Neuromuscular reinnervation efficacy after nerve repair or nerve graft in YFP mice

Alexander CS Woollard

UCL

PhD

Acknowledgements

I would like to my supervisors in both London (A.O.Grobbelaar and K. Rolfe) and Cambridge (J.W. Lichtman) for all their wisdom and patience. In particular Jeff, for guiding me through the world of neuroscience with such care. I am indebted to my wife for her support of me in this endeavor and her willingness to stand by me, wherever that took us.

This work has been presented in the following forums:

2011 New England Society for Microscopy Annual Spring Symposium
Woods Hole, USA
"Facial Reanimation: A transgenic approach to muscle reanimation".
Woollard AC

2013 Society of Academic and Research Surgery Annual Meeting
Royal Society of Medicine, London, UK
"Reinnervation of the interscutularis muscle after nerve repair or graft in YFP mice".
Woollard AC, Rolfe K, Grobbelaar AO

2013 Insight into Surgical Training
Royal Society of Medicine, London, UK
"A Royal College of Surgeons Research Fellowship, My Experience".
Woollard AC

2013 12th International Facial Nerve Symposium
Boston, USA
"Neuromuscular reinnervation efficacy after nerve repair or graft in YFP mice".
Woollard ACS, Rolfe K, Lichtman JW, Grobbelaar AO

2014 EURAPS
Ischia, Italy
"Axonal Regrowth After Nerve Repair or Graft in YFP Transgenic Mice"
Woollard AC, Rolfe K, Lichtman JW, Grobbelaar AO

I, Alexander CS Woollard, confirm that the work presented in this thesis is my own. Where information has been derived from other sources, I confirm that this has been indicated in the thesis.

Abstract:

Introduction: The gold standard reconstruction for facial reanimation is the functional muscle transfer. The reinnervation of a muscle is never complete and clinical results are variable with 20% not achieving a satisfactory outcome (1). This study uses transgenic YFP mice to investigate the patterns of reinnervation through a nerve repair and a nerve graft.

Method: 81 YFP-16 mice were studied in three intervention groups (nerve repair, nerve graft and nerve cut) over three time periods (four, six and twelve weeks post intervention). Two parameters were investigated: the number and surface area of reinnervated neuromuscular junctions and the number and calibre of regenerating axons. An assessment was made of motor unit proportions. 14 YFP-H mice were used to further investigate the patterns of axon regeneration through a nerve repair and graft.

Results: In the nerve cut group there was no reinnervation of the muscle at any time period. In all cases of nerve repair and nerve graft the muscles were completely reinnervated by regenerating axons with no significant difference between either intervention group and controls. The number and calibre of the regenerating axons was significantly different to controls for both intervention groups. The motor units were smaller in both intervention groups, but when the axons were thresholded to within two standard deviations of the control axon populations, the motor units were larger.

Discussion: Reinnervation after nerve repair or graft appeared adequate, however the neuromuscular junctions showed some evidence of morphological change that persisted. The number and type of axons after repair or graft differed from the control groups. There were more small calibre axons, suggesting the arbor had been reinnervated by a smaller number of axons that branched to increase their influence. These axons showed evidence of remodeling in the repair group, but not in the graft group.

Contents

List of Figures and Tables

1. Introduction

In 2008 I was presenting a clinical poster on reconstructive options in Möebius syndrome at the annual meeting of the American Association of Plastic Surgeons in Boston, Massachusetts. The keynote speaker at the meeting was a neuroscientist called Jeff Lichtman who presented his work on the nervous system using transgenic animals expressing Green Fluoroescent Protein. It was a before-and-after moment for me, and I knew that I wanted to exploit this tool to help me understand the biology behind the clinical applications of nerve regeneration in facial palsy reconstruction. I pestered Jeff for nearly two years until he agreed for me to join him in his laboratory in Harvard. The work set out in this thesis represents that journey. After a brief training in animal husbandry, laboratory experimentation and the theory and use of the confocal and two photon microscopes I set off. All the experiments, data collection and analysis presented here were performed by me at Jeff Lichtman's laboratory in Harvard University. The contemplation and write up were done back in London with the support of my supervisors. The results have been presented at several international meetings of both the plastic surgical and neuroscience communities. Papers are in preparation for submission to the plastic surgical literature.

The near infinite complexity of the human smile has challenged artists and physicians for centuries. There are over twenty paired muscles in the head and neck innervated by the facial nerve, and most of them are involved in enabling us to smile. A smile can be voluntary or spontaneous, or a combination of both. It encompasses the mouth but also the eyes and even the nostrils in a way that is unique in every individual. When this system fails to function it is usually due to a problem with the facial nerve. Evidence of facial palsy can be seen from over four thousand years ago in Egyptian statues. Today facial palsy has an estimated incidence of 50 per 100,000 population per year (6,7). Schaitkin identified over a hundred possible aetiologies from causes as varied as leprosy and Lyme's disease to injury or surgical trauma. 13% of cases are associated with a significant, treatable or life-threatening disorder (8). Two thirds of cases are of unknown cause and as such classified as Bell's palsy, a diagnosis of exclusion (6,9). Freidrich's original description in the 18th Century attributed this to "rheumatism" (10). For a while in the 1930s Bell's palsy was thought to be caused by oedema of the nerve in its narrow intracranial course, leading to a brief vogue for surgical decompression of the bony canal (11,12). Bell's palsy is probably associated with a viral infection, most likely herpes simplex (HSV-1) though this has not been definitively confirmed to date (13-15). Whatever the cause facial palsy has a tremendous impact on a person's life. The American Medical Association Guide to the Evaluation of Permanent Impairment rates disabilities according to their "percentage whole body impairment". A unilateral facial palsy scores 10-15% and a bilateral facial palsy 30-45% (16). The loss of an index finger by comparison scores 18%. This reflects the devastating impact of a seventh nerve palsy, which results in a raft of both functional and aesthetic problems. Depending on the degree of sub-branch involvement there can be loss of facial expression, oral and ocular incontinence, difficulty with eating and drinking, poverty of articulation and social interaction. The inability to close the mouth adequately results in drooling and ultimately dental caries. Similarly, poor eye closure can result in dysfunctional eye lubrication and toilet, leading to corneal ulcers and permanent reduction in visual acuity. The impact on social participation makes patients shy and unwilling to communicate. In children this is detrimental to their development and often contributes to bullying and introversion. A unilateral paralysis creates an asymmetry, and a bilateral paralysis leads to an expressionless face.

1.1 The facial nerve

Part of what makes the treatment of facial palsy fascinating is the complexity of the facial nerve itself (Fig 1). It is the seventh of twelve cranial nerves and was first described in an account given by Sir Charles Bell to the Royal Society in 1821 (17). The facial nerve nucleus is one of the largest motor cranial nuclei with 7,000-10,500 cells spatially divided into groups that correspond to individual mimetic muscles of expression in the face (18-20). Closely associated with the facial nerve is another nerve, the intermediate nerve, which carries visceral and somatic afferent fibres as well as general visceral efferent fibres. The intermediate nerve is also referred to as the sensory component of the facial nerve. The two are so intertwined that they can almost be considered as a single entity and this has implications for how we consider the nerve in clinical scenarios.

The motor element arises from the pons and has a tortuous intracranial course, joining the intermediate nerve at the internal auditory meatus of the ear canal. Halfway along this canal, after a small branch is given off to the stapedius muscle of the inner ear, the facial and intermediate nerves divert to exit the skull through the stylomastoid foramen via the facial canal. Extracranially, small branches are given off to supply the stylohyoid and digastric muscles in the neck, and the posterior auricular muscle behind the ear. The nerve then passes into the parotid gland. It is the only nerve in the human body to pass through the substance of a gland. Within the parotid the facial nerve divides into its five main branches to supply the mimetic muscles of the face: temporal, zygomatic, buccal, marginal mandibular and cervical (21).

The particular dominance of the oral and ocular musculature in man is reflected in the high degree of differentiation between the areas that control these muscles in the motor nucleus. Most of the facial nerve motor axons are large, 7-10μm in diameter, and the motor units are small, in keeping with the high degree of subtlety in their movements (22). Feinstein estimated the human platysma to have approximately 25 muscle fibres per axon (23). What is unusual is the relative paucity of muscle spindles found in the muscles innervated by the facial nerve. Given the precision with which the facial muscles are utilized it might be expected that they would be more heavily populated by these proprioceptors that govern muscle tension and tone. Voss found only six in a human stylohyoid muscle and Bruesch identified only 140 afferent fibres in the facial nerve branches of the cat (24,25). However, even when the trigeminal nerve, which provides sensation to the skin of the face, is anaesthetised, proprioceptive signals are preserved (26,27).

The cell bodies of the intermediate nerve reside in the geniculate ganglion. It has some general visceral efferent fibres that stimulate a number of glands in the face (lacrimal, submaxillary, sublingual). There are also small, mainly myelinated sensory nerves. Most of these are gustatory afferents that are distributed to the tongue and mucosa of the oral cavity via the greater petrosal (33-35%) and chorda tympani (45-55%) nerves. However 12-15% of the fibres continue within the facial nerve to innervate an area of skin behind the ear (28,29). There is a similar sensory cutaneous branch of the facial nerve in man which probably tracks to the trigeminal nuclei (30-35). Likewise, though most facial reflexes probably rely on afferents in the trigeminal nerve, there is some involvement of afferent fibres travelling in the facial nerve (21,36). The facial nerve is often thought of as purely motor to the mimetic muscles of the face. In fact it is a much more complicated nerve. It has a mixture of myelinated axons that are mainly motor though there are some sensory cutaneous and muscle afferent fibres (21).

Figure 1.

Anatomy of the facial nerve

Anatomical representation of the course facial and intermediate nerves in humans (2)

1.2 Facial Palsy

Facial palsy can be classified in several ways. It can be complete or partial depending on how many of the muscles of the face are involved. It can also be unilateral or bilateral depending on whether one or both sides of the face are paralysed. Bilateral cases are rarer and more often congenital, where they are frequently associated with other defects (37). It is possible to have an acquired bilateral case in adulthood (38). Given that Bell's palsy is the commonest cause of paralysis it is perhaps reassuring that all Bell's palsies recover some movement, with 71% regaining full movement. In those with some residual paralysis the deficit correlates well with both the initial degree of paralysis (partial or complete) and the speed of recovery over the first weeks and months after onset. Patients with abnormal movement after six months are unlikely to make a full recovery (8,39).

If the palsy has been caused by division of the nerve as a result of surgery or trauma it is recommended to repair the nerve immediately if possible, or within thirty days if there is contamination that requires debridement. If there is a nerve gap, from tumour excision or debridement, repair with a nerve graft (eg. sural nerve harvested from the same individual) is preferable to a nerve repair under tension. If the injury occurs proximal to where the facial nerve has subdivided into its main branches in the cheek there is a higher incidence of synkinesis (40). It is thought this occurs due to individual axons entering more than one terminal branch and abnormally innervating multiple muscles. Synkinesis results in uncoordinated movements in areas of the face that would normally be isolated from one another. If an urgent progressive cause of the palsy has been ruled out the initial clinical management is supportive and prophylactic. It focuses on measures to reduce the incidence of permanent sequelae. Most patients will recover some, if not all, movement and any return of natural expression is generally more aesthetically pleasing than a reconstruction. Most surgeons would not consider intervening until at least twelve to eighteen months after there has been no further improvement in function (41). If there is residual deficit, facial reanimation can be considered.

1.3 Facial reanimation

Functional muscle transfers were first described in 1970 when Tamai transplanted the biceps brachii and rectus femoris muscles from one leg to the other in a dog model and repaired the motor nerve (42). It was reliant on two advances that created the modern specialty of microsurgery: a better understanding of the blood supply to muscles, bone and skin that allows parts of the anatomy be removed and reconnected elsewhere, and the development of the instruments and techniques that facilitate operating under a microscope (43-45). Adding muscle functionality to the already burgeoning field of microsurgery opened up a new rung on the reconstructive ladder. Free functioning muscle transfers are now the gold-standard for facial reanimation and can also be used in some extremity reconstructions (46-53). A muscle is harvested along with its blood supply and nerve so that it can be transferred *en bloc* to a new location where it is reconnected to a new blood supply and to a new nerve input, which restores muscular contraction. The survival rates in free flaps have steadily improved over time, however the functional outcomes in muscle transfers remain less predictable. In the case of facial reanimation the final results are a complex mixture of symmetry both at rest and in movement. This relies on striking a balance between muscular power, bulk and excursion in a muscle that gradually atrophies and then re-innervates over eighteen months to two years. A recent series of 637 muscle transfers for facial reanimation graded 20% of results as sub-optimal (54). These are muscles that either have too little movement or, perhaps more depressingly, initially good results that have become tight and contracted over time. The underlying cause of these poor results is unclear. The best results for FFMT are in children under ten years old, and they are not reliably satisfactory in patients over fifty five (54,55). This is probably due to impaired neural regeneration in older subjects.

The two-stage facial reanimation with a free-functioning muscle transfer was first described in the late 1970s (46,47,49,56-58). At the first operation a nerve graft is harvested, normally the sural nerve. This is reversed to reduce the chance of regenerating axons getting lost at old branching points. What was the distal end is connected to a terminal arbor of the buccal branch of the facial nerve on the un-paralysed side of the face. The remaining length is then tunneled under the skin to the opposite, paralysed side as a cross-facial nerve graft (CFNG). Growth through this graft is tracked using a Tinel's sign where sensation is provoked by tapping the growing end of the nerve. The presence of this Tinel's sign is confirmation of the presence of some sensory fibres within the facial nerve. The second stage is performed when the CFNG has regenerated axons across the face to a sufficient length so that when it is connected to the new muscle the delay in reinnervation is a short as possible. Regenerating axons grow at approximately 1mm per day and the CFNG is usually 15 cm in length. Whilst the timing of the second stage depends on the individual, most axons will have traversed the graft after five or six months. A muscle is then harvested (usually the pectoralis minor, a segment of the latissimus dorsi or gracilis) and inserted into the paralysed cheek. Its blood supply is restored by connecting its vessels to the facial vessels and its nerve is connected to the freshened end of the CFNG. The muscle ends are sutured to the corners of the nose and mouth, and to the zygomatic fascia in front of the ear to recreate the vector of smile that is seen on the unparalysed side for that individual (Fig 2).

Figure 2.

Two-stage facial reanimation procedure

a) b)

The first stage operation involves the placement of a cross-facial nerve graft from the functioning facial nerve to the paralysed side. The second stage transfers a muscle into the cheek, restores its blood supply and connects it to the end of the graft.

a) A cross facial nerve graft (CFNG) from the normal right facial nerve buccal branch to the paralysed left cheek.
b) A free-functioning muscle graft in the left cheek anastomosed to the facial blood vessels and the CFNG.

1.4 Evaluating Free-Functional Muscle Transfers

This procedure is arguably amongst the most intricate operations in modern surgery. The outcome depends upon a combination of technical expertise, aesthetic judgment, and the unpredictable element, the adequacy of the reinnervation of the muscle by the new nerve. Even with microsurgical techniques the reinnervation of muscles by peripheral nerves is far from perfect. The results of facial reanimation are subjective and hard to assess. There are a number of grading systems quoted in the literature that all rely on a combination of a score given by the operating surgeon and a score from an independent panel (49,54,59-64). The aim is to relate the outcome to the goals. In the case of the reconstruction of a smile these are symmetry, both at rest, and during movement, and the degree of excursion, by which we mean how much movement the muscle produces at the corner of the mouth. In addition there is the spontaneity of the smile, something that is very difficult to provoke in the relatively sterile environment of the clinic or hospital photographic department and often it can only be captured in unguarded moments. Ho has pointed out that the patient satisfaction is often absent from these grading systems (65). All the complexity of the smile is boiled down to excellent, good or poor. Excellent and good both encompass results where the muscle transfer has been successful and there is some movement recreating a smile, but variable degrees of symmetry. This is usually as a result of inadequate contraction of the muscle or an inferior vector of contraction due to its placement. Poor results represent 20-49% of cases and can occur for a number of reasons (54,59,66). All free tissue transfers, even when they are not free-functioning muscle transfers, have a failure rate associated with their blood supply of 5-10% (67). Even if the muscle survives in 7-11% of cases it will not re-innervate which results in little or no movement (54,68). There can also be synkinesis where the new muscle doesn't contract synchronously. This is thought to be due to imperfect reinnervation of the transferred muscle. Perhaps most disheartening is late-onset tightness seen in 8-13% of muscles (54,68). This occurs when a muscle that was initially working well seems to tighten up and contract within the cheek over the course of a few years. Overall approximately one fifth to half of patients have an unsatisfactory result (54,59,66). The underlying process that results in these poor outcomes remains unclear. It is probably due to problems with the reinnervation of the muscle.

It has been estimated that as many as 90% of all nerve repairs leave some degree of deficit despite achieving return of function, be that sensory or motor (69,70). Repairs that require a graft have a poorer outcome than a simple repair of the proximal and distal stump (71-73). It is not clear if this is simply due to there being two repairs instead of one. Investigations into possible nerve graft substitutes have tried everything from freeze-thawed muscle tissue, veins and even synthetic conduits, but none have consistently compared favourably with autograft of a host's own nerve (71,74,75).

It is a given that in free functional muscle transfers that once a muscle has been transplanted the new source of innervation (the donor nerve) will be different from its original nerve. Nerves can be composed of a number of different types of axons depending on their function. They can be purely sensory, motor or mixed, and within that there is variation in the properties of the individual axons according to their role (Table 1). The effect of connecting a muscle to a nerve that has a different makeup of axons from its original supply is poorly understood. MacQuillan has shown, by transplanting a hindlimb muscle in a rabbit model, that attaching a muscle to a peripheral nerve with more axons than its original does not improve the functional outcome (76). However, in the same scenario, comparing cranial nerve branches with differing numbers of axons, there is a difference in the tension generated. The larger of the two branches produced more tension than the repaired original nerve, though still less than the uninjured muscle (77). It would seem that cranial nerves are capable of increasing the functional output of a muscle in a way that peripheral nerves are not. In trying to model facial reanimation it would seem prudent to use a cranial nerve.

Moreover, it would seem logical to try and match the properties of the original and donor nerves to minimise the discrepancies in reinnervation. There is very little in the literature regarding the axonal composition of the branches of the facial nerve or of nerves supplying the muscles commonly used for functional muscle transfer in humans (78). Frey has investigated the medial pectoral nerve which supplies pectoralis minor. It has 1500 axons which are all myelinated with an average diameter of 8.5µm (79). The other two mainstays of facial reanimation, the latissimus dorsi and gracilis muscles, remain relatively undescribed in humans. Terzis has biopsied the nerve from the donor muscle in 35 patients undergoing a second stage free-functional muscle transfer for facial reanimation. She doesn't clarify which muscle was being transferred in each case but states that the axonal load was 1222 ± 324 (80).

Table 1.

Axon subtypes and properties

	Type	**Erlanger-Gasser Class**	**Diameter (µm)**	**Myelin**	**Conductance (m/s)**	**Function**
Motor	α	Aα	13-20	Yes	80-120	Muscle fibres
Motor	γ	Aγ	5-8	Yes	4-24	Muscle spindles (efferent)
Sensory	Ia	Aα	13-20	Yes	80-120	Muscle spindles (afferent)
Sensory	Ib	Aα	13-20	Yes	80-120	Golgi tendon organ
Sensory	II	Aβ	6-12	Yes	33-75	Muscle spindles (afferent), Cutaneous mechanoreceptors
Sensory	III	Aδ	1-5	Thin	3-30	Cutaneous pain, touch, pressure, cold
Sensory	IV	C	0.2-1.5	No	0.5-2	Cutaneous pain and heat
Autonomic	Pre-ganglionic	B	1-5	Yes	3-15	
Autonomic	Post-ganglionic	C	0.2-1.5	No	0.5-2	

In a study of 30 patients undergoing two-stage reanimation Jacobs took biopsies from the stump of the buccal branch of the facial nerve at the first stage operation At the second stage several months later he also took biopsies of the cross facial nerve graft to compare the characteristics of the original nerve and the graft. He found that the total number of axons doubled from 5500 in the biopsy of the buccal branch to 11,500 at the distal end of the graft. Jacobs concluded that a buccal branch, via a cross facial nerve graft, provided an adequate number of axons to power a functional muscle transfer. However, the number of myelinated axons fell by over half and as a proportion of all fibres dropped from 31% to 4%. The diameter of the regenerated axons was small with an average of 2.5µm and a maximum of 3µm (81). Given what we know about the anatomy of the facial nerve it is hard to explain the presence of so many unmyelinated fibres in the normal buccal branch. The increase in the number of axons suggests that there has been a substantial amount of branching within the graft, something supported by other work on nerves that are regenerating without target organs (82,83). Jacobs took the biopsy of the distal nerve graft prior to the insertion of the new muscle at the second stage. The lack of a target muscle during regeneration would have influenced the nature of the axons growing through the graft. In one case where a functioning muscle had to be revised after five years for unrelated reasons the proximal graft was re-evaluated. It now contained fascicles "packed with large regeneration clusters of well myelinated fibres with a maximum diameter of 13µm". Unfortunately the number of fibres is not mentioned. This suggests that the cross-facial nerve graft without a target muscle has a different composition from one that is connected to a muscle. Terzis performed a similar study in a number of patients undergoing a variety of facial reanimation procedures. 35 underwent free-functioning muscle transfer (*vide supra*). Biopsies of the facial nerve showed that the zygomatic branch (998±705, n=59) has more axons than the buccal branch (683±506, n=25) which correlates with MacQuillan's work in rabbits (77,84). The sural nerve contained 1762 ± 953 (n=37) axons at the first stage but at the time of the second stage this had fallen to 453±265 (n=34). Interestingly she compared these axonal counts with the final clinical outcomes. A donor nerve with more than 900 axons correlated significantly with an improvement in functional and aesthetic outcomes. The only other significant finding was a correlation between the number of axons in the donor nerve and the number of axons at the distal end of the graft. Terzis does not give any raw data regarding the number of axons that were myelinated but she does mention that the number of myelinated axons in the distal nerve graft correlated with the counts at the donor nerve, but not with improved outcome (84). The differences in nerve composition and the changes that occur in axons after repair would seem to be likely contributing factors to the variability in results.

There is a considerable amount of literature on the reinnervation of muscles after nerve injury, either nerve crush, nerve cut or nerve repair (85-103). However the methods available until recently have meant that investigation has been reliant on indirect measurements from techniques such as electrophysiology to estimate the size of axons and their motor units. Even retrograde labeling, which can highlight the number of nerve cell bodies in the central nervous system that have made projections to a target, cannot separate out those axons which made functional connections, from those that were misdirected there and make no contribution (104). Actual visualization has necessitated segmentally dividing up the nerve-muscle complex and imaging it sequentially. Serial sections in the electron microscope which can provide immense resolution have, to date, only been used to reconstruct relatively small volumes of neuropil (105). It is not a suitable tool to reconstruct the entire picture from the proximal nerve, through an area of injury, into the muscle and onto the neuromuscular junction. The recent advent of transgenic animals that can express green fluorescent protein in their neurons now makes it possible to visualize neurons in continuity and trace their pathways both intra and extra-muscularly. It is possible to evaluate reinnervation in a completely new way and unpick the relationship between the returning axons and the muscle they are reinnervating.

1.5 Neurons

Our current understanding of the structure and function of nervous tissue had its beginnings with the work of Golgi and Cajal just over a century ago. Before that the prevailing view was that the brain was a gland and the nerves conduits to transport the fluids, which it produced around the body. In 1873 Camillo Golgi developed a histological technique for staining nervous tissue with silver. The silver offers the dual advantage of being fully absorbed by a neuron along its entire length, but only being taken up in a small proportion of the total number of cells. This allowed Golgi to study cells in isolation without background noise from its neighbours. It was Ramón y Cajal who then applied this technique, and through his observations of neuron structure developed many of the fundamental tenets of modern neuroscience (106). He recognized that there was connectional specificity. Neurons had no cytoplasmic continuity but formed precise connections, and those connections were not random but organized. He also elucidated that within each neuron information always flows in a very organized pattern of dynamic depolarization. A signal arrives at a set of receiving sites (dendrites and sometimes the cell body) and then a trigger zone (axonal hillock) initiates an action potential which propagates in one direction down the axon to the pre-synaptic release sites in the axon terminal. This work at the end of the nineteenth century dramatically altered the paradigm for studying the nervous system, and initiated the neuronal doctrine: this states that the system is made up of individual cells capable of producing signals and communicating between one another via connections. It was supported by concurrent research in related disciplines. Harrison used tissue cultures to study embryological development, and showed that the dendritic and axonal processes of the neuron are continuous with the cell body and project from it. He also demonstrated the presence of a growth cone at the tip of the advancing axon as it extends towards its target organ (107).

Physiological work by pioneers such as Galvani and von Helmholtz unraveled some of the mysteries of the electrical activity of nerve cells and how signals were conducted along their processes. Pharmacologists such as Bernard, Ehrlich and Langley, showed how drugs could interact with receptors on the surface of neurons, and started the process of understanding the way the electrical impulses are converted to a chemical signal at the synapse (108).

Neurons can be classified according to their connections and their structure. Afferent neurons carry signals into the nervous system. Efferent neurons carry signals away towards effector organs such as muscles and glands. Inter-neurons carry signals between other neurons and make up most of the cells within the brain. A typical motor neuron is a multipolar cell with its cell body located in the anterior horn of the spinal cord. It has 7 – 18 primary dendrites, which gather information, and a single axon which propagates information over a variable distance to the presynaptic terminal (108). If a threshold membrane potential from the dendritic inputs is reached an axon potential is initiated in an all-or-nothing signal (109). Once the axon reaches the muscle it ramifies into an arbor and each branch ends at a neuromuscular junction (NMJ). Here the terminal swelling of the axon contains vesicles that deliver the neurotransmitter acetylcholine into the synaptic cleft. A single axon from each nerve cell will connect to multiple muscle fibres, but each mature muscle fibre will only receive input from a single axon. The fibres collectively innervated by each nerve cell are defined as a *motor unit,* and within a single muscle there will be a distribution of units of varying sizes. The proportion of small to large units and their orderly recruitment dictates the overall function of the muscle (110). Henneman postulated that within each muscle the motor units are recruited according to the size principle: smaller units are excited first and most often. Larger units are added to them as the size of the stimulation is increased and more power is required from the muscle (111,112).

One of the key defining characteristics of nerve cells is their excitability. This feature results from changes in electrical potential difference across the cell membrane due to the rapid shift of charged ions between the intra and extracellular spaces. This shift depends on the ion channels that span the phospholipid bilayer of the cell membrane, which can initiate a wave of coordinated depolarisation as an action potential. The speed with which this signal can travel is dependent on electrical resistance of the membrane and axonal cytoplasm. This resistance is inversely proportional to the diameter of the axon. However, it is advantageous to keep axon diameters small to maximize the number of conduits available to transmit large volumes of information to and from the periphery. Insulating the axons by wrapping them in myelin reduces the resistance by more than an equivalent increase in axonal diameter (108).

Glial cells, are intimately associated with nerve cells and their signal transduction properties. Schwann cells are the glial cell of the peripheral nervous system. These cells are not actively involved in signal processing but they play important roles in supporting and nourishing the axons. They buffer potassium ion concentrations, phagocytose debris (see *nerve injury* below) and assist in axonal migration and growth guidance. Schwann cells produce myelin which wraps around each axon in concentric rolls to sheath and insulate them (108). Myelin is very similar in structure to plasma membranes consisting of 70% lipid and 30% protein, with a high concentration of cholesterol and phospholipid molecules. In development, before myelination, the nerve cells lie in a trough formed by rows of adjacent Schwann cells. These then surround the axon and form mesaxons, a double-membraned process that then spirals around the axon as it elongates. As it does this, the cytoplasm of the glial cell is squeezed out and the concentric rings condense into a lamellar structure called the myelin sheath. The axon makes contact with the muscle at neuromuscular junctions which tend to be gathered in a region of the muscle defined as the end-plate zone. The myelin sheath terminates just short of the point where the axon forms thin tendrils that branch out over the junction. A non-myelinating Schwann cell variant covers the junction.

1.6 The neuromuscular junction

Once an action potential has travelled the length of an axon it arrives at the synaptic terminal. Much of nerve anatomy is concerned with the rapid and precise conduction of information between two cells over a considerable distance. Within the cell processes, both dendritic and axonal, this is in the form of an electric potential. The point of contact between cells is called a synapse. Synapses can vary greatly depending on the anatomy of the pre and post synaptic cells and the function they perform, but it is vital that the speed and precision of the action potential be maintained. In most cases the signal is transferred by the conversion of the electrical signal to a chemical one at the synaptic junction, which then influences the postsynaptic cell. This is uni-directional and can be excitatory or inhibitory, and expressed through a myriad of neurotransmitters (e.g. acetylcholine, noradrenaline, serotonin, dopamine, γ-aminobutyric acid). The type of transmitter is specific to the pre-synaptic cell and, once mature, that cell only secretes that transmitter at all its synapses, however the same neurotransmitter may have excitatory effects on some postsynaptic cells and inhibitory effects on others. The neurotransmitter at the neuromuscular junction (NMJ) is acetylcholine (ACh) which acts in an excitatory capacity via a nicotinic receptor on the surface of the muscle fibre. ACh is synthesized from the non-specific metabolic substrate acetyl coenzyme A (acetyl CoA) by the substitution of choline for CoA by the enzyme acetyltransferase (108).

When the action potential arrives at the terminal it opens voltage-gated calcium channels which results in a secretory potential at the bouton (108). Thousands of vesicles containing ACh fuse with the presynaptic membrane releasing ACh by exocytosis. A concentration of ACh receptors reside in the post-synaptic membrane and are associated with voltage-gated sodium channels.

The receptor is a transmitter-gated ion channel with a central pore that is large and non-specific. It allows passage of potassium, sodium and even calcium ions. During the millisecond that ACh is, on average, bound to its receptor there is a net influx of sodium ions and efflux of potassium ions resulting in a depolarization of the membrane. ACh channels can only be opened by binding with ACh and are therefore limited to the concentration of ACh molecules in the cleft. This keeps the size of the depolarization proportional to the concentration of ACh released. This concentration peaks at the moment the action potential initiates the exocytosis of the vesicles in the presynaptic membrane, then fades due to diffusion of ACh out of the cleft and the action of acteylcholinesterase. The depolarization caused by the ACh receptor channels opens the voltage-gated Na+ channels which then instigate a positive feedback loop. This is sufficient to provoke an action potential in the muscle fibre. The area on a muscle that is in contact with a nerve contains all the neuromuscular junctions and is known as the end-plate band. Once the action potential arrives at an NMJ it generates an end-plate potential which propagates along the surface of the muscle.

1.7 Nerve Injury

Peripheral (PNS) and central (CNS) nerves have very different responses to injury. Centrally the ability to repair damage is very limited. Neurons cannot regenerate axons. In contrast neurons in the periphery are able to re-grow axons over large distances and re-establish connections to target organs. The exact mechanisms behind these differences are not fully understood. There are theories suggesting that it might be due in part to differences in the extracellular matrix that surrounds the injured nerve cells. Cajal noted that by bringing the proximal end of an axotomised nerve in the PNS into contact with CNS by transplanting a segment of optic nerve, it immediately arrested any regeneration (113). In contrast when a segment of rat sciatic nerve (PNS) was grafted onto an axotomised optic nerve (CNS), nerve fibres were encouraged to regenerate (114).

When an axon is severed axoplasm seeps from the cut ends of both the proximal and distal segments. This stops once the axonal membrane seals across the open ends. The ends then swell and retract away from one another as they fill with the substances that normally travel along the axon. The discontinuity of the axon means that the proteins synthesized in the cell body can no longer reach the terminal bouton. Synaptic transmission rapidly ceases as it cannot regenerate vesicles. The nerve segment that is not in continuity with the cell body begins to degenerate. This process was first described by Augustus Waller in 1850 (115) and has become known as Wallerian degeneration (WD). The cytoskeleton of the axon forms into clumps and disintegrates into a 'string of beads' mediated by calcium influx which activates axonal proteases (116). Depending on the size of the nerve there is disintegration of the axon within one to two days (117). During this time the myelin sheath also pulls away from the axon and breaks apart. The proximal axon stump retracts back to the next node of Ranvier. The cell body swells and undergoes a series of changes known as chromatolysis (100). The nucleus increases in size and moves away from the centre of the cell towards the axonal hillock and the rough endoplasmic reticulum breaks up. The cell switches from a state of signal transmission to one of growth, and with that there is a change in gene expression with up-regulation of those genes responsible for growth cone elongation and stability (118). mRNA and protein synthesis is accelerated to support axon growth (119). These genes include those for cytoskeletal proteins (tubulin and actin) and growth associated proteins, especially growth associated protein-43 (GAP-43) and cytoskeleton-associated protein-23 (CAP-23) (120,121). Regenerating axons are thinner than normal due to the down-regulation of genes for neurofilament cytoskeleton production and therefore reduced neurofilament:tubulin ratio within the growing axon (122,123).

Within two days the Schwann cells dedifferentiate and down regulate the genes that produce myelin, which would normally support axonal transmission (124). There is a highly coordinated up-regulation of regeneration associated genes (RAGs) which code for neurotrophic factors (nerve growth factor (NGF), brain-derived neurotrophic factor (BDNF) and glial cell derived neurotrophic factor (GDNF), cytokines and cell adhesion molecules (125). Schwann cell proliferation occurs in a non-myelinating form that promotes axonal growth (126,127). These cells scavenge myelin debris from the fragmenting sheath and form it into ovoids, the classical 'ground glass' appearance associated with Wallerian degeneration (128-130). Release of nerve growth factor (NGF) causes Schwann cells to migrate across the site of injury and form bands of Büngner which are important in supporting and guiding the regenerating axons (131-133).

Macrophages infiltrate the site by the third day post injury, and remain in the nerve stump for at least a month. They are the principle agent for removing the myelin debris such as myelin associated glycoprotein (MAG) which is inhibitory to axonal growth (134-139).

1.8 Nerve growth and regeneration.

The proximal stump develops a growth cone similar to that seen in development. Axons grow by adding components at their distal extremity at an area known as the growth cone (140-142). This cone was recognized by Cajal, but he imagined it to be akin to a simple snowplow that opened the route within the packed stroma for the axon to pass through (143,144). The presence of filopodia extending out from the growth cone were first noticed by Harrison working with embryonic neural tubes in cultures, and then by Speidal *in vivo* in tadpoles (145,146). It appears that growth cones have two potential morphologies (147). When the axon is following a path that has already been laid down by previous axons the growth cone is exactly that, a cone, with very few filopodia. However, when it reaches an area where a 'decision' has to be made: to defasiculate, follow an alternative path, or contact with a target, the cone flattens out and forms multiple filopodia (148-150). The increase in axonal length occurs at the growth cone tip (151). The production of new membrane mainly occurs through the calcium-dependent fusion of vesicles at the tip of the cone (152). Likewise the polymerizastion of axonal architecture, of tubulin into microtubules and actin into microfilaments, also occurs at distal tip of the axon (153-157). Microfilaments seem to be more important for growth of the filopodia, whilst microtubules are concerned with advancement of the whole growth cone (158). Filopodia are capable of generating retrograde tension that drags the axon forwards (159). This allows them to affect the direction of the growth cone as they interact with their surroundings. Growth cones are guided towards their targets by a number of processes. They are able to respond to physical and chemical signals in their local environment[1]. In this way they interact with the substrate they are

---

[1] Guidance of axonal growth cannot be explained entirely by physical means. In experiments where the optic nerves were transplanted to different areas of the brain they still managed to find their correct targets (160). The adhesiveness of the surface the axon is grown on also makes a difference to the activity of the growth cone (161-165). McKenna *et al* showed that there is a threshold concentration of adhesion molecules required to facilitate

growing on as well as adjacent cells, cell adhesion molecules and diffusible agents that can promote or inhibit growth. Experiments have shown that growth cones can be impeded by physical breaks in the tracts they would normally follow, but that they can also be facilitated by an artificial pathway (184). This underpins how we can use nerve grafts to overcome gaps in injured nerves.

As the growth cone extends from the proximal nerve stump in regenerating axons it travels on the surface of the Schwann cell or along the inner surface of the basal lamina of the Büngner's band (185). These have the dual function of providing a scaffold for regenerating axons to grow along and the adhesion molecules to encourage that growth (186-189). The Schwann cell columns and the denervated target both produce neurotrophic factors that support the growth of axons (102,190,191). Multiple growth cones form, with each of the damaged axons producing on average 5 branches and some of those can co-exist within a single Schwann cell column or basal lamina tube (82,98,101,192,193). If the nerve reaches a target the number of fibres shrinks and the average size of each axon increases. It is thought that the reduction in branches takes place through pruning of those that have not made adequate or appropriate connections (94,95). This

---

growth but they are not necessarily instructive (166). There are numerous molecules in the extracellular matrix (ECM) that have been shown to promote axon growth (167). Whilst all can support growth some seem to be preferred by particular subsets of cells: CNS axons prefer laminin whilst peripheral axons prefer fibronectin. This specificity may lie in the makeup of the expression of integrin molecules at the tip of the growth cone (168). In addition the combination may alter as an axon matures and encounters different environments (169). Most axons grow along the surfaces of other cells and axons. These express cell adhesion molecules (CAMs) on their surface which support axonal growth and have a number of specialized functions. NCAM is probably the most studied of the CAM family. It seems to be expressed on all neurons and glia but can be highly modified in its extracellular portion and therefore exists in multiple forms (170). It is thought that this variation may assist in the direction of nerves as they advance through complex regions such as the brachial plexus (171). The family of CAMs seems to keep growing and interrupting their action produces a huge variety of changes in axonal growth. This has led to the 'labeled pathway' hypothesis of axon guidance whereby a pioneer axon grows towards the target and lays down CAM signals that all subsequent axons follow (172-175). The understanding of how the original pioneer axons reaches its targets is still not clear though it is thought it might be through local cues or chemotaxis towards a diffusible signal from the target, as demonstrated by the ability of growing axons in culture to detect and grow towards a higher concentration of neurotrophic factor (176-179). This is a complex topic and one that is not resolved. It seems likely that growth cone guidance is a combination of attractive and repulsive forces acting in concert (180-183).

may occur through a process similar to that undergone in development, when competition between axons at polyinnervated neuromuscular junctions eventually gives way to single innervation (194-201). In regeneration it is unclear whether each axon is pruned back to a single fibre. Multiple collateral branches are capable of function as seen in synkinesis. Mackinnon has shown that the initially increased number of branches is reduced to normal levels after twenty four months in a rat model (202). However this doesn't allow for the natural reduction of axon numbers with ageing in a similar timeframe which can be as much as 30% (5).

The size of regenerating axons change as they mature. Initially there is a large population of small, unmyelinated axons and as they mature they become fewer, larger and myelinated (82,203,204). The most important factor for the maturation of the regenerating axons is a connection with the target, regardless of the degree of target regeneration (82,205-207). However, target size has been shown, at least in sympathetic fibres, to be influential on the size of axons (185,208). The size of axons is also the deciding factor in their myelination, with all axons greater than 2µm becoming encased in a sheath (209). This may explain the disproportionate increases in unmyelinated axons over myelinated than have been reported (81,98,210). Branches that have not reached a target may stay small and therefore remain unmyelinated. Those that have made a connection with a target may be able to mature, enlarge and myelinate. Whilst the axon characteristics seem to be restored after nerve crush this is not the case after axotomy and repair where axons are noted to be smaller and slower with thinner myelin sheaths (86,204,211). Despite some recovery over time, the normal distributions are not regained (87,203).

Although axon damage and target denervation stimulate regrowth, it has long been known that the functional recovery is worse after periods of denervation (212-215). The assumption has been that this recovery problem is secondary to the severe muscle atrophy following chronic denervation (216). However, more recently this idea has begun to be revised, to incorporate the changes that occur in both chronically denervated axons and intramuscular Schwann cell sheaths. Regeneration of muscle fibres from satellite cells has shown that it is possible to maintain a normal number for as long as ten months post denervation (217,218). Bagust has shown that the number of axons crossing a fresh nerve repair is approximately 50% (219). If the repair is delayed this number falls to 35% by three months, and then remains stable for at least a year. The axons that do make connections (in this case to a freshly denervated muscle) are able to increase their motor unit size threefold, so that the functional recovery is complete (220). This corresponds to the four to six fold increase in sprouting ability seen in uninjured axons expanding to occupy partially denervated muscles (221,222). However there is some evidence to suggest that whilst motor units two to four times larger than normal are stable, those four to six times are less so (222-225). Muscles that have been denervated for more than six months and reinnervated by freshly cut nerves do not recover as well. The returning axons still increase their motor unit size threefold but the number of motor units fell by 85%. This corresponds to fewer than 50% of the original muscle fibres being reinnervated (226). Interestingly this result was replicated with no delay by suturing the nerve directly to the muscle instead of to the distal nerve stump. Fu, in a rat model, suggests that this is evidence that poor reinnervation is due to the deterioration within the intramuscular nerve sheaths, as a result of either reduced numbers of Schwann cells secondary to poor trophic support, fragmentation of the basal lamina, or collagenisation of the endoneurial tubes. Rich has shown in mice that following nerve crush reinnervating axons accurately reoccupy old junction sites, and that new junctions are almost never established (227). Kang has shown in mice that the non-myelinating terminal Schwann cell that covers the neuromuscular junction, is involved in guiding axons back to vacant junctions (228). If the intramuscular sheath system deteriorated this would reduced the number of axons that manage to make connections with the original junctions.

The patterns of nerve regeneration in muscle are dependent on the nature of the injury to the nerve. Nguyen, in mice, has shown that after nerve crush there is an extraordinary degree of accuracy of reinnervation with axons not only reoccupying their previous junctions but even repeating their original branching patterns. After axotomy this situation is reversed with almost total loss of the original connectome (103,229). Brushart, in a mouse model, noted that after even individual fasicular division and repair, retrograde labeling of the dorsal horn nuclei showed more diffuse staining than the tight segregation seen in controls (92). In the case of full axotomy this effect was compounded (230-232). If there are multiple possible targets for a regenerating axon this confusion is reinforced. Cutaneous sensory axons that do not reach the skin cannot provide useful information, and motor axons that do not reach muscles cannot induce contractions. Regenerating branches that arrive at different muscles will produce synkinesis. There is an extensive literature on factors that might influence axons to preferentially reinnervate motor branches over sensory ones (93,94,233-238). There remains some uncertainty as to whether this occurs at all, or is a feature of subsequent axon pruning as mentioned above, that helps to restore the connectivity patterns (94,97,194,200,201,239). This may be an evolutionary advantage of collateral branching as the wiring can only be revised when there are connections made to 'good' and 'bad' targets. A motor neuron that only makes a cutaneous contact receives no trophic support and is unable to improve its situation (94).

1.9 Changes at the neuromuscular junction after denervation.

Neuromuscular junctions in the neonatal period evolve from a plaque-like structure into the familiar pretzel shape during the process of synapse elimination. This is intricately associated with the conversion from poly to single innervation. Asynchronous stimulation from multiple axons elicits a loss in postsynaptic receptor density, which precedes the withdrawal of the overlying axon (197,240). As this progresses the plaque perforates and forms, resulting in the mature receptor morphology (201,241). These are relatively stable, enlarging uniformly with age through intercalary growth (242). After denervation there is total loss of the presynaptic signal. This total inactivity doesn't result in immediate receptor disassembly, and junctions are lost gradually with the normal turnover of receptor sites in a process that can take several weeks (201). In reinnervated junctions Kang has shown that receptor areas that are no longer covered by the processes of terminal Schwann cells disappear (243). The area of receptor loss was increased with a delay in reinnervation after a double nerve crush. He has suggested that this may be akin to the mechanism of asynchronous receptor loss described by Rich. Areas of permanent receptor loss were seen where there was competition between axons at reinnervated junctions (197). Once the junction has become singly innervated, the areas of the receptor that were eliminated remained unoccupied, and new acetylcholine receptors were not inserted. These changes after reinnervation may resemble the characteristic changes that occur at the neuromuscular junction associated with senescence. There is often partial dissociation of the synaptic terminal from the receptor site leaving it partially innervated. In other cases there is a return to the polyinnervation of the neonatal period. The axon can become irregular, either very thin, or bulbous and varicose. The receptor area can become fragmented and break up into islands (5). These changes could represent a decreased efficiency of the neuromuscular junction.

1.10 Green fluorescent protein

In 2008 Chalfie, Tsien and Shimomura were awarded the Nobel prize in chemistry for the discovery and development of green fluorescent protein (GFP). It was Shimomura's painstaking work on the *Aequorea victoria* jellyfish that unraveled how it produced its bioluminescence through two proteins rather than the luciferin/luciferase pathway used by most other bioluminescent organisms. The first protein was a calcium binding protein, *aequorin,* that emitted a bluish light. The second absorbed that blue light and emitted a greenish one resulting in the moniker: green fluorescent protein, GFP (244). The gene for GFP was then sequenced by Prasher and subsequently inserted into the touch receptor neurons of *Caenorhabditis elegans* by Chalfie (245,246). Hazelrigg, Chalfie's wife, manufactured a fusion protein which allowed GFP to be expressed and functionally replace an original protein, paving the way for GFP to act as a label for particular cells expressing that protein (247). Tsien expanded the spectrum of GFP to produce a range of fluorescent proteins emitting wavelengths from 440nm to 648nm (248) (for review see (249)). GFP is a protein that requires no co-factors to render a cell fluorescent, and results in a label that is non-toxic and stable both in live tissue and after fixation. It has no impact on normal developmental or ageing changes and is still present in axons that have been injured and subsequently regenerate. By fusing it to particular proteins it can be used to label specific subgroups of cells (250). Combining GFP with the thy-1 gene promoter created transgenic mice where the GFP is expressed in several neuronal types but almost not at all outside the nervous system. The transgene is inserted randomly into the chromosome which generates large variation between lines in the cell subtype and proportion of axons where GFP is expressed. However there is minimal inherited change once the expression is established giving stable transgenic lines. This, and the use of spectral variants of GFP, has provided a number of tools to study nerves (250). Lines can be generated that express GFP in all axons (YFP-16), or a few as 5-10% (YFP-H), akin to the sparse silver staining of Cajal and Golgi. Combined with more traditional labeling of neuromuscular junctions with bungarotoxin conjugated to alexa-fluorphores it is possible to build up a picture of the entire nerve-muscle complex that can be studied both *in vivo* and *in vitro*. Single motor units can be mapped as opposed to inferred (251,252). By mixing lines it is possible to generate lines in which axons of more than one colour are expressed in a single nerve. As such the behaviour of a single axon can be picked out against all of its neighbours, or two motor units can be labeled and their interactions observed (253,254). Nguyen has used YFP-H mice to investigate patterns of reinnervation after nerve crush (103). Here I have used the same approach, but adapted it to a model mimicking facial palsy to examine the changes occurring in a nerve-muscle complex after nerve repair and nerve graft.

1.11 Hypotheses.

The aim of this study is to get an overview of the changes taking place across the entire neuromuscular system in the context of reinnervation. I wanted to follow a regenerating axon from the proximal stump, through a nerve repair or graft, right into the muscle to the junction.

To do this I have used two lines of transgenic mice that express yellow fluorescent protein in their axons: YFP-16 expresses in all axons, the YFP-H in approximately 5-10%. The YFP-16 allowed me to study the overall reinnervation patterns of the whole muscle. The YFP-H mice are more akin to the silver staining used by Cajal, enabling me to see the regenerating pathways of just a few axons, without the background noise of the entire nerve.

Cross sections of the axons at proximal and distal sites in the terminal branch to the muscle provided data on the number of axons, the amount of branching, and their caliber. Antibody staining reiterated the proportion of these axons that were myelinated.

Labeling neuromuscular junctions with alexa-594-bungarotoxin illustrated the number of junctions that were reoccupied by the regenerating axons as well as any changes in the morphology of the junctions.

The first null hypothesis is that there is no difference in the pattern of neuromuscular innervation between a control muscle and a muscle that has been reinnervated after a complete division of the nerve and restoration of continuity.

The second null hypothesis is that there is no difference in the pattern of neuromuscular innervation whether that restoration of continuity occurred through a nerve repair or a nerve graft.

Both of these hypotheses are broken down to focus on specific markers of reinnervation:

a) the reoccupied neuromuscular junctions

b) the regenerating axons

c) the reinnervated motor units

2. Methodology

2.1 Transgenic Mice

All experiments were performed in transgenic mice originally produced in the Lichtman laboratory at Harvard University. The genetic lines are maintained internally by individual researchers and pure colonies by a technician. The genetic lines are available through Jackson Laboratories (Jackson Laboratories, Bar Harbor, Maine, USA). All surgeries took place with both National Institues of Health (NIH) and Institutional Animal Care and Use Committee (IACUC, USA) approval. These ethical standards are equivalent to standards set out by the Animal Welfare and Ethical Review Body (AWERB) under the Animals (Scientific Procedures) Act, UK.

YFP-16 is a line that expresses yellow fluorescent protein in all axons in both sensory and motor nerves (255). These animals were used to study the reoccupation of neuromuscular junctions and regenerating axonal load.

YFP-H is a line that expresses yellow fluorescent protein in approximately 5-10% of axons in each nerve (255). These animals were used to look at branching patterns within the regenerating nerve.

2.2 Interscutularis

The interscutularis is a superficial muscle that crosses the parietal skull and connects the cartilaginous base of the ears. It is encased in loose connective tissue and embryologically derived from the *panniculus carnosus* so it has no bony connection, in keeping with the muscles of facial expression in humans. In the midline there is no definitive aponeurosis and the muscle fibres of each side interweave directly (Fig 3).

The interscutularis is innervated by a branch of the posterior auricular nerve (PAN), itself a branch of the facial nerve. The facial nerve exits the stylomastoid foramen of the skull caudal to the base of the ear. The nerve passes cephaladad and immediately divides into two main trunks, one passing ventrally under the ear to become the five branches to the face, the other passing dorsally as the posterior auricular branch (Fig 4). This travels deep to the parotid and a fat pad between the mastoid process and the external ear (3).

The PAN divides into 4 or 5 main branches before it arrives at the posterior surface of the conchal bowl. These run parallel to each other in close proximity to the cartilage of the posterior auricle and supply the superficial muscles of the dorsal neck and head (levator auris longus, interscutularis, auriculolabialis, cervical platysma).

Figure 3.

The interscutularis muscle

Anatomical drawing of the anatomy of the interscutularis muscle in a rat. Anatomically the rat and the mouse are identical in this regard. There are no anatomical atlases of the mouse that show this degree of detail. (3)

Figure 4.

The facial nerve in the rat

Anatomical drawing illustrating the course and branches of the facial nerve in the rat (3). There is no equivalent anatomical atlas showing this degree of detail in a mouse, but the anatomy is very similar between the species in this regard.

2.3 Pilot studies (various XFP lines)

10 animals were used to explore the dynamics of nerve repair and nerve graft. Initially (n=5) this followed a protocol previously used in the Lichtman laboratory focused on the sternomastoid and cleidomastoid muscles (103).

Anatomical studies were performed to develop the surgical approach to the interscutularis and posterior auricular nerves. It was essential that the operation to carry out the nerve division, repair or graft should not violate the tissues around the muscle and induce scarring. It was also necessary for the nerve to be accessed at a location where its calibre was large enough to facilitate neurorraphy.

In the pilot methodology for this study we planned to use the contralateral muscle as a control in each specimen. The interscutularis muscle inserts laterally into the cartilage of the ear on its superior and posterior aspect. In the midline its fibres interweave with the muscle from the other side. There is no bony attachment and the muscles are separated from the skull on their deep surface, and the platysma superficially by layers of loose connective tissue. This allows the muscle complex to slide freely over the skull as the ear moves cranially or caudally. It also means that the insertion of the muscle into the ear on one side acts as the anchor point for the action of the muscle on the opposing side. The effect of a contraction on one side can therefore be transferred across the midline. There are very few muscles (the orbicularis orii and the anal sphincter, for example) that have this kind of action across the midline of the anatomy. In pilot studies it was apparent that there was significant variation in the number of neuromuscular junctions between specimens. There was no evidence for right or left dominance (p=0.4, see figure 17) but the variability within each individual (p=0.01, see figure 18) was sufficient to make comparisons between them invalid. This made the use of the contralateral interscutularis from each specimen as a control impractical. A separate cohort of specimens where no interventions had been performed, matched for age and weight, were used as a control group.

All animals in the anatomical pilot studies came from a pool of adult mice of various fluorophore lines (Green FP, Cyan FP, Yellow FP) that were otherwise allocated for euthanasia.

In honing the methodology for this study we explored several other avenues that were eventually excluded.

The use of native fluoroescent protein expression to identify structures *in vivo* is a new and powerful technique to understand biological events. In this study we have used YFP to focus on regenerating axons in the facial nerve. However, XFP technology has expanded in its scope significantly since Chalfie first managed to splice it into the genome of the *C.elegans*. Lichtman has been working on exciting variants such as the Brainbow mouse where multiple fluorophore colours are inserted into the genome and each gene is turned on randomly. This generates a palate of colours and allows each axon in a nerve to have a different hue [Livet 2007]. We attempted to use the technique of multiple fluorescent labeling within our methodology to answer two questions. Firstly we attempted to use a double transgenic CHAT Cre:Thy 1 mouse to identify exclusively motor axons. In these animals the YFP gene would only be expressed in axons that produced actylcholine and therefore would preferentially label motor axons over sensory ones. Secondly we attempted to produce a line of S100 CFP:Thy 1 YFPdouble transgenics. In these animals we hoped to label the schwann cells with one colour of fluorescent protein (cyan) and the axons with another colour (yellow). This would negate the need for separate immunohistochemical labeling of the myelin. Unfortunately, both these lines proved to suffer with very poor fertility. We only managed to breed very small numbers, insufficient for any experimental groups.

Measures of functional outcome, such as toe spreading, have been described when investigating functional outcomes in the hind limbs. There is no such outcome measure with respect to the ear. We tried to develop a technique to assess ear movements using video of a number of white dots of paint on the rim of the ear. The theory was that we could measure the range and scope of movement in the normal ear and the denervated ear and compare the quality of the muscle reinnervation. This proved technically impossible. We could not reliably get standardised video footage of the mice. We couldn't keep the animal in a standarised position with some degree of anaesthesia which then affected ear movement. When footage was achieved it proved too complex to define a "normal" range of ear movement, let alone quantify the change seen in reinnervated muscles.

One of the main aims of this study was to investigate changes in motor unit size. A compromise of the study design is that by examining the terminal nerve to the muscle we were unable to say with certainty that there have not been axonal branches prior to the proximal sampling point. An alternative method of assessing the number of individual axons reinnervating the muscle would be to perform retrograde labelling. This would label the cell bodies of the axons that had made connections with the muscle, independently of how many branches they had made as they regenerated. We set up a pilot study to look at this. I supervised an undergraduate student (K Lee) who performed this work as her final year neurobiology extended project. Unfortunately the location of the facial nerve nucleus within the brain stem, and thus within the skull, complicated this experiment. Results were inconsistent in control animals, and even more difficult to interpret in experimental animals and we ultimately abandoned the technique.

2.4 YFP-16

YFP-16 animals were divided into four groups:

One control group:	pure controls with no intervention (N), n=9
Three experimental groups:	unilateral nerve repair (R), n=27
	unilateral nerve graft (G), n=27
	unilateral nerve cut (C), n=18

R, G and C groups were equally subdivided into 3 time intervals (Table 2).

Table 2.

YFP-16 specimen distribution.

Group/Time	Controls (N)	Cut (C)	Repair (R)	Graft (G)
4 weeks	6	6	9	9
6 weeks	-	6	9	9
12 weeks	3	6	9	9

2.5 YFP-H

In the YFP-16 line we were looking for changes in the axon and NMJ populations during regeneration after nerve injury. The YFP-H line has sparse expression of the fluorescent protein so only 5-10% of axons are labeled. This is akin to the silver staining used by Cajal and Golgi which enabled single axons to be identified from the background noise of the entire nerve (106). The YFP-H was used to examine branching patterns after the nerve has reconnected to the muscle. Once axons have undergone remodeling unsuccessful axons are pruned and only the successful axons remain. The routes and branches that occurred during the process of reinnervation are preserved and represent a record of the axon regeneration process.

YFP-H animals were allocated to the same experimental groups as the YFP-16 animals. However all Cut, Repair and Graft specimens were harvested at twelve weeks post-intervention (Table 3). This allowed for the process of reinnervation and remodeling to occur, giving a route map of the progress the successful axons took. In the Cut group only the neuromas on the cut side were harvested for analysis.

Table 3.

YFP-H specimen distribution between the control and experimental groups

Group/Time	Controls (N)	Cut (C)	Repair (R)	Graft (G)
4 weeks	1	0	0	0
6 weeks	0	0	0	0
12 weeks	3	3	5	2

2.6 *Surgical protocols*

All surgery took place in adult mice of either sex between seven and eight weeks of age under NIH guidelines and an animal protocol approved by Harvard University Animal Studies Committee and the Standing Committee on the Use of Animals in Research and Teaching (IACUC, USA). Animals were anaesthetised using a standard mixture of Ketamine:Xyalazine (KX 17.38mg/ Lloyd Inc, Shenandoah, Iowa, USA) at 0.1ml/20g body weight. Deep sedation was verified using a standard foot pinch test. All surgeries took place in a warm, clean room using a Leica fluorescent operating microscope (Leica MZ 16FA, Leica Microsystems GmbH, Wetzlar, Germany). In transgenic animals this can greatly assist in accurate identification and dissection of relevant structures. With fluorescent illumination the nerves of YFP mice are easily visible as green/yellow against the background tissue (Fig 5). Animals were placed on gauze on a metal operating plate and retraction was performed with custom made retractors fitted to magnetic stands.

Anaesthetised animals were placed in a right lateral position and the right lateral neck was depilated (Nair, Church and Dwight Inc, Princeton, NJ, USA) and the skin prepped with 70% alcohol solution. An incision was made caudal and parallel to the conchal bowl exposing the fat pad and the parotid gland.

The tissue was blunt dissected away from the auricle taking care not to disrupt the posterior facial vessels, which were retracted ventrally. A branch of the cutaneous sensory nerve to the skin of the neck was encountered superficial to the parotid, running in the same vector as the

Figure 5.

Intraoperative photographs of the posterior auricular nerve (PAN) in a mouse

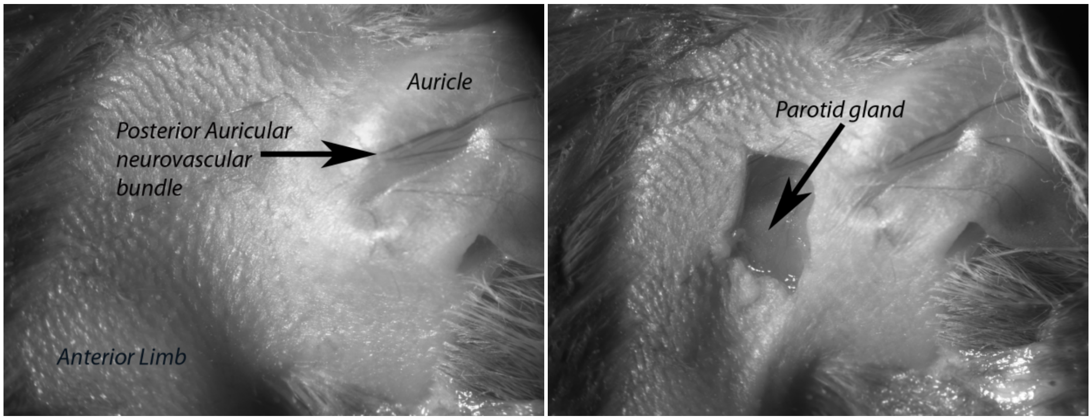

The image on the left shows the animal in the right lateral position with the ear folded forward and the operating area depilated. On the right the skin incision has been made exposing the parotid gland.

Figure 6.

Intraoperative photographs of the surgical approach to the PAN in a mouse

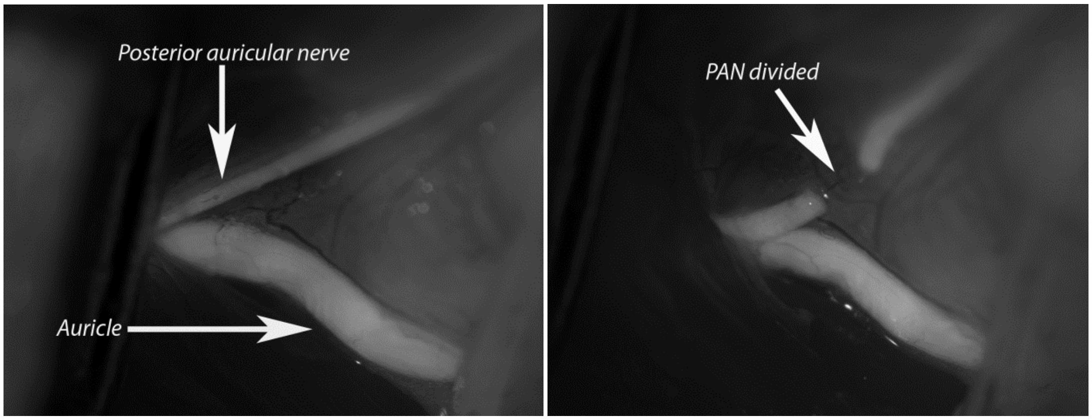

In the image on the left the fluorescent nerves are highlighted against the background tissue under the fluorescent dissecting microscope. The posterior auricular nerve has been divided in the image on the right.

cranial nerve. Since the dissection was carried out cephaladad to the parotid through a small incision care must be taken not to mistake this for the PAN. In YFP animals this nerve is often less intensely labeled with fluorophore. The branches of the PAN can be seen arising deep in the neck medial to the parotid gland, which must be retracted, and clearly coursing onto the posterior aspect of the concha. By following the terminal nerve branches caudally they can be seen to coalesce and run as a single nerve in the lateral neck towards the skull. This is where the nerve is large enough to effect a repair or graft.

Animals were divided into 3 surgical groups:

a) In the nerve cut group (C) the nerve was divided and the wound was closed (Fig 6). It was noted that in some of the animals in the twelve week nerve cut group a degree of reinnervation of the distal nerve was observed. Examining the site of nerve division a large neuroma was evident (Fig 7). Some axons had crossed the division site and where the axons had encountered the distal stump they reorganized and fasiculated. As a result the method was adapted to make the control more robust. The nerve was still divided but more distally and the proximal stump was mobilized sufficiently to bring it superficial to the parotid, thus interposing the gland between the two cut ends of the nerve.

b) In the nerve repair group (R) the nerve stumps were approximated with a single 11/0 nylon suture (S&T AG, Neuhausen, Switzerland) through the epineurium. This provided adequate approximation of the cut ends (Fig 8). More than one suture frayed the fascicles like a

Figure 7.

Two photon microscope montage of a neuroma in a nerve cut mouse (pilot methodology)

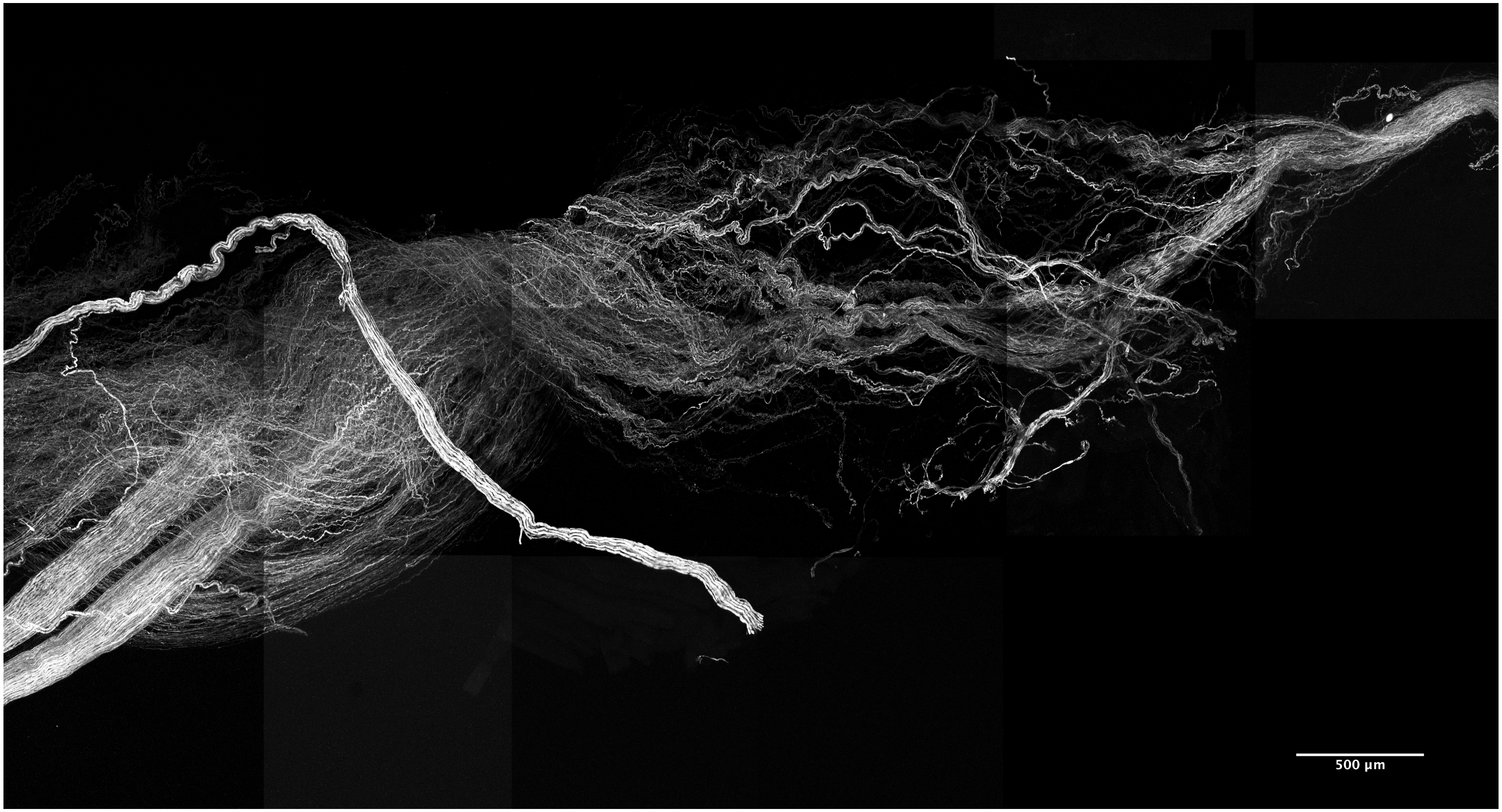

This image shows a neuroma in continuity in a nerve cut specimen, twelve weeks after the intervention (original protocol). The axons form a helical structure as they “seek” the distal stumps. Once the axons have reached the distal stumps (top right) they again assume a tight fasciculated bundle.

Figure 8.

Intraoperative photographs of a surgical repair in a mouse

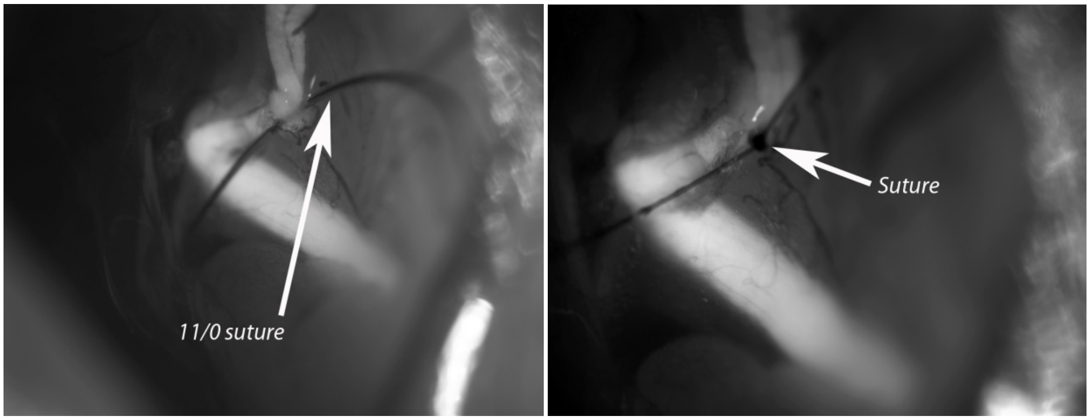

Here the divided stumps of the posterior auricular nerve have been opposed with a single nylon 11/0 suture.

horse tail, leaving the nerve ends more disrupted than with no sutures at all. The parotid gland was then repositioned over the repair and the wound closed.

c) In the nerve graft group a section of the saphenous nerve was harvested before the exposure of the muscles in the neck. With the animal supine the ventral hind leg was depilated and prepped with 70% alcohol. A longitudinal incision exposed the ventral neurovascular bundle (Fig 9).

The saphenous nerve was dissected away from the adjacent blood vessels and divided proximally. A single 11/0 suture was placed in the distal stump (outside to inside) and left untied. The distal nerve was then divided so that 5mm of graft could be removed suspended on this suture and placed in Ringer's lactate solution [manufacturer] until the neck was prepared. This prevents the graft from drying out. The wound in the leg was closed.

Once the nerve in the neck had been exposed and divided the graft was reversed and placed in situ in the space the gap between the nerve ends. The suture in the graft was then passed through the proximal nerve stump (inside to outside) and secured. A second suture was placed between the distal end of the graft and the distal nerve stump (Fig 10). Finally the parotid gland was repositioned and the wound closed. This added 5mm to the length of the distal nerve in the grafted group, increasing the distance axons had to regenerate to reinnervate the muscle. This does potentially affect our ability to compare the repair and graft groups at the three time points as the distances are not equivalent. Given the very small length of PAN in the lateral neck before it starts to branch into multiple terminal nerves, this was unavoidable. We decided that it was acceptable given the speed with which the nerves had regenerated after nerve repair or graft in the pilot studies.

All skin wounds were closed with 6/0 nylon sutures (Ref: 911B, Angiotech, Reading, Pennsylvania, USA) and the animals revived with Antisedan (atipamezole hydrochloride 0.25 mg/ml, Pfizer, New York, USA). Two doses of buprenorphine (0.08 mg/ml, PharmaForce Inc. Hilliard, Ohio, USA) were given in the first twenty four hours post surgery and the animals monitored for four days as per the Harvard University protocol approved by the Standing Committee on the Use of Animals in Research and Teaching (IACUC, USA).

Figure 9.

Intraoperative photographs (mouse) and anatomical drawings (rat) of the nerve graft donor site

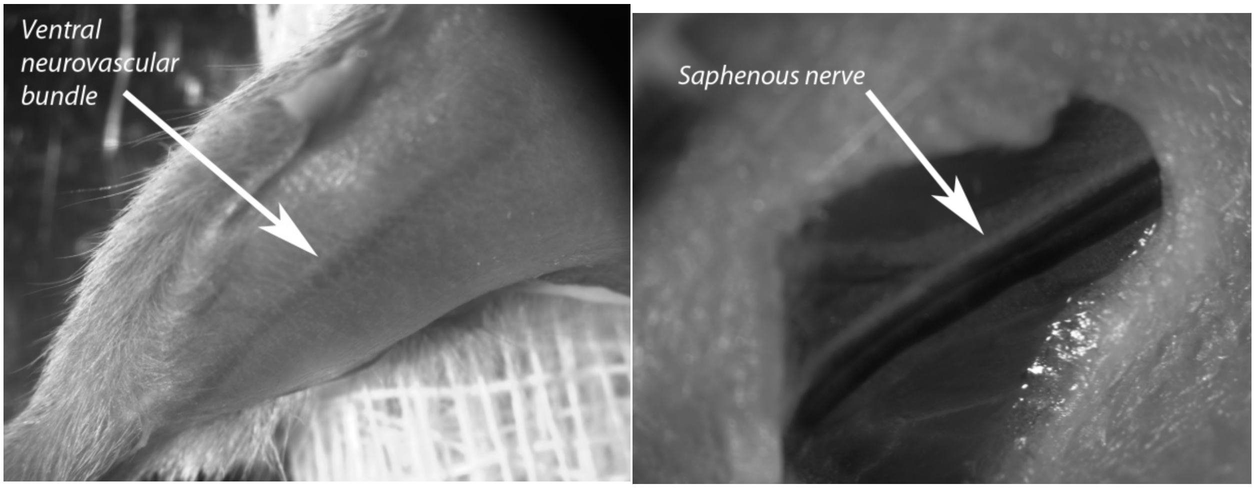

In the surgical images above an incision in the ventral lower limb exposes the neurovascular bundle in a mouse. Below is an anatomical drawing illustrating the saphenous nerve in a rat, which was used as the donor nerve graft (3).

Figure 10.

Intraoperative photographs of a nerve graft in a mouse

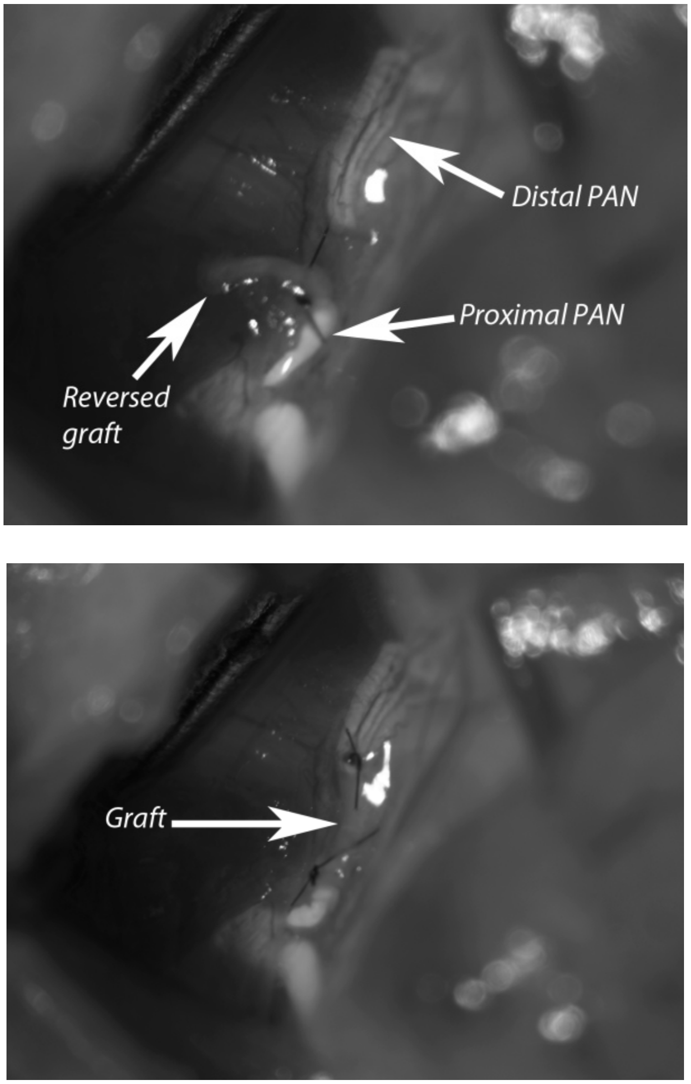

A section of saphenous nerve is secured by an 11/0 nylon suture to the proximal stump of the posterior auricular nerve. It is then sutured to the distal stump to bridge the defect as a nerve graft.

2.7 *Perfusion and specimen harvest*

At the time of euthanasia animals were sedated with sodium thiopental at 5mg/20g body weight. The ventral thorax was depilated with Nair (Church and Wight Co. Inc., Princeton, New Jersey, USA) and prepped with 70% alcohol. Incisions were made from the xiphisternum along both sides of the thorax in the mid lateral line to expose and divide the ribs in a shield shape. This provided access to the medastinum and heart. A cut was made in the right ventricle to allow blood to vent. A 5ml syringe of ice cold Ringer's lactate was slowly perfused through a 30 gauge needle to empty the vascular system of blood. This was then repeated with 5mls of ice cold 4% paraformaldehyde (PFA) in 4% phosphate buffered solution (PBS).

The skin of the dorsal neck and head was then depilated and prepped as before and a sagittal incision made in the dorsal head and neck that could be extended laterally caudal to the ears. The entire right and left interscutularis muscles were harvested *en bloc* with attached nerves back to the point of entry with the skull. In all intervention groups the contralateral muscles and nerves acted as an additional control. They were harvested in the same way as the intervention side simultaneously and put through the same immunohistochemical protocols. In the interscutularis the two sides of the muscle are contiguous, the central fibres interwoven without an aponeurosis, allowing the entire construct to be removed *en bloc* as a single tissue complex.

The muscle-nerve complex was post-fixed in 4% paraformaldehyde (PFA) for 30 minutes on a rocking platform protected from light and then washed twice in phosphate buffered saline (PBS) for a total of 60 minutes. The complex was then manually cleared of excess fat and connective tissue in a 4% PBS bath before being put through immunohistochemical protocols.

The complex was incubated in bungarotoxin (5µg/ml Invitrogen Corp., Carlsbad, CA, USA) for 30 minutes on a rocking platform protected from light. Alexa 594 bungarotoxin was used for all YFP mice unless otherwise stated. The tissue was then washed twice in 4% PBS for 60 minutes total. Finally the tissue complex was immersed overnight in Vectashield (Vector Laboratories Inc., CA, USA). Vectashield is glycerol-based and partially dehydrates the muscle, replacing some of the water within the tissue, though sufficient water remains to allow the fluorophores to function. The glycerol changes the refraction index of the tissue to bring it into line with the slide cover slip and also increases the transparency of the muscle fibres which improves the imaging on intramuscular structures such as the neuromuscular junctions.

The tissue complex was finally mounted on glass slides using Vectashield as a mounting medium. It is optically clear and has both anti-fading and anti-bleaching properties reducing the loss of signal from fluorescent proteins during laser imaging. Care was taken to make sure that muscle was unraveled and as flat as possible with the nerve arranged orthogonally to the muscle in imitation of the natural *in vivo* scenario. The bilateral interscutularis/nerve complex could be mounted on a single slide. This measure enabled the nerve to be traced back to the repair or graft during imaging which ensured that the correct side of the muscle was identified in each case. In addition, during imaging, the proximal (intervention) and distal (muscle) ends of the nerve could be reliably identified.

Glass cover slips of 1.0mm thickness were used, to reduce optical refraction during imaging. Magnets were placed on top of the glass cover slips for 20 minutes to compress the muscle and provide a flatter specimen for imaging. The cover slip was then sealed with nail varnish and stored at -20ºC.

2.8 *Myelin labeling*

The natural fluorescence in YFP-16 and YFP-H animals only labels the axoplasm of the nerves. To identify the presence of a myelin sheath required an immunohistochemistry approach. Myelin Basic Protein was labeled according to the following protocol:

- Forty eight hours in a starting block of 1% Triton X-100 (Sigma-Aldrich, St Louis, USA), 4% bovine serum albumin (BSA) , 5% normal goat serum and 0.1% sodium azide.
- Three days in the primary antibody in fresh starting block (1:400), Rabbit-anti-Human Myelin Basic Protein (AbD setotec, Morphosys UK Ltd, Oxford, UK)
- Three hours wash in PBS
- Twenty four hours in secondary antibodies (1:500), 594 Goat-anti-Rabbit (AbD serotec, Oxford, UK)
- Three hours wash in PBS

Samples were then remounted on glass slides in Vectashield (*vide supra).*

2.9 Image Capture

Confocal microscopy

Samples were imaged on a confocal microscope (Olympus FV-1000MPE) using a 20X oil immersion optical objective (1.35 Å, 0.8 NA) and excited by 488nm and 568nm lasers through a dichroic mirror (440/488/568/633 nm). Emission light was divided into two channels. The first by a dichroic mirror at 560nm and then through a filter at 505-550 nm, the second by a mirror and then a filter at 575-675nm. Channels were sampled sequentially with twice Kalman sampling. Scan speed, laser power, gain and offset were all optimised for resolution with minimal bleaching. Images were captured at 1024 by 1024 pixels which corresponds to an image size of 635.283μm^2.

The intervention and control sides of the muscle were imaged in one session as a series of stacks using the montage settings of the Olympus software. Each stack was independently arranged to encompass the upper and lower limits of the axons and neuromuscular junctions at a slice thickness of 0.70μm.

Montages were taken in a single channel (488nm laser) at 20X (1.35 Å, 0.8 NA) of the nerve from the point of repair through to the point of entry into the muscle. This was done in both YFP-16 and YFP-H animals.

Myelin antibody labeling was imaged on the same microscope using a 60x oil immersion objective (1.35 NA). The same laser lines and dichroic filters were employed as described above. Z slice thickness was set at 0.37µm to ensure over-sampling and maximum resolution.

Two photon microscopy

To obtain images of axons with a high enough resolution in 'Z' samples were imaged using a two photon microscope (Zeiss, 710 NLO, Axio Examiner microscope). Stacks were taken of the proximal and distal ends of the terminal branch of the PAN to the interscutularis for both intervention and control samples. A 950nm excitation laser was used through a dichroic filter. The emission light was streamed through a 525-560nm filter. Images were taken using a 63x oil immersion optical lens (1.45 NA) with a slice thickness of 0.38µm to acquire maximum Z resolution. Scan speed, laser power, gain and offset were all optimised for resolution even at the expense of some bleaching. Images were captured at 828 by 828 pixels, which corresponds to an image size of 134.79µm^2.

2.10 Image processing

Neuromuscular junctions

Each confocal stack was opened in ImageJ (256). Each channel was then assigned an appropriate colour: nerves green and neuromuscular junctions red (*Image*; *Color*; *Channels Tool*: Select *color* from drop down: Assign colours to each channel: Select *composite* from dropdown). A *maximum intensity* projection was then generated (*Stacks*; *z-project*: *maximum intensity*) and saved as a tiff file. All the *maximum intensity* tiff files for a given muscle's montage were then stitched together in Adobe Photoshop CS5.1 (Adobe Systems Inc., CA, USA) to create a single montage of the entire neuronal arbor. Each image (now a *layer*) was adjusted for gamma in red and green to standardise the background across the whole montage.

The junctions were counted and measured in ImageJ from the stitched montage with the *Region of Interest* tool (*Analyze; Tools; ROI manager*) using a tracing tablet and stylus (Wacom Cintix 12WX, Wacom Co, Ltd, Vancouver, WA, USA). At 150% zoom the circumference of each NMJ was traced with the *freehand selection* tool and the outline adjusted to an ellipse (*Edit; Selection; Fit Ellipse*). This was measured (*Add*. nb: the *Show all* box of the *ROI manager* should be ticked to prevent double counting). Once all the junctions have been measured the data can be collated (*ROI manager; measure*) and the results copied to an Excel (Microsoft Office 7 Professional) spreadsheet. This provides both a numerical count of all the junctions, and measures their cross sectional areas (Fig 11).

Figure 11.

Region of Interest (ROI) tool to count and measure the number and area of neuromuscular junctions

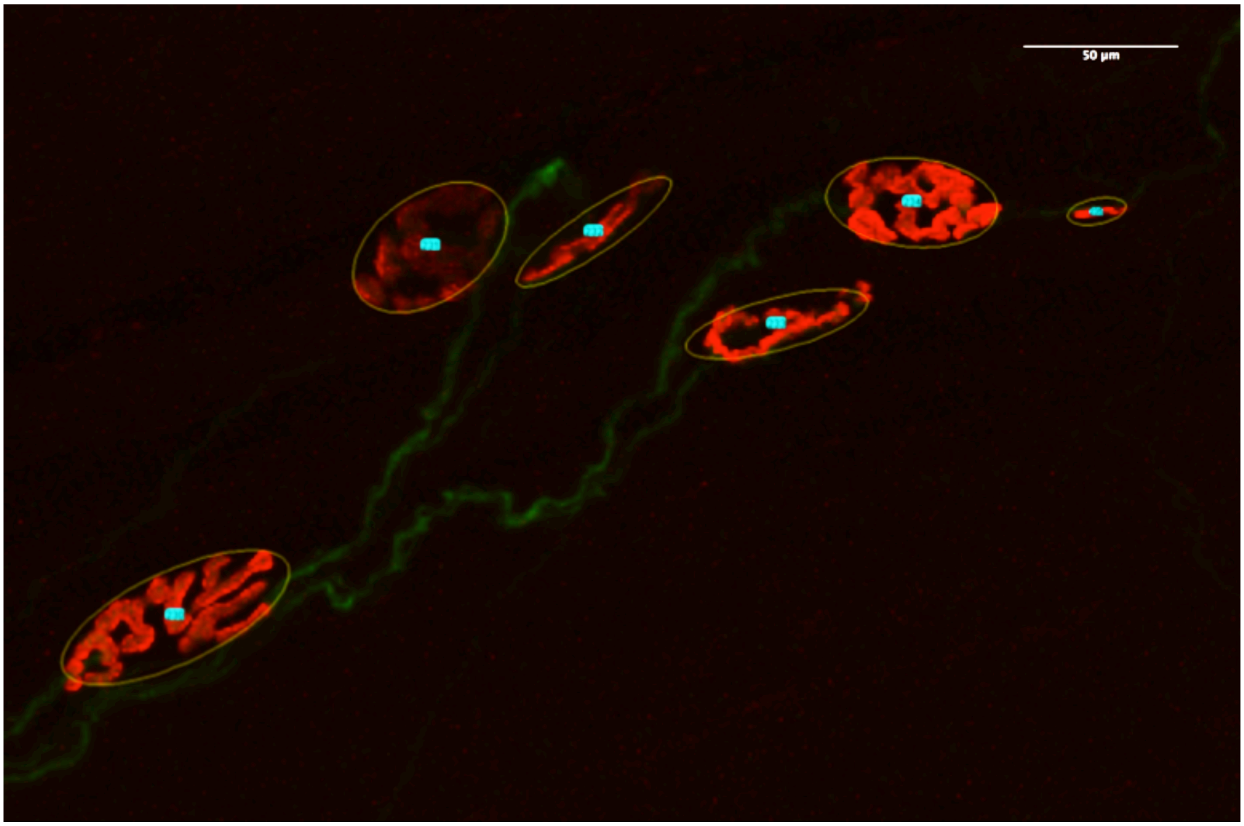

Counting of neuromuscular junctions that are double-labeled with alpha-bungarotoxin and YFP fluorophore using the ROI tool which avoids errors through double counting. Each junction is numbered, and then encircled using an ellipse tool to estimate cross sectional area.

Axonal load

Each terminal nerve to interscutularis was sampled at two points: its most proximal and distal extent. Each two photon stack was opened in ImageJ. The stack was scrolled through to locate an area where the nerve was most clearly resolved and ran straight. A line was drawn orthogonal to this area using the *line* tool and a perpendicular stack created (*Stack; Reslice*) of 100 slices. This gave a digital reconstruction of 100 cross sections at a separation of 0.38µm. This stack was saved as a NIFTI file.

The NIFTI file was opened in itk-SNAP (www.itksnap.org) and a 5 consecutive slice section selected for tracing (257). For tracing each axon was given a different designated colour (*Label editor*; *new*) and a single operator (A. Woollard) traced the outline of each axon in each slice. The tracing was performed using a Cintiq 12WX interactive tablet, as above. The axonal volume data (*Segmentation; Volumes and statistics*) was copied to an Excel file (Microsoft Office 7 Professional).

Myelin

Stacks were opened in ImageJ and translated as described above. In this case axons were assigned red and myelin green to improve clarity. Stacks were scrolled through in an XY plane and in Z as a *reslice* to ascertain the presence of a myelin sheath.

Axon branching

Axonal branching was analysed in two ways:

- measuring the change in axon number between proximal and distal cross sections in YFP-16 animals.

- tracing individual axons in YFP-H animals in a montage of the nerve. This was done in Adobe Photoshop CS5.1 (Adobe Systems Inc., CA, USA).

2.11 Statistics

Almost all the data sets were analysed using a two way ANOVA test. In addition paired T tests and one way ANOVA were used to analyse some the data in the control population. A number of statistical software programs were used: PRISM 6 (GraphPad Software Inc., La Jolla, CA, USA) and SigmaPlot (Systat Software Inc., San Jose, CA, USA), and SPSS (IBM, UK). Significance was set as a P value of less than 0.05.

All the data sets failed the Kolomoglov-Smirnoff test for normality. Khan and Mendes have shown that despite the lack of normality, a two way ANOVA was the most appropriate statistical test in this scenario (258-260). Tukey’s test was used for post hoc comparison of each variable to ascertain significance between time periods and between interventions.

3.

The normal pattern of innervation in the interscutularis muscle

3.1 Introduction

This study aims to model the scenario of facial reanimation where a functional muscle transfer is reinnervated by a terminal branch of the facial nerve through a nerve graft. The goal is to analyse the patterns of reinnervation in a muscle after nerve repair and nerve graft. Elucidating changes that occur in the nerve and the muscle and how they interact will provide information about the deficits encountered in clinical reinnervation scenarios.

To understand the deficits however, it is first necessary to characterize the relationship between nerve and muscle in an uninjured control. A requirement of the selected model is that the muscle be innervated by a cranial nerve, as Macquillan and colleagues demonstrated the peripheral and cranial nerves have different capabilities of reinnervation (261,262). The muscle selected for this study was the interscutularis in a mouse. This is a muscle on the dorsal aspect of the head that moves the ears and its neural arbor has previously been characterized in detail (263,264). The muscle is thin and flat making it possible to image the entire muscle and its neural arbor.

Interscutularis is innervated by a terminal branch of the posterior auricular nerve, itself a branch of the facial nerve. A further advantage is its anatomical location as it is possible to operate on the nerve in the lateral neck without disturbing the tissues around the muscle, therefore reducing scarring that may interfere with subsequent imaging.

After injury to a peripheral nerve there is a loss of function of the muscle-nerve complex. The distal nerve segment undergoes Wallerian degeneration (265). The proximal segment dies back to the last node of Ranvier. The glial Schwann cells dedifferentiate and convert to a form that supports axon growth through their empty Büngner's bands. Myelin sheaths disintegrate and the debris is phagocytosed. The absence of depolarizing supra threshold potentials at the neuromuscular junctions effectively leaves the muscle stranded with no stimuli. Unable to contract, the fibres atrophy and the receptor plaques are reabsorbed over time.

The proximal axons begin the process of regeneration by resuming their developmental state. Growth cones form and seek the distal stump endings to their target organ, in this case the muscle. The nature of the injury has an impact on the ability of axons to return to their appropriate distal course. Nguyen has shown that after a nerve crush the original configuration of branching is restored 93% of the time (103). If there has been a total axotomy with disruption of the proximal-distal continuity the accuracy of reinnervation is greatly reduced. The reoccupation of synapses by their original axons can be used as a marker for the accuracy of reinnervation. This dropped from over 90% in nerve crush to less than 5% after nerve cut (103). Two factors are often cited to contribute to the disruption: axon loss and axon misdirection. Some axons get stuck in the neuroma at the site of injury and fail to enter the distal stumps, not contributing to the reinnervation (Fig 12). Of the axons that do enter the distal stumps many are unlikely to enter their previous endoneurial tubes. This mismatch results in axons occupying different synapses on the target muscle and leading to a new branching pattern. Axons have several strategies to compensate for the reduced number that enter the distal tubes. Axons can divide extramuscularly to produce several branches. Intramuscularly axons can produce both collateral and terminal sprouts to occupy more synapses. It is thought each axon can effectively increase the size of its motor unit by a factor of between four to six (221,222). Subsequent remodeling can compensate for the abnormal wiring of the connectome through the pruning of inappropriate axon branches.

In clinical neurotomy scenarios a surgical nerve repair attempts to reduce the deficit of the injury. This secures the proximal and distal stumps in close approximation aiming to reduce the number of axons that escape the distal stump. There was a vogue for fasciular repair but this has not been shown to improve results, although alignment of motor and sensory anatomy in mixed nerves appears beneficial (266-268). Tension across a repair negatively effects nerve regeneration (269-271). If the gap between the two nerve stumps is too great to effect a repair without tension, bridging the gap with a graft improves the outcomes (272-274). To date autologous grafts have been shown to provide better results than other materials. Cadaveric allografts have recently shown some promise, especially since they avoid a donor site morbidity (275,276). The use of allograft requires immunosuppression but does offer the potential to graft using mixed sensory/motor nerves, which has shown to produce better results in muscle reinnervation than the purely sensory donors that autologous grafting is restricted to (277-279).

Figure 12.

Two photon microscope montage a neuroma in a nerve repair mouse

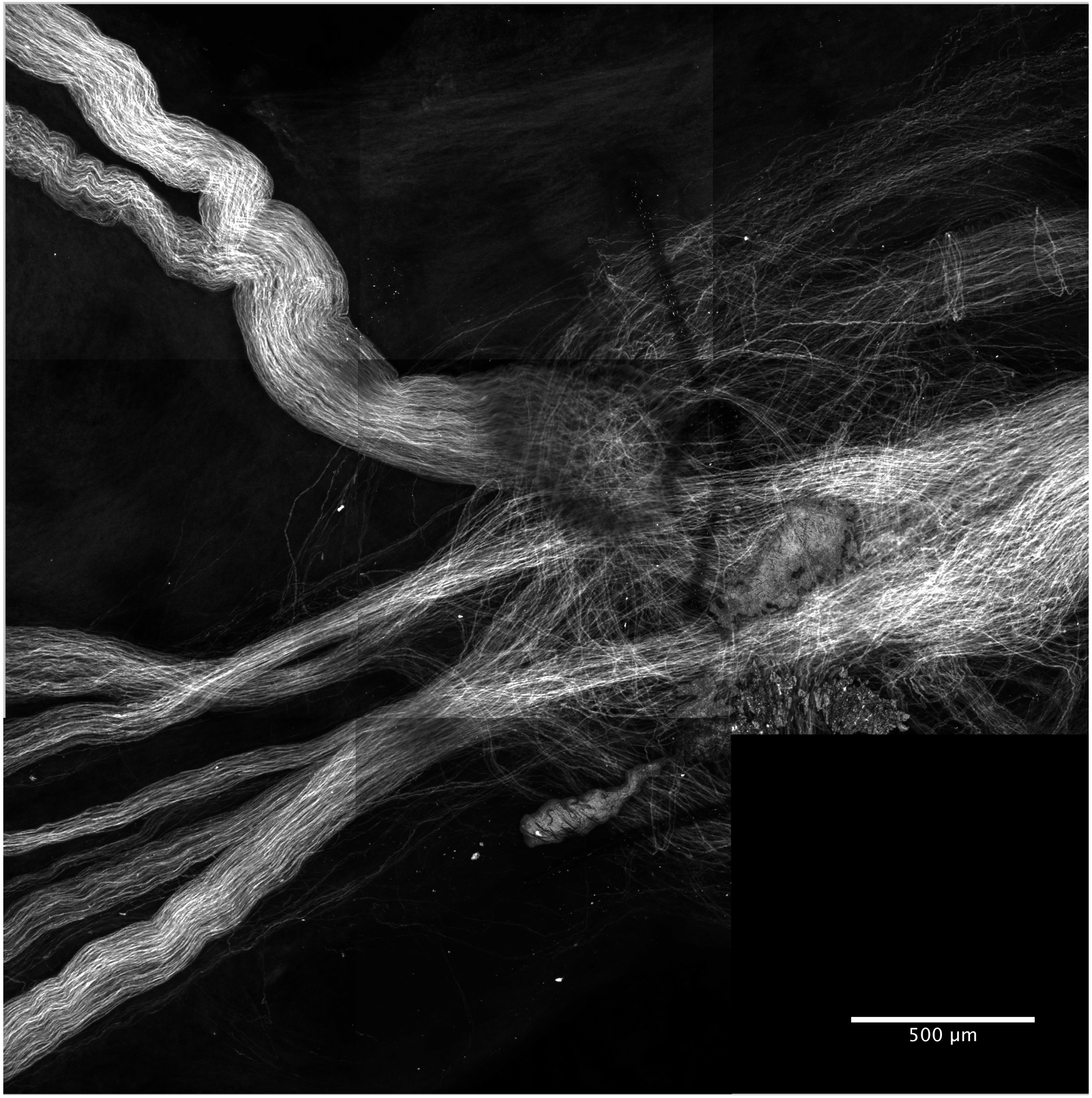

A neuroma forming at the site of a nerve repair. The shadow of the suture is visible. Fasciculated axons arrive in the donor nerve (right). There is apparent chaos at the site of repair and then order is restored as axons re-enter the distal stumps. Some axons do not navigate the site of injury and are misdirected into adjacent tissue (upper right).

Conduits demonstrate reasonable results in small defects (280). These are materials that provide a scaffold tube for the regenerating axons to cross the gap to the distal stump. They can be either biological such as arteries, veins and skeletal muscle, or synthetic such as silicone, polyglycolic acid polymer, polytetrafluoroethylene, collagen, poly-DL-lactide-caprolactone (281-285). These techniques are suitable for very small defects (280). However, any sort of graft introduces an extra repair site, as well as a non-vascularised segment of tissue, for regenerating axons to cross. Birch showed in clinical cases the regenerating axons sometimes crossed the first repair site but stopped advancing within the substance of the graft (272). In a traditional two-stage facial reanimation a graft is used to carry the axons of the facial nerve on the functioning side across the face to the paralysed side, a distance of 10-14cm. One of the aims of this study was to ascertain if there was a difference in the patterns of reinnervation of the muscle between nerve repairs and nerve grafts.

3.2 Methods

The main body of this study was conducted using YFP-16 mice that express the yellow fluorescent protein in all their peripheral axons. These mice were used to analyse the axons in the terminal nerve to the interscutularis. Digital cross sections were taken at the proximal and distal end of this nerve providing a count of the number of axons and their caliber (Fig 13). Antibody staining for myelin basic protein identified the axons that have reconstituted a myelin sheath. The muscle's neuromuscular junction acetylcholine receptor sites were labeled with a fluorescently tagged alpha-bungarotoxin. The junctions have a distinctive pretzel-like morphology made up of an end-plate zone that forms a continuous gutter (Fig 14). Each junction is distinct, much like a fingerprint, making it possible to use them as fiduciaries (286).

By using YFP-16 transgenic animals and an alpha-bungarotoxin with a fluorescent label at 633nm it is possible to excite the two fluorophores separately with different lasers. Innervated junctions are double labeled and the signals can be separated to show the terminal axon conforming to the shape of the end-plate gutter. This double labeling provided a count of how many junctions were innervated and information about the morphology of the junctions (Fig 14).

The normal interscutularis has been characterized previously by Lu *et al.* in four YFP-16 mice. There each connectome had 14.5 ± 1.5 axons supplying 198 ± 11 muscle fibres (junctions). Six percent of axons branched within 3mm of the muscle edge but there was no branching seen

Figure 13.

Two photom microscope montage of proximal and distal nerve sampling

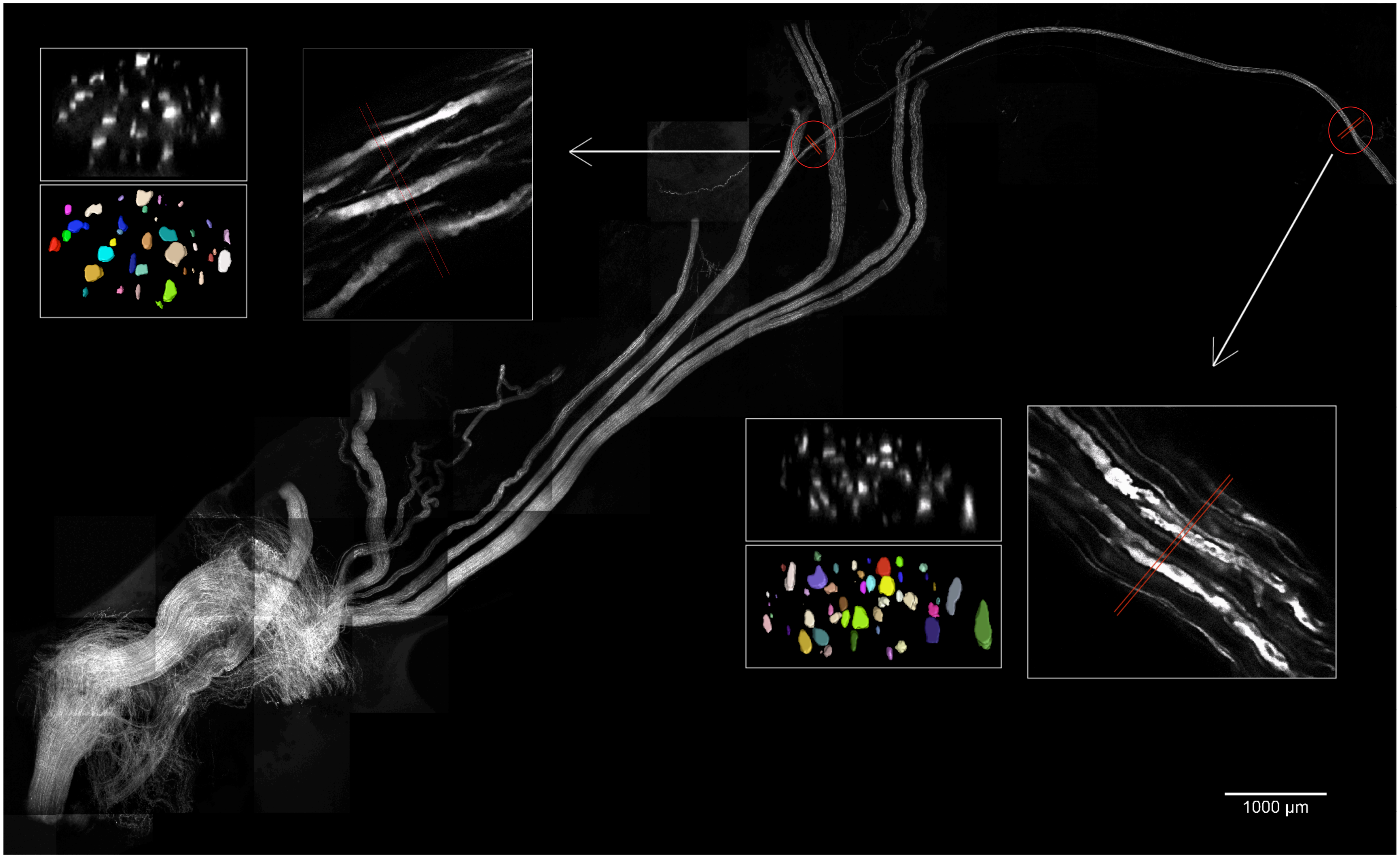

The proximal stump of the nerve is seen in the bottom left corner. This has regenerated through a graft and into the distal nerve bundles. The terminal branch to interscutularis has been digitally cross-sectioned at two points (proximal and distal) and the number and caliber of axons traced and measured.

Figure 14.

Confocal microscope image of axons and double-labeled neuromuscular junction morphology

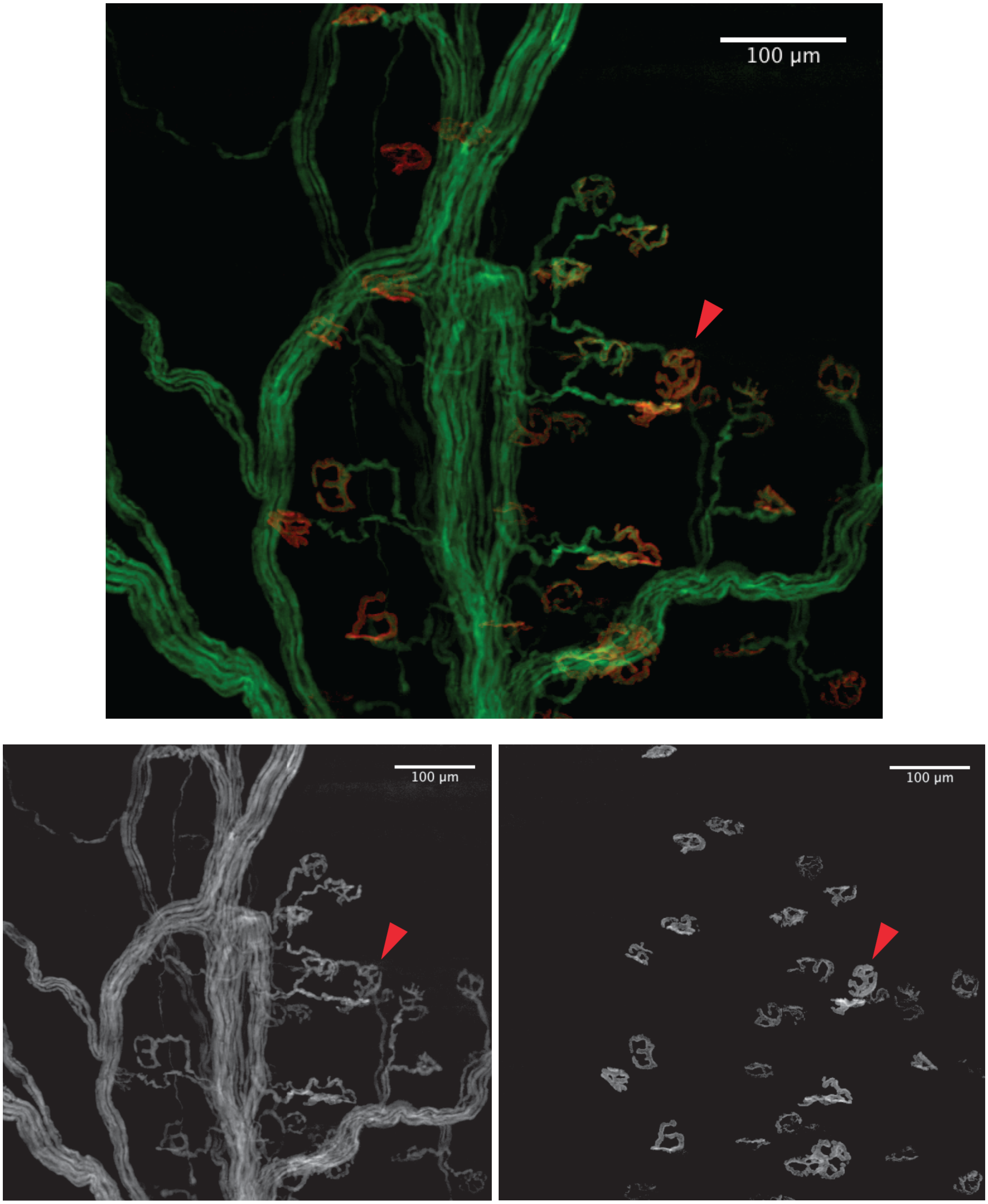

In the upper double-labeled image from a control specimen, axons are labeled in green (YFP fluorophore) and the neuromuscular junctions in red (alpha bungarotoxin). The lower images show the green channel (left) and the red channel (right) separately. Innervated junctions (eg red arrow) exhibit the same shape in both channels showing complete occupation of the receptor gutter by the axon.

between 3mm and 5mm from the edge of the muscle. The mean motor unit size was 7.7 ± 2.8 fold. The smallest motor unit had just one junction and the largest 37 junctions. Motor unit sizes were skewed in favour of smaller units where each axon innervates fewer muscle fibres. Axon cross-sectional areas correlated with their motor unit size according to a power law. The area scaled to the square root of the motor unit size (252).

3.3 Results

The controls for this current study came from 18 muscles in 9 animals (Fig 15). They were used to characterize the normal muscle and nerve parameters. The mean number of neuromuscular junctions in normal muscles was 265.4 ± 32.0 (n=18) (Fig 16). There was variability between animals, and between sides in individual animals. The difference between left and right in each individual was not statistically significant (P=0.4, paired T test, Fig 17), however the inter-specimen variability was found to be significant (P = 0.013, one way ANOVA, Fig 18).

As an animal gets older it gains mass (Fig 19) and the cross-sectional area of each muscle fibre increases in size (287). The size of each neuromuscular junctions varies with changes in the diameter of the muscle fibre it innervates (242). The mean age of the control animals at the time of perfusion was 90.4 ± 55.1 days. The mean mass of the animals was 30.4 ± 9.2g. To control for the difference in age, and therefore mass, the data was normalized (area for each junction was controlled for by animal mass in grams at time of perfusion). The mean size of each junction was 33.9 ± 7.7 $\mu m^2/g$. and there was no difference left and right side of the same individual (P = 0.9, unpaired T-test, Fig 21) supporting the absence of “handedness” shown in the NMJ numbers. The mean total surface area of receptors per muscle is 10040 ± 2872 $\mu m^2/g$ (n=18) (Fig 20). The difference in the mean total surface area between individual control animals was statistically significant (P<0.0001, one way ANOVA).

Figure 15.

Confocal microscope image of axonal arbors in a YFP-16 control mouse

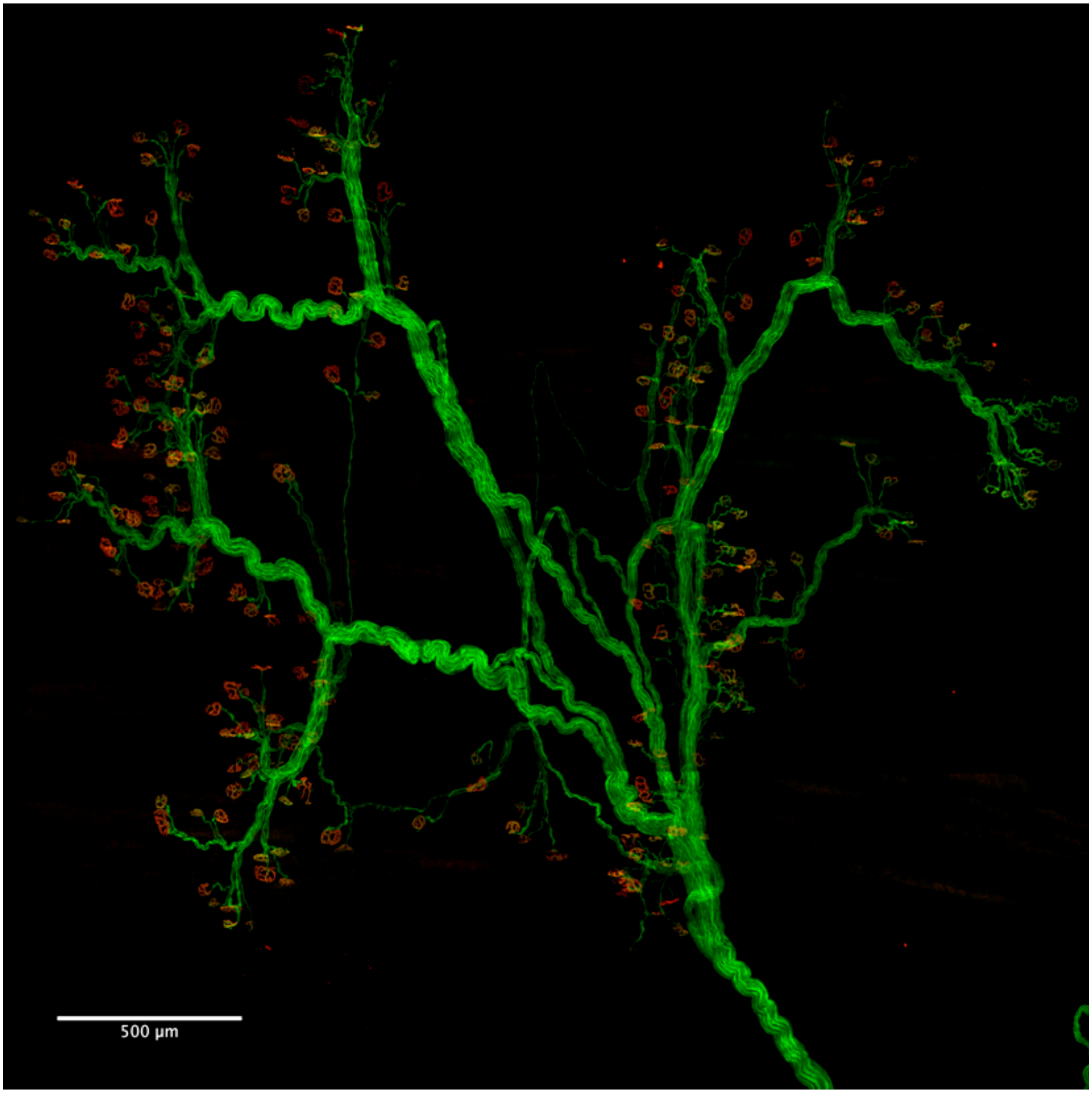

These are examples of YFP-16 neuronal arbors in control specimens. They have a typical branching pattern that enters the end-plate zone of the interscutularis muscle.

Neuromuscular junctions are labeled red with bungarotoxin. The nerve is labeled with native fluorescence by yellow fluorescent protein. In this YFP-16 animal all of the axons are labeled and the entire arbor is visualised.

Figure 16

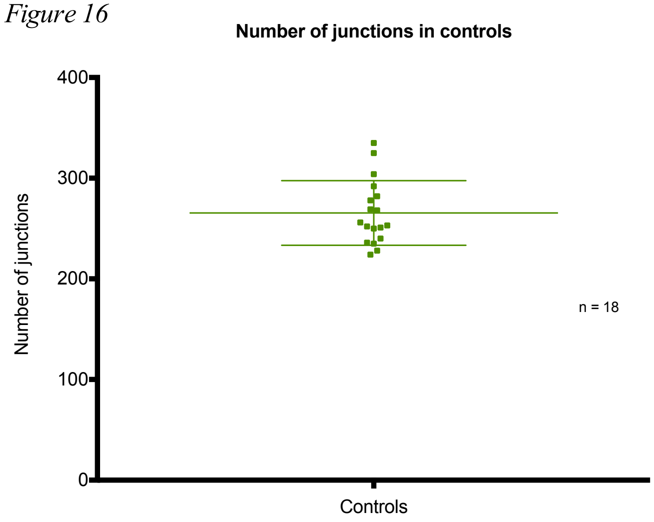

Figure 18

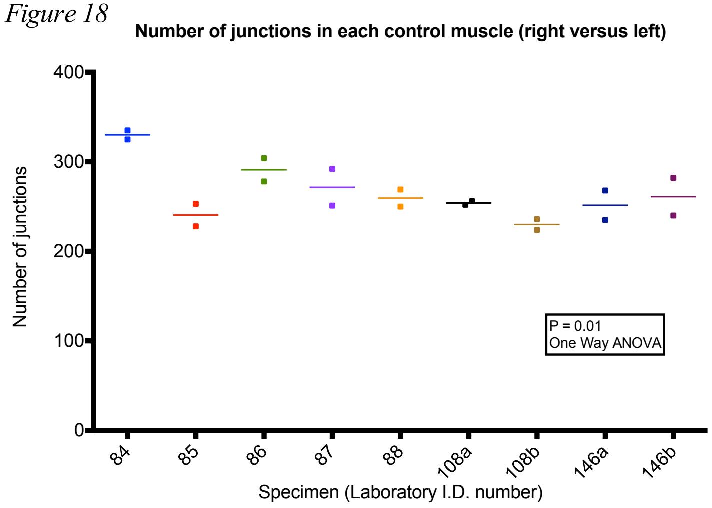

Figure 17

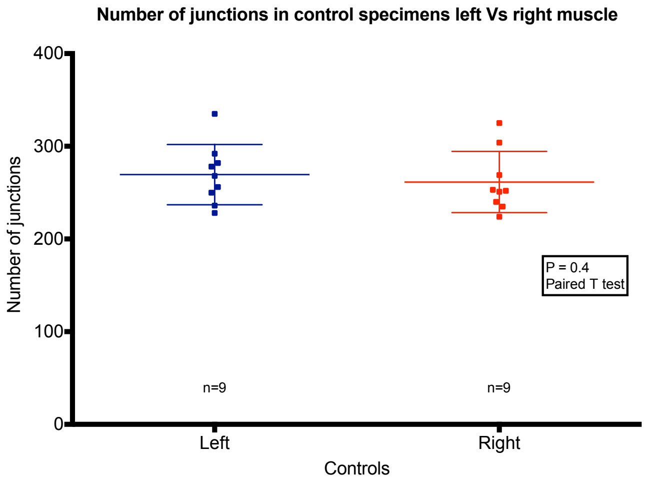

Figures 16-18 illustrate the number of neuromuscular junctions in the control specimens, 18 muscles taken from 9 animals. There is no overall difference between the number of junctions in right and left muscles. However, in each individual the difference between right and left (each side is plotted in fig 18) is significant.

Figure 19

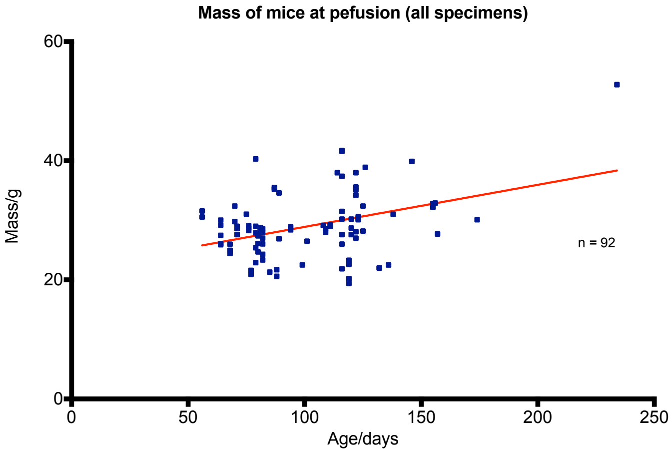

Figure 20a

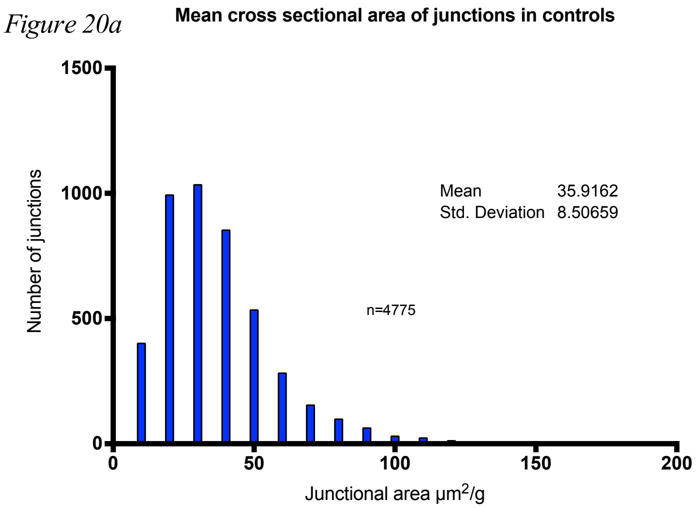

Figure 20b

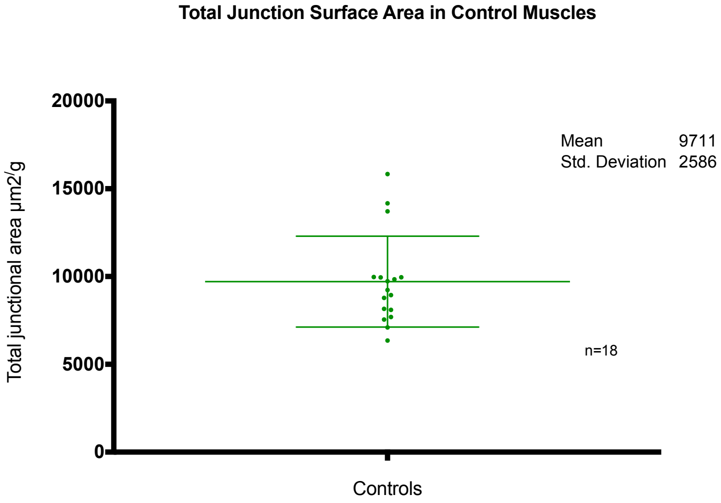

Figure 21

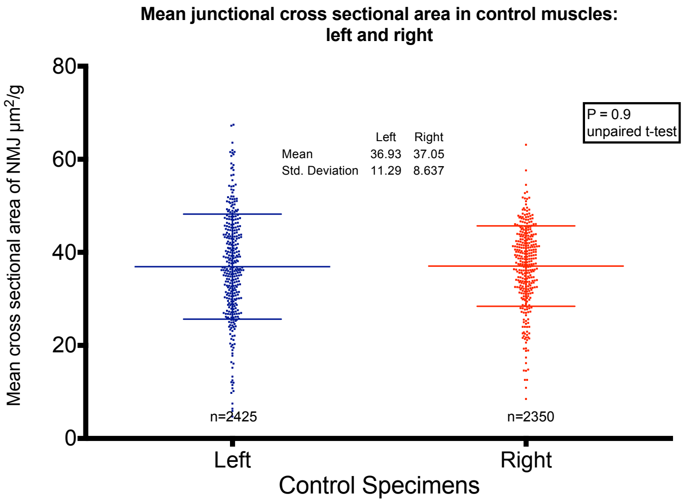

Figures 19-21 Junctional area increases linearly with increasing age as the animal's mass increases. Cross sectional areas were controlled for mass. The mean junctional area is unimodal and there is no difference in area between the junctions in right or left muscles. The total junctional surface area of muscles is clustered around 10,000µm.

Axons

The number of axons supplying the interscutularis muscle were measured by taking cross sections at two points in the terminal nerve to the muscle. These two points were at the proximal end of the terminal branch (when all remaining axons are only supplying the interscutularis) and at the distal end just as it is about to enter the muscle. There were anatomical variations in two animals where the terminal nerve to interscutularis was short. In these cases there was inadequate length after the final division of the terminal nerve to acquire proximal axon data. These specimens were excluded from analysis. The mean number of axons was 19.6 ± 4.6 proximally (n=16), and 23.1 ± 5.8 distally (n=16) (p=0.0002 paired t-test, Fig 22). There was a mean increase of 19.7% ± 16.5% in the number of axons over the course of the terminal branch of the nerve. This figure encompasses a wide range from 0% to 57.9%.

The mean diameter of axons proximally was 8.0µm ± 1.2µm (n=313) and 7.7µm ± 1.2µm (n=393) distally (Fig 23). The total cross-sectional area of axons represents the sum of the individual cross-sectional areas of all the axons within a particular nerve. This increased from 1191μm^2 ± 429μm^2 proximally to 1325μm^2 ± 374μm^2 distally (Fig 24). This increase, despite a fall in the mean axon diameter as the axons taper distally, was due to the increase in the number of axon fibres.

Antibody labeling to myelin basic protein shows that all axons were enclosed in a myelin sheath. In a small subset of the two-photon images of nerve there was some fluorescent expression within the connective tissue surrounding the axons. In these samples there was bright fluorophore expression in the axon and faint expression in the connective tissue. Between the

Figure 22

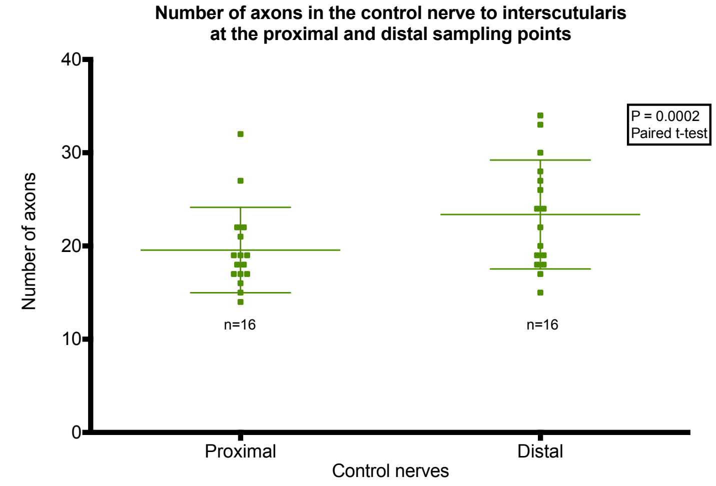

Figure 23

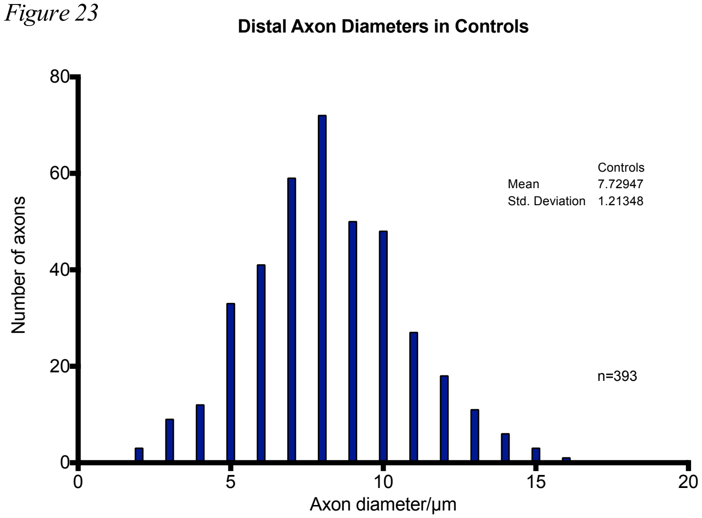

Figure 24

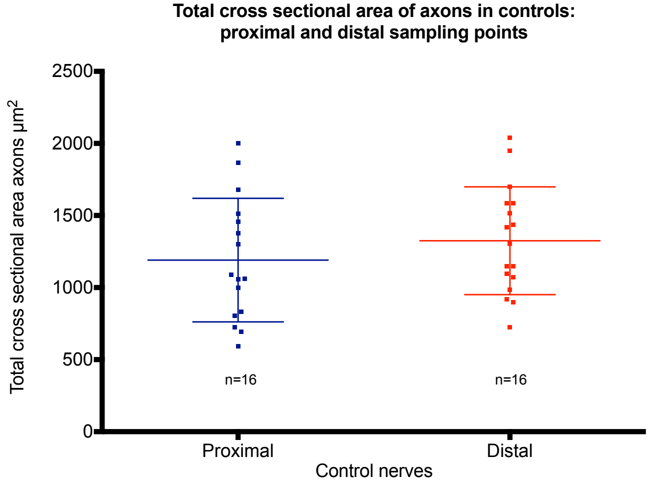

Figure 25

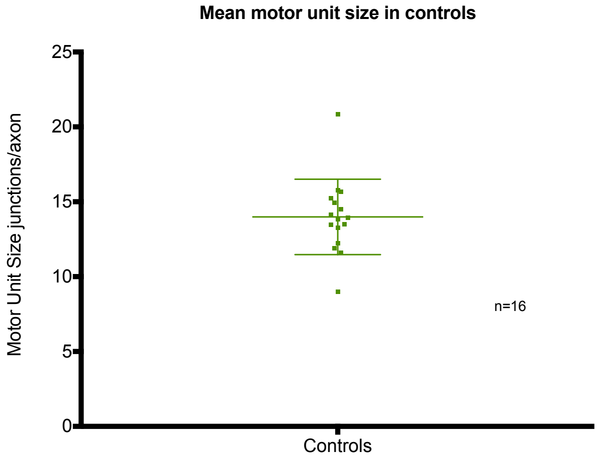

Fig 22-5 illustrate changes that occur in the terminal nerve to interscutularis. There is an increase in the number of axons as a result of branching in the terminal nerve to the muscle. The mean diameter of distal axons shows a unimodal distribution around a mean of 7.7µm and the total cross sectional area of axons increases as the nerve approaches the muscle. The mean motor unit size (number of neuromuscular junctions/number axons) cluster around a mean of 14 NMJ/axon two there was a dark halo corresponding to the presence of the myelin sheath (Fig 26).

The mean size of the motor units can be calculated by dividing the number of neuromuscular junctions by the number of axons that supply the junctions. The increase in axon number in the terminal nerve, from proximal to distal, represented branching of the proximal population. Whilst the proximal number may have included some branches that have divided more cephaledad, it still represents a more accurate estimate of the number of individual axons supplying the muscle for the purpose of calculating mean motor unit size. Lu *at al.* produced a "wiring diagram" for four interscutularis muscles in which he traced each axon through to each of the NMJ that it innervated. However, whilst this produced an actual size of motor unit for each axon, he only picked up the axons 5mm from the muscle edge, essentially our distal sampling point. We have shown that there are approximately 20% more axon fibres at the distal end of the terminal nerve than at its proximal origin. This suggests that not all of the axons at the point where it meets the muscle are isolated individuals. We believe our methodology represents a more accurate way of calculating mean motor unit size than the Lu e*t al.* data.

The number of innervated junctions was divided by the number of axons at the proximal site for each muscle. In control muscles the mean motor unit size was 14.0 ± 2.5 junctions/axon (Fig 25).

Figure 26.

Confocal and two photon microscope images of axons showing the presence of myelin sheaths

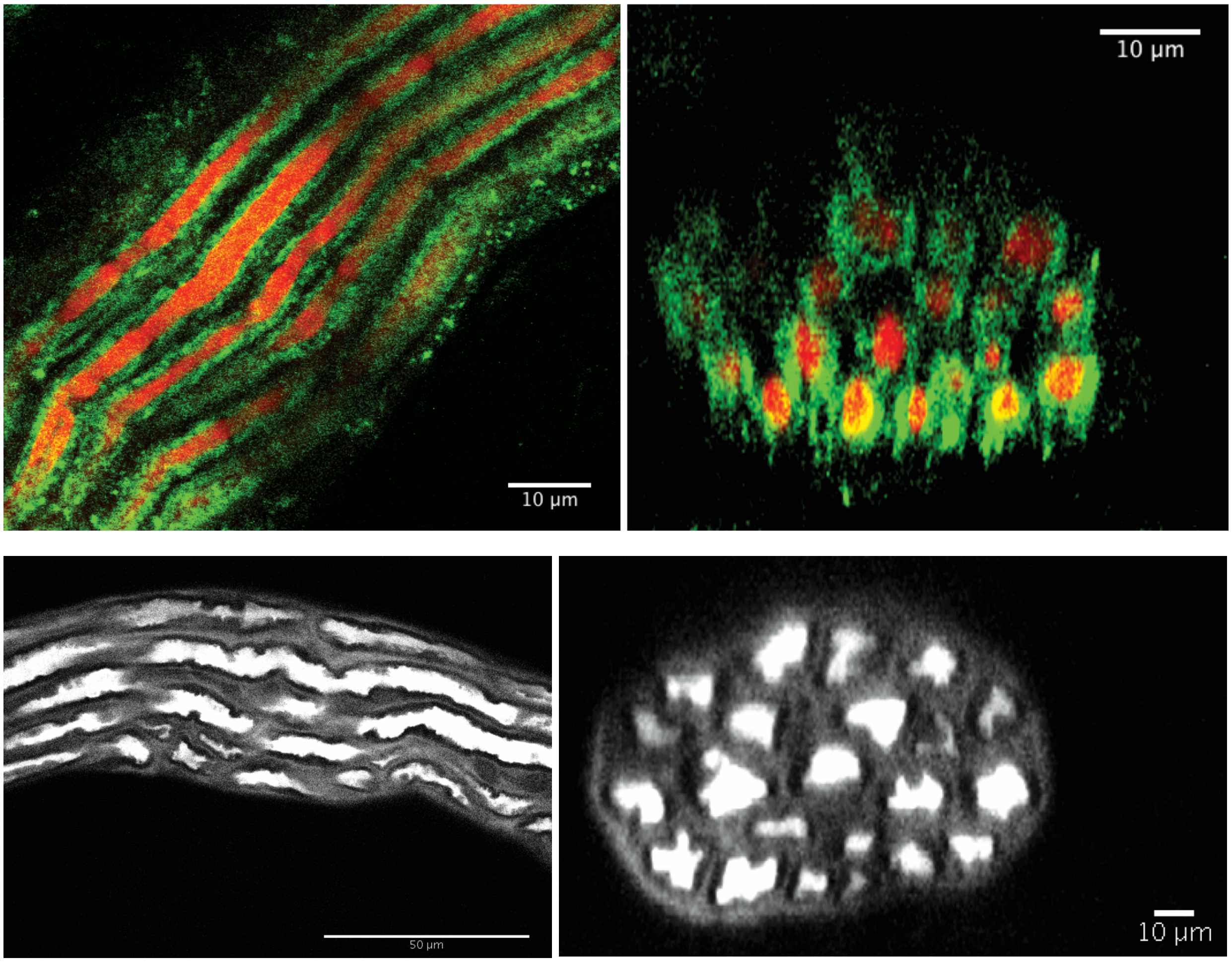

In the upper images the axons' native fluorescence is labeled red and antibodies to Myelin basic protein are labeled green. Each axon is enclosed in a separate myelin sheath. The lower images are taken in a single channel, two photon microscope, that show bright labeling of the axons and faint labeling of the connective tissue. The black areas that surround each axon are myelin.

3.4 Summary

The characteristics of the interscutularis muscle are suitable for modeling nerve repair and nerve graft in a facial palsy. It is innervated by a cranial nerve, and we know from MacQuillan's work that cranial and peripheral nerves behave differently when re-innervating muscles (288). The interscutularis has been used in previous studies analysing both its neural arbor, and its response to reinnervation after nerve injury (289,290). The characteristics of the have been further elucidated by our control group. The muscle-nerve complex also has certain advantages from the methodological perspective. There is a terminal nerve branch supplying the muscle that can be accessed easily without disturbing the muscle itself. This allows for surgical interventions without producing scarring around the muscle which would interfere with subsequent imaging. However, one disadvantage of this system is that the nerve originates within the cranium. This means that it is not possible to ascertain how many of the axons at the start of the terminal branch are individuals or sub-branches.

In summary the interscutularis is a thin muscle supplied by a terminal branch of the facial nerve. It has approximately 265 muscle fibres supplied by 20 axons. This gives a mean motor unit size of 14 muscle fibres per axon. At the proximal end of the terminal branch to the muscle the axons are a relatively homogeneous population with an average diameter of 8.0μm and all are myelinated. Some axons do branch extramuscularly, but the degree of branching is variable between specimens.

4

Characterisation of the changes seen in the interscutularis muscle after reinnervation through a nerve repair or nerve graft in YFP-16 specimens

4.1 Introduction

A nerve enters a muscle at the end-plate zone, an area rich in neuromuscular junctions. In the interscutularis this zone is a well-defined and compact area towards the lateral pole of the muscle. Once the nerve enters the muscle the axons spread out and arborise to cover the end-plate zone like the branches of a tree. Each axon will contact several junctions, but each mature junction is only innervated by a single axon. All of the junctions innervated by the same axon are collectively referred to as a motor unit. The arbors of reinnervated muscles closely resemble the controls (Fig 27).

Figure 27.

Confocal microscope images of the arbors of YFP-16 mice after nerve repair and nerve graft

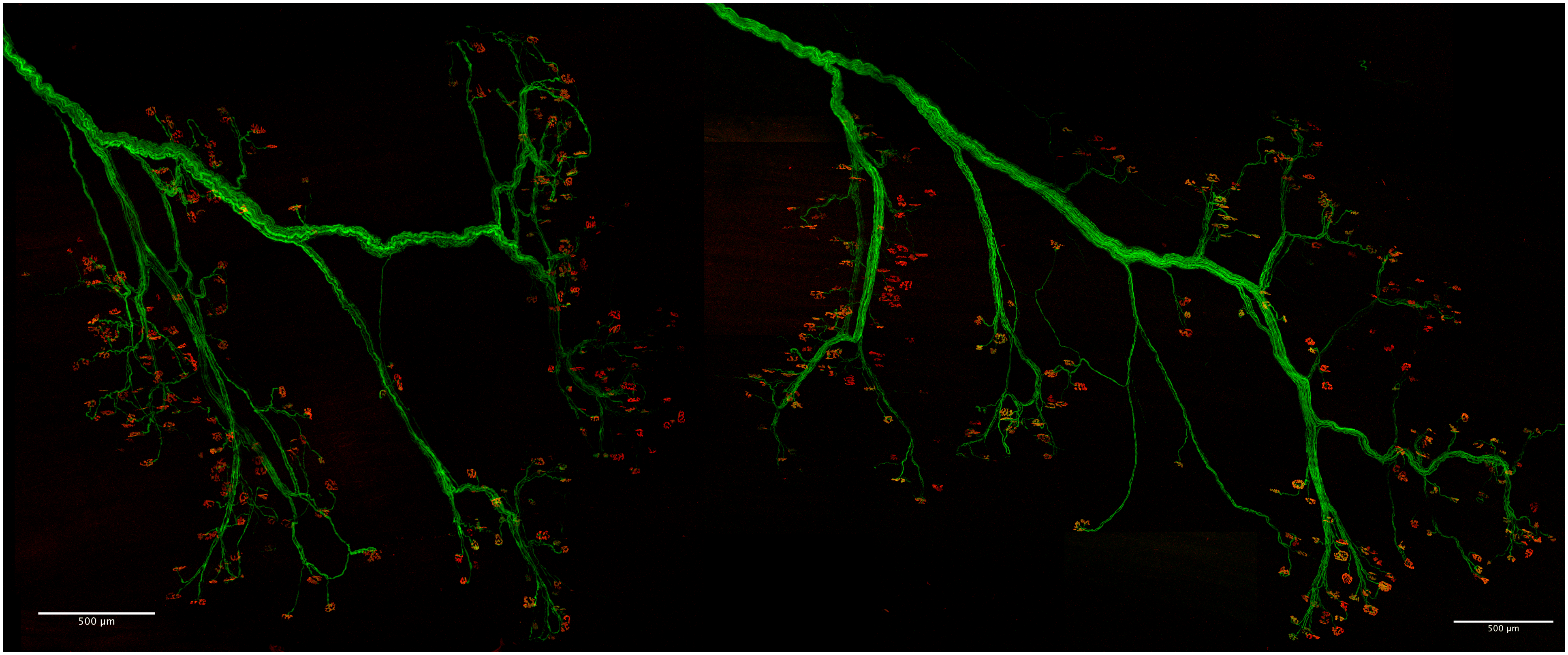

The arbors of reinnervated muscles twelve weeks after nerve repair (left) and nerve graft (right). They closely resemble the control arbor (Figure 14).

4.2 Results

Skeletal muscle fibres are typically innervated at a single neuromuscular junction site. To assess the number of muscle fibres remaining after interventions the number of occupied neuromuscular junctions were counted in reinnervated muscles (Fig 11).

There was no significant difference between the number of junctions in reinnervated muscles and controls at any time period (P=0.37, Two-way ANOVA (Fig 28, Table 4). In the nerve cut group (C) where the nerve was divided and a segment removed (nerve cut) there were no reinnervated junctions at four, six or twelve weeks (Fig 29).

Table 4

Mean junction number per group at four, six and twelve weeks.

Mean ± Standard deviation (n)

Group/Time	4 weeks	6 weeks	12 weeks	Overall
Repair	263.1 ± 43.2 (9)	303.0 ± 31.7 (9)	261.8 ± 52.1 (9)	**276.0 ± 45.8**
Graft	276.3 ± 53.2 (9)	270.0 ± 46.3 (9)	242.6 ± 43.0 (9)	**263.0 ± 48.2**
Controls				**265.4 ± 32.1**

Figure 28.

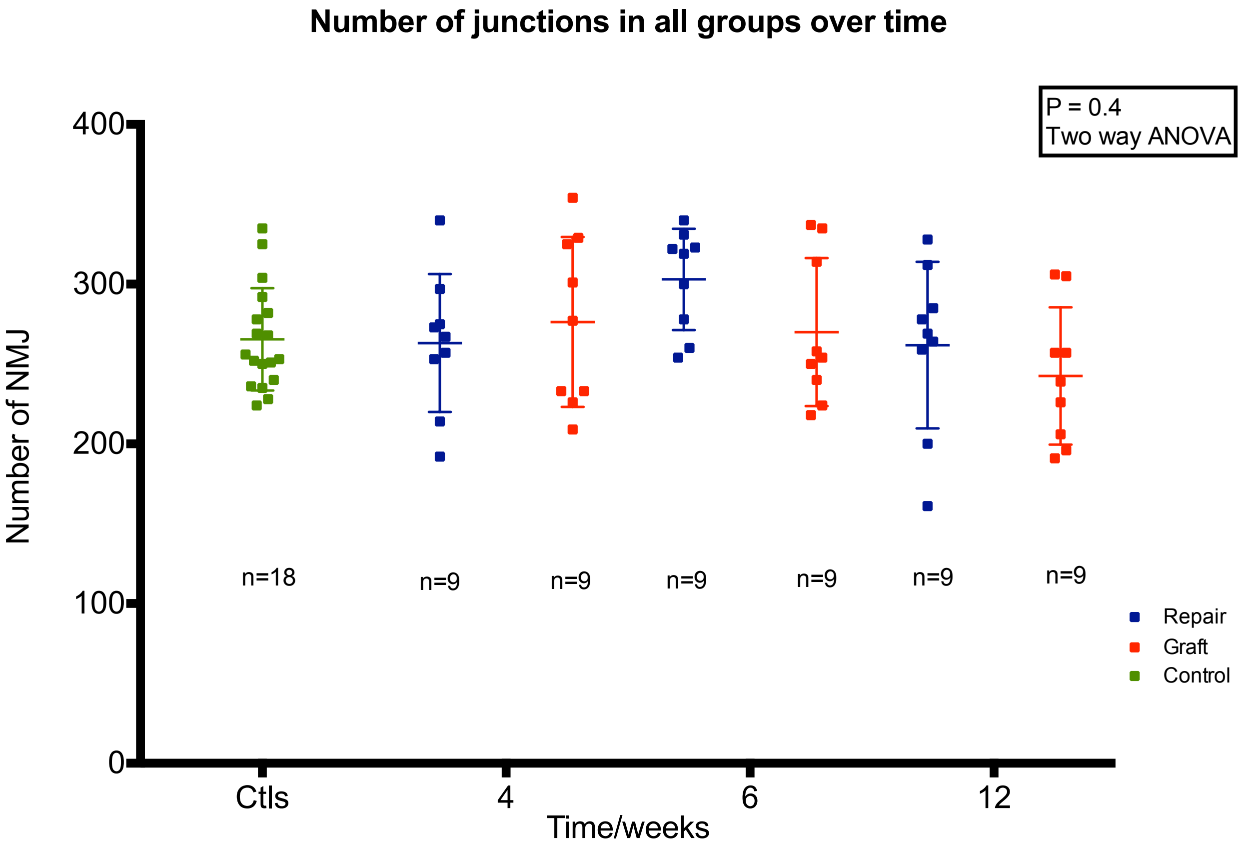

There was no significant difference in the number of neuromuscular junctions between the control group and either of the intervention groups at any time period after reinnervation. There is only one junction per muscle fibre so the number of fibres has remained constant.

Figure 29.

Confocal microscope image showing the end plate zone of a nerve cut mouse

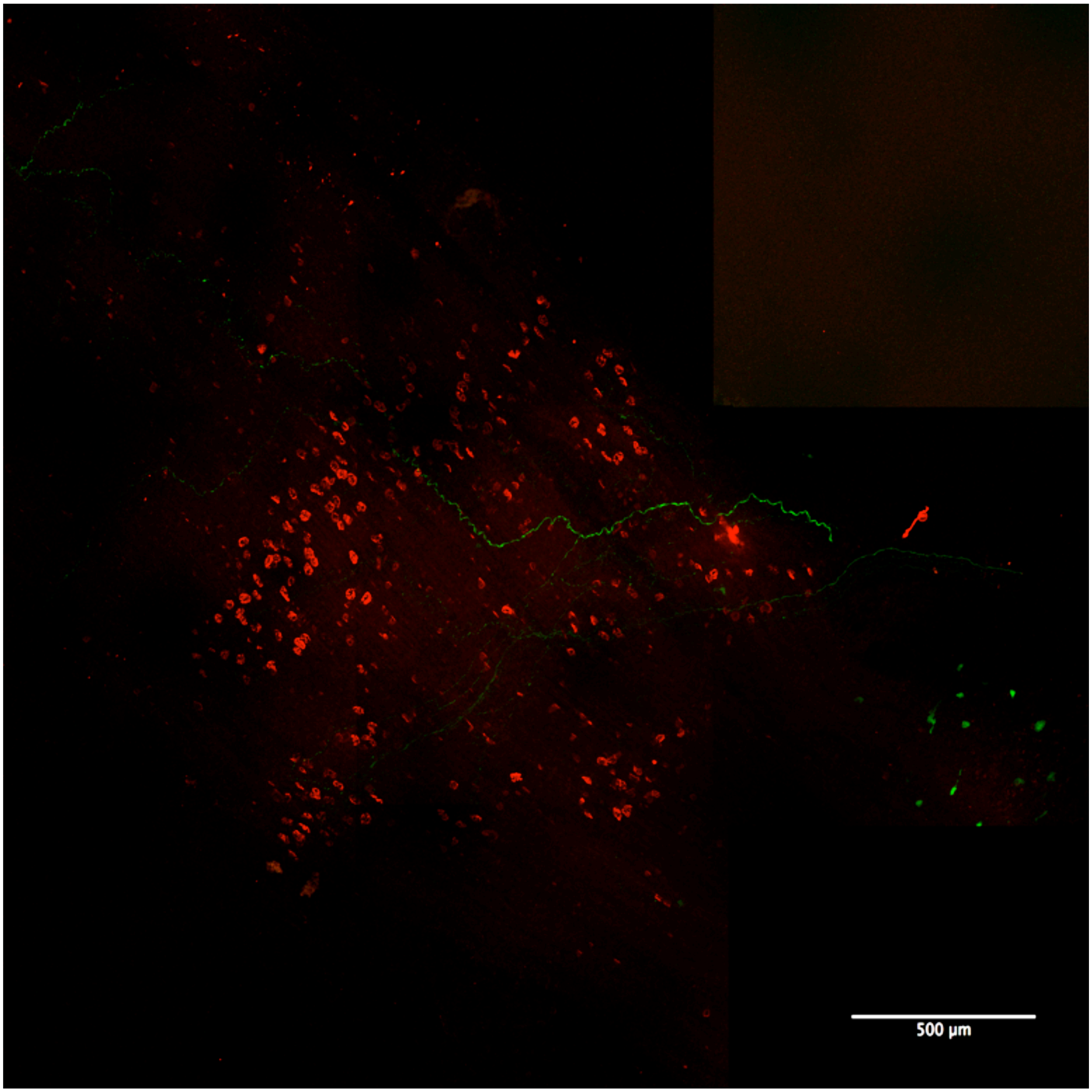

This double-labeled image is a nerve cut specimen four weeks post intervention. No neuromuscular junctions were reinnervated at any time period where the nerve was divided and not repaired or grafted. In this image an axon has regenerated into the arbor, but it has not made any connections with neuromuscular junctions. This axon has a wavy appearance (also see Fig 51) unlike the motor axons seen in control specimens and perhaps represents a sympathetic axon.

Figure 30.

Confocal microscope image of axons and labeled NMJ four weeks after a nerve graft

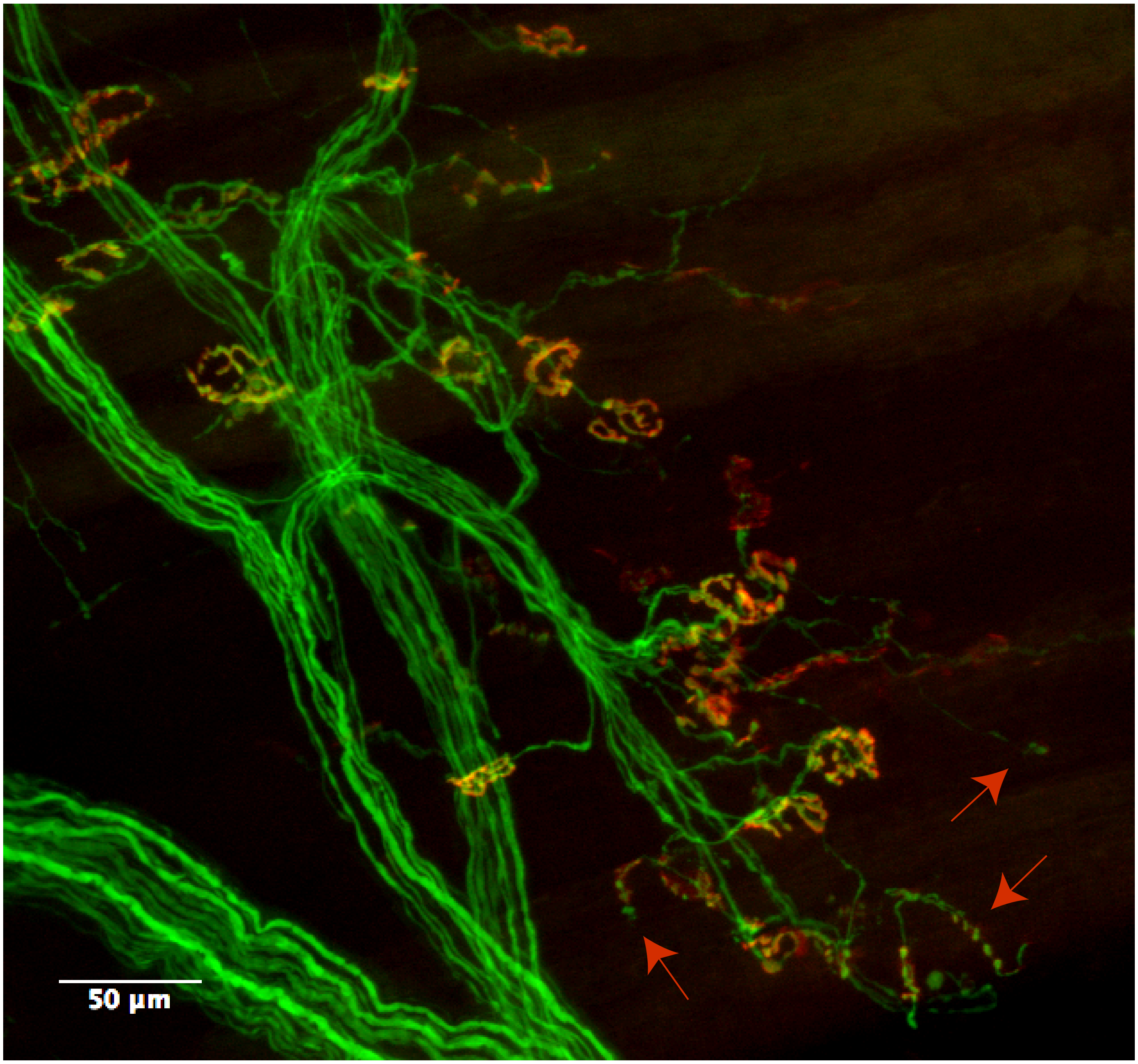

This double-labeled image is a nerve graft specimen four weeks post innervation. Terminal axon sprouts extend from occupied junctions and innervate small areas of neuromuscular receptor labeled with alpha-bungarotoxin (red arrows) that resemble a 'string of beads'. These areas of receptor may represent degenerated junctions, or areas of *de novo* receptor on denervated muscle fibres.

The surface area of all reinnervated NMJ was estimated using ImageJ and standardised by controlling for the mass of each animal at the time of perfusion. The mean NMJ size was smaller in the intervention groups than in the controls at all time points. Taking time and intervention as variables, two way ANOVA was not statistically significant ($p=0.88$). However, whilst there was no change over time ($p=0.816$), the difference between the interventions was significant ($p<0.001$). Tukey's test demonstrates that although the NMJ size in the repair and graft groups were not dissimilar ($p=0.596$), they were both significantly smaller than those in the control group ($p<0.001$). The NMJ increased in size in both repair and graft groups with time from intervention but never recovered their original surface area (Table 5, Fig 31). At twelve weeks the mean size of NMJ in the repair group is 94% of controls whilst the graft group remained smaller at 77%.

Table 5.

Mean NMJ size μm^2/gram in each of the intervention groups at four, six and twelve weeks.

Mean ± Standard deviation (n)

Group/Time	4 weeks	6 weeks	12 weeks	Overall
Repair	30.5 ± 13.6μm^2 (2368)	25.1 ± 6.3μm^2 (2729)	31.7 ± 10.9μm^2 (2360)	28.3 ±6.9μm^2 (7457)
Graft	22.2 ± 10.7μm^2 (2491)	25.5 ± 9.3μm^2 (2430)	26.0 ± 7.0μm^2 (2195)	25.8 ±10.0μm^2 (7116)
Cut	26.7 ± 5.3μm^2 (872)	23.5 ± 6.8μm^2 (152)	N/A	
Controls				33.9 ± 7.7μm^2 (4775)

The mean total surface area of high-density receptor sites per muscle increased over time in both intervention groups, but remained smaller than controls at all time points (Table 6).

Table 6.

Total NMJ cross sectional area of repairs & grafts at four, six and twelve weeks in μm^2/gram.
Mean ± Standard deviation (n)

Group/Time	4 weeks	6 weeks	12 weeks	Overall
Repair	$6925 \pm 1659\mu m^2$ (9)	$7759 \pm 1552\mu m^2$ (9)	$7694 \pm 2223\mu m^2$ (9)	$7459 \pm 1085\mu m^2$ (27)
Graft	$5388 \pm 1321\mu m^2$ (9)	$6187 \pm 699\mu m^2$ (9)	$6095 \pm 1395\mu m^2$ (9)	$5904 \pm 1190\mu m^2$ (27)
Controls				$10040 \pm 2872\mu m^2$ (18)

Two-way ANOVA of the total NMJ surface areas showed no significant difference between the groups (p=0.937). However, whilst the time difference is not significant (p=0.521) the difference between the interventions and controls showed the total surface area of receptor to be significantly smaller post reinnervation (p<0.001, Fig 32). This significance existed between each intervention and controls as well as between nerve repairs and nerve grafts (Table 7).

Figure 31

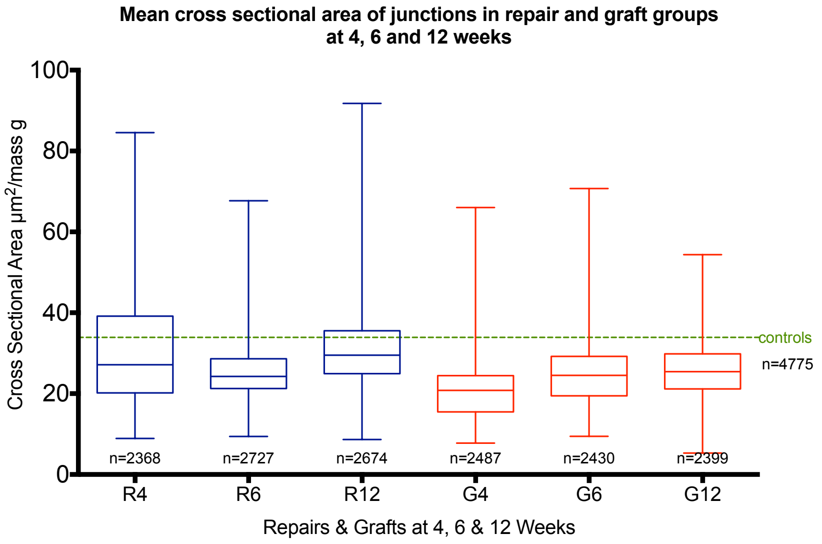

Mean cross sectional area of junctions in repair and graft groups at 4, 6 and 12 weeks

Figure 32

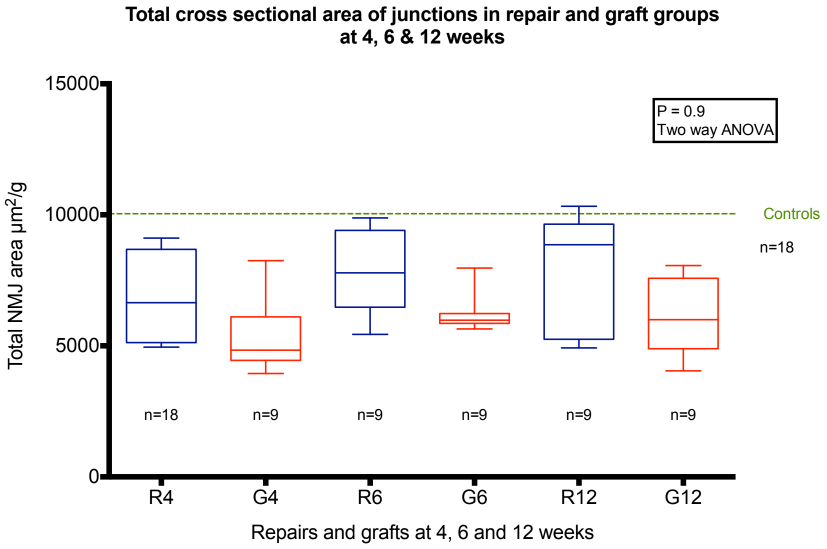

Total cross sectional area of junctions in repair and graft groups at 4, 6 & 12 weeks

Figure 33

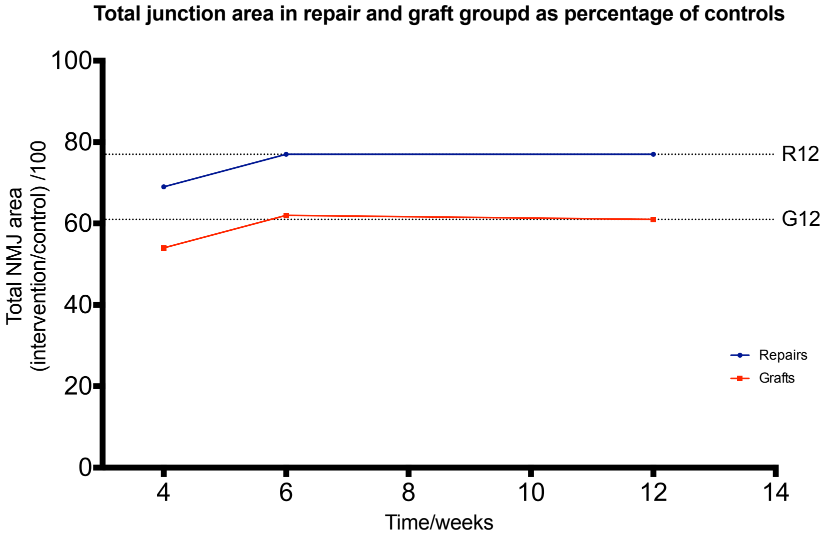

Total junction area in repair and graft groupd as percentage of controls

Boxes represent the 25th bto 75th percentiles, whiskers are minimum and maximum values. The green dotted line is the mean for all junctions in the control group.

The mean cross sectional area of neuromuscular junctions is smaller in all reinnervated muscles than controls. The trend is for the mean size of junctions to increase the lpnger they have been reinnervated. This is also apparent in for the total cross sectional area of junctions/muscle.

Whenr the total crosss sectional area of NMJ is represented as a percentage of the controls both interventional groups achieve an asymptote at six weeks. The nerve repair group achieve 77% of the area of controls and the nerve grafts 61%.

Table 7.

Two way ANOVA and Tukey's multiple comparisons of neuromuscular junction total surface areas for nerve repairs and nerve grafts at four, six and twelve weeks post intervention versus controls.

Variables	P	Tukey's Test	P
Time	0.521		
Intervention & Time	0.937		
Intervention	<0.001		
		Control Vs Graft	<0.001
		Control Vs Repair	0.002
		Repair Vs Graft	0.020

The mean total surface area of receptor expressed as a percentage of controls shows that after an initial increase in area in both repairs and grafts there was no change between 6 and 12 weeks (Fig 33). Values reach an asymptote of 77% for repairs and 61% for grafts. This illustrates that the total area of receptors increased after reinnervation but reached a stable state that was less than the original surface area.

In the nerve cut group there was no reinnervation of the neural arbor. The NMJ gradually diminished in size over time and lost their architecture. At four weeks most NMJ were still present with normal morphology but some had already become smoother, losing the intricacy of the folds in the gutters. Some NMJ maintained their original architecture even at six weeks post denervation but by twelve weeks all recognizable junctions have disappeared (Fig 34).

Figure 34.

Confocal microscope images of the end plate zone in a nerve cut specimen at four, six and twelve weeks after division of the nerve

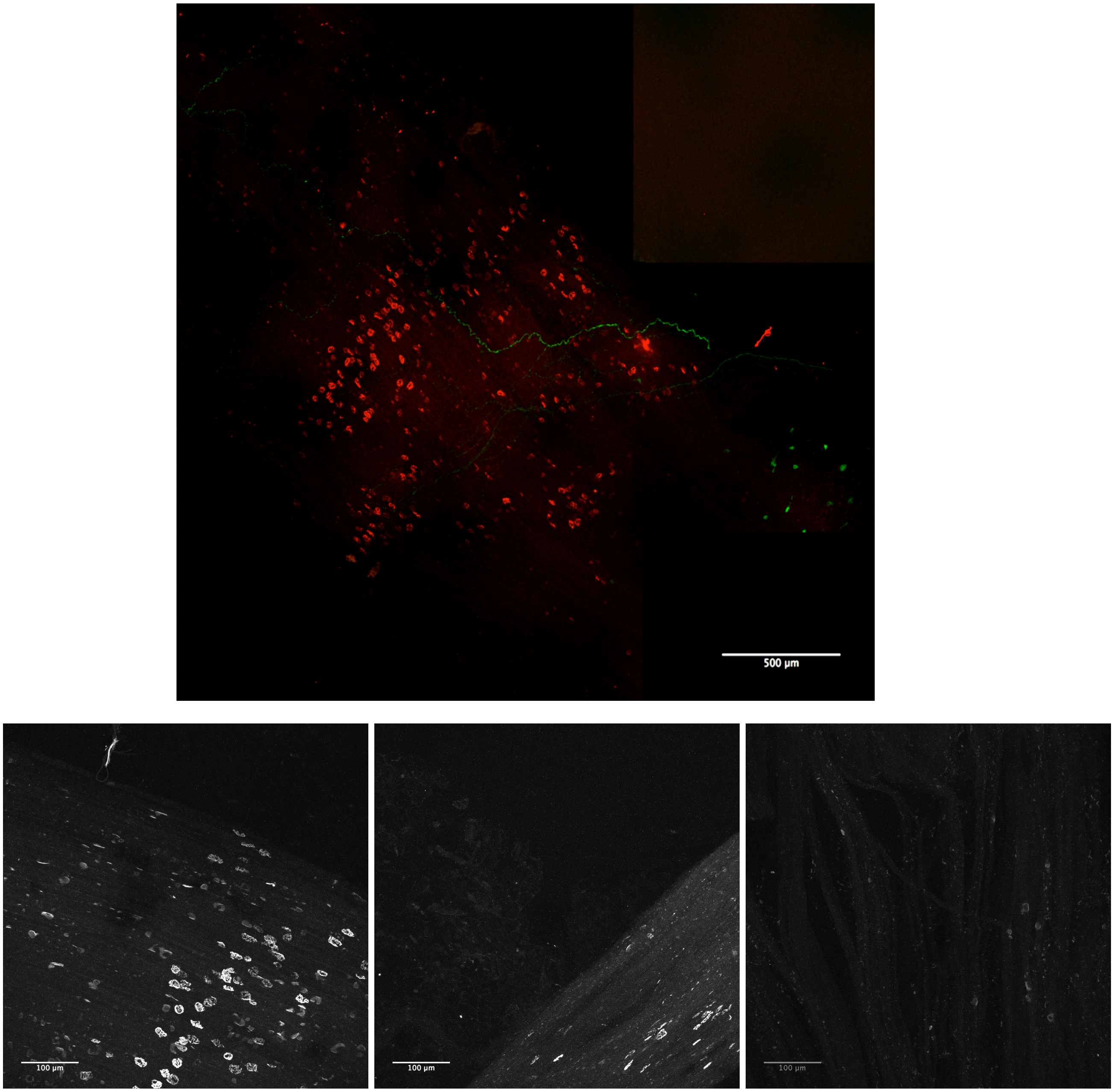

4 weeks 6 weeks 12 weeks

In the upper, double-labeled image of a nerve cut specimen at four weeks post denervation there is no reoccupation of the arbor. A single axon has grown back along the terminal nerve and is seen crossing the muscle from right to left. It has a wavy appearance unlike the motor axons seen in control specimens and perhaps represents a sympathetic axon (see Fig 51).

The nerve cut specimens (four, six and twelve weeks) show a gradual atrophy of the NMJ with prolonged denervation. The number of recognizable NMJ reduces over time, and their size also shrinks. By twelve weeks there are only fragments of NMJ persist.

4.3 Summary

In summary the number of neuromuscular junctions remained constant in both the nerve repair and nerve graft groups compared to controls, which suggests that there was no loss of muscle fibres. The mean size of the NMJ was smaller after intervention (repair or graft) compared to controls, and though they enlarged with time they stabilized at a smaller size. The mean total surface area of receptor sites increased between four and six weeks but remained stable thereafter. The repair group recovered more receptor area than the graft group. Both groups regained more than the 20% of receptor area that Wood suggested is the minimum required for normal neuromuscular transmission (300). On balance it appears that the innervation parameters of the muscle have been restored after both repair and graft.

5.

Characterisation of the changes seen in the terminal nerve to the interscutularis after reinnervation through a nerve repair or graft in YFP-16 specimens

5.1 Introduction

The characteristics of a muscle are dependent on a ratio between the numbers of muscle fibres and the axons that innervate the muscle. In the previous chapter it was demonstrated that the number of muscle fibres remains constant with reinnervation through either a nerve repair or nerve graft. Nguyen showed that after a nerve crush axons recapitulate their original patterns extremely accurately (103). However, this was not the case after nerve cut. Here the aim was to analyse the patterns seen after nerve repair and nerve graft. It is perhaps intuitive that after a full nerve cut there will be a complete disruption of the axons between the proximal and distal stumps. Even with accurate apposition of the cut ends reinnervation cannot be perfectly restored as prior to the injury. Scar tissue forms at the site of injury which can disrupt the ability of axons to locate the appropriate distal pathway (Figs 12 & 35). Axons that manage to enter the distal Büngner's bands are unlikely to precisely find their original distal path and therefore be delivered to their previous target muscle fibres. Axons have been shown to increase their field of influence to compensate for axons that no longer innervate the target (221,222). Remodeling has been shown to be a powerful tool in manipulating this misalingment (94,95,296). The aim of this study is to analyse the patterns and morphology of the axons that re-innervate the muscle after nerve repair of graft. We have shown in normal controls that there is a homologous population of myelinated axons innervating the interscutularis that have a consistent diameter of 8μm throughout their course in the terminal nerve. All of these axons make connections with motor end-plates so can be assumed to be motor axons. Lu has demonstrated that the interscutularis has no spindle fibres which further confirms this finding (252) (personal communication with JW Lichtman).

Figure 35.

Two photon microsope montage of the PAN after a nerve graft

This is a montage of stacks of a nerve graft specimen six weeks post intervention from a two-photon microscope. The graft, with a repair at its proximal and distal extent, is seen in the bottom left. The terminal nerves are included through to the beginning of the arbor at the top right.

5.2 Results

The number and size of regenerating axons were measured at two locations: the proximal and distal ends of the terminal branch to interscutularis. These points were both distal to the site of surgical intervention. Antibody labeling of myelin basic protein was used to assess whether the axons were myelinated. The n values for the proximal and distal sampling points were not equal due to anatomical variations in the branching of the terminal nerve to interscutularis. Occasionally the final branch to the muscle would occur very late which did not allow for a proximal sampling point (Table 8). The four muscles (two repairs at four weeks, one repair at six weeks, one repair at twelve weeks) that do not have a proximal sample were excluded from subsequent calculations of branching or motor unit size (see below).

Table 8.

Number of specimens in each group proximally and distally

Group	Experimental Specimens Total	Proximal Sampling	Distal Sampling
Controls	18	14	17
Repair 4 weeks	9	7	9
Repair 6 weeks	9	8	9
Repair 12 weeks	9	8	9
Graft 4 weeks	9	9	9
Graft 6 weeks	9	9	9
Graft 12 weeks	9	9	9

The mean number of axons (Table 9) for both interventions at each time period was greater than controls.

Table 9.

Mean axon numbers for repairs and grafts at four, six and twelve weeks. Mean ± Standard deviation (n)

	Weeks	Proximal Axon Number Mean (S.D., n)	Distal Axon Number Mean (S.D., n)
Controls		19.6 ± 4.6 (16)	23.1 ± 5.8 (16)
Repair	4	34.7 ± 9.8 (7)	51.7 ± 16.3 (7)
	6	34.3 ± 8.3 (8)	45.9 ± 10.2 (8)
	12	28.0 ± 10.5 (8)	29.1 ± 9.3 (8)
Graft	4	29.8 ± 9.8 (9)	38.0 ± 11.1 (9)
	6	25.9 ± 6.9 (9)	35.3 ± 10.9 (9)
	12	29.0 ± 6.9 (9)	40.7 ± 18.1 (9)

The mean number of axons in the nerve where it entered the muscle (distal) was significantly greater in nerve repairs [43.7 ± 15.4 (n=27)] and in nerve grafts [37.9 ± 13.5 (n=27)] than controls [23.1 ± 5.8 (n=16)] ($P=0.004$, two way ANOVA, Fig 36). The significance of the mode of intervention ($p<0.001$) was much stronger than time ($p=0.055$). Breaking down the results (Tukey's test) there was no significant difference between the graft groups at any of the time points. In the repair group the change between the four and twelve week points was significant ($p<0.001$), with at first an increase and then a decrease in axon numbers. This demonstrates remodeling over time. This trend was reinforced when comparing the repairs and grafts against controls (Table 10). The grafts remain significantly different from controls throughout the time frame whilst the repairs trend towards the controls, and by 12 weeks are no longer significantly different in axon number.

Table 10.

Tukey's comparison of axon numbers in the distal nerve after nerve repair or nerve graft over time with controls (p values)

Comparison/weeks	4 weeks	6 weeks	12 weeks
Repair Vs Control	<0.001	<0.001	0.062
Graft Vs Control	0.003	0.014	<0.001
Repair Vs Graft	0.003	0.184	0.254

The mean number of axons at the proximal sampling point [Repairs: 32.9 ± 8.5 (n=23); grafts: 28.2 ± 7.9 (n=27); controls 19.6 ± 4.6 (n=16)] displayed a slightly different pattern (Fig 37). Two way ANOVA was not statistically significant ($p=0.577$). Whilst there was no change associated with time ($p=0.319$), the difference between each of the interventions was significant ($p<0.001$). Pairwise multiple comparison (Tukey's test) showed that both interventions were significantly different from the controls ($p<0.001$), but not from each other ($p=0.073$).

The total number of proximal axons possibly represents a combination of axons and their branches. Since no axons join the nerve in this terminal section the increase in axon number between the proximal and distal counts represent branching of the proximal group. Due to the

Figure 36

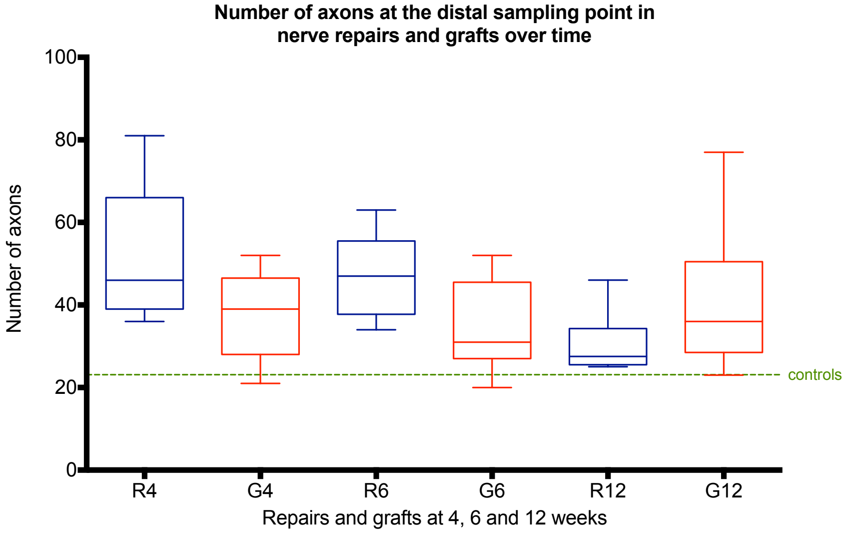

Figure 37

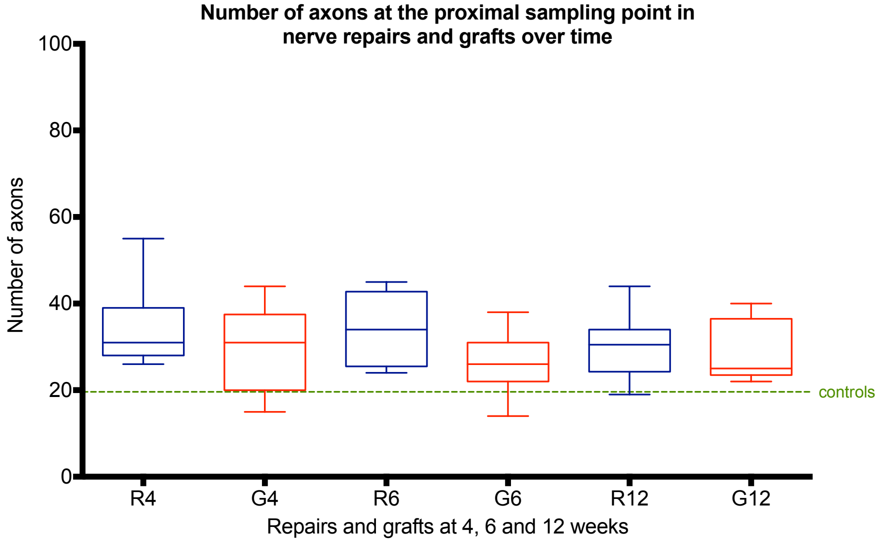

Figure 38

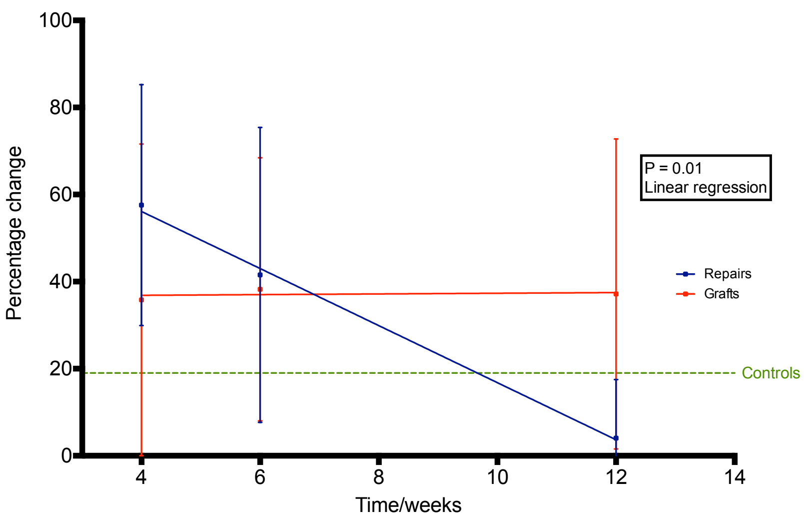

Figures 36 and 37 illustrate the change in the number of axons at the proximal (37) and dsiatl (36) sampling points at 4, 6 and 12 weeks post reinnervation. At both sampling points and at all time points the number of axons in the intervention groups is greater than the control group. Distally the number of axons in the repair group reduces over time and this is significant ($p<0.001$, Tukey's test, from two way ANOVA).

Figure 38 illustrates the percentage change in axon number from proximal to distal (i.e. branching). In the repair group the degree of change falls over time. This does not occur in the graft group.

considerable variability in total axon numbers between specimens the degrees of branching were normalised as a percentage change proximal-to-distal (Fig 38). A comparison between nerve repairs, nerve grafts, and controls showed significant difference in percentage change (P=0.007, two way ANOVA). The percentage change in the graft group did not change with time. However, in the repair group the percentage increase in axons numbers (i.e. branching) fell over time. Whilst there was no difference between four and six weeks in the repair group the change between six and twelve weeks was significant (p=0.013) and that difference was even stronger when comparing the four and twelve week points (p<0.001).

The percentage change in the graft and repair groups diverge significantly over time (P= 0.01, linear regression, Fig 39) which supports the idea that the repair group is undergoing a change that is not occurring in the graft group. The fall in percentage change and the overall reduction in the number of distal axons possibly represents the pruning of axons that did not successfully innervate distal targets (94,95). The percentage change in axons in the graft group remained constant over time suggesting that whatever process was occurring in the repair group was not replicated in the graft group. This may reflect a lack of remodeling of the axons in the graft group.

Axon diameters were measured at the proximal and distal locations (Fig 13). In both intervention groups the mean diameter of axons increased over time (Table 11). In addition the mean diameters increased from proximal to distally but did not achieve the mean of the control group at either position (Fig 39). The mean diameters of axons in the repair and graft groups were smaller than the control group both proximally and distally. In the intervention groups there are

Table 11.

Axon Diameters proximally and distally in repairs and grafts compared to controls. Mean ± Standard Deviation (n)

	Weeks	Proximal Diameter µm	Distal Diameter µm
Control		8.0 ± 1.2 (313)	7.7 ± 1.2 (393)
Repair	4	4.2 ± 1.8 (243)	3.9 ± 1.5 (489)
	6	4.3 ± 1.4 (273)	4.5 ± 1.3 (394)
	12	5.6 ± 1.7 (239)	6.5 ± 1.6 (295)
Graft	4	3.7 ± 1.4 (268)	4.4 ± 1.3 (342)
	6	4.4 ± 1.6 (233)	5.3 ± 1.8 (318)
	12	4.9 ± 1.6 (261)	4.9 ± 1.9 (365)

Figure 39.

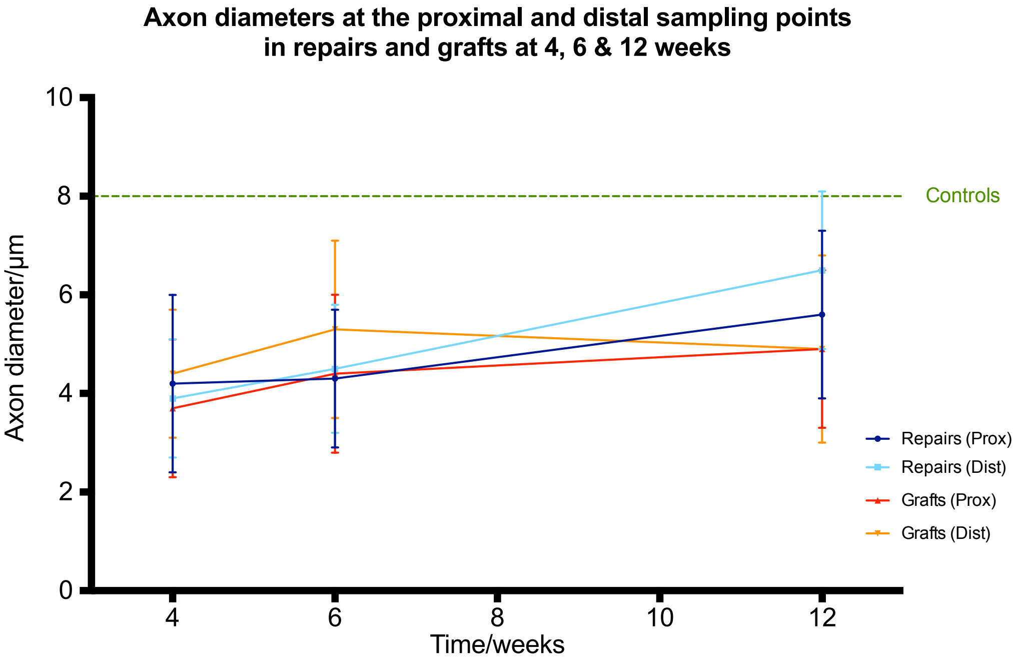

In both repairs and grafts the mean diameters of axons increase over time, at both sampling points. However, they never achieve the diameters of the control axons.In the grafted group the mean diameter of distal axons reaches asymptote at six weeks.

more axons per muscle, but the axon fibres were smaller than those in the control group. The axons in the intervention groups gradually increased in size over time. Two way ANOVA comparing intervention and time was not significant, either proximally or distally (Table 12). However, the intervention variable was significant at both sampling points (p<0.001).

Table 12.

Two way ANOVA and Tukey's test of axon diameters comparing controls with nerve repairs and nerve grafts over time (p values).

Source of Variation	Proximal p value	Distal p value
Intervention	<0.001	<0.001
Time/weeks	0.116	0.163
Intervention * Time	0.452	0.130

All pairwise multiple comparison analysis (Tukey's test) of the interventions shows that both repairs and grafts are significantly different from controls, but not from each other, proximally and distally (Table 13).

Table 13.

Two way ANOVA and Tukey's test of axon diameters comparing controls with nerve repairs and nerve grafts (p values).

Comparison	Proximal p value	Distal p value
Controls Vs Repairs	<0.001	<0.001
Controls Vs Grafts	<0.001	0.163
Repairs Vs Grafts	0.490	0.759

Figure 40

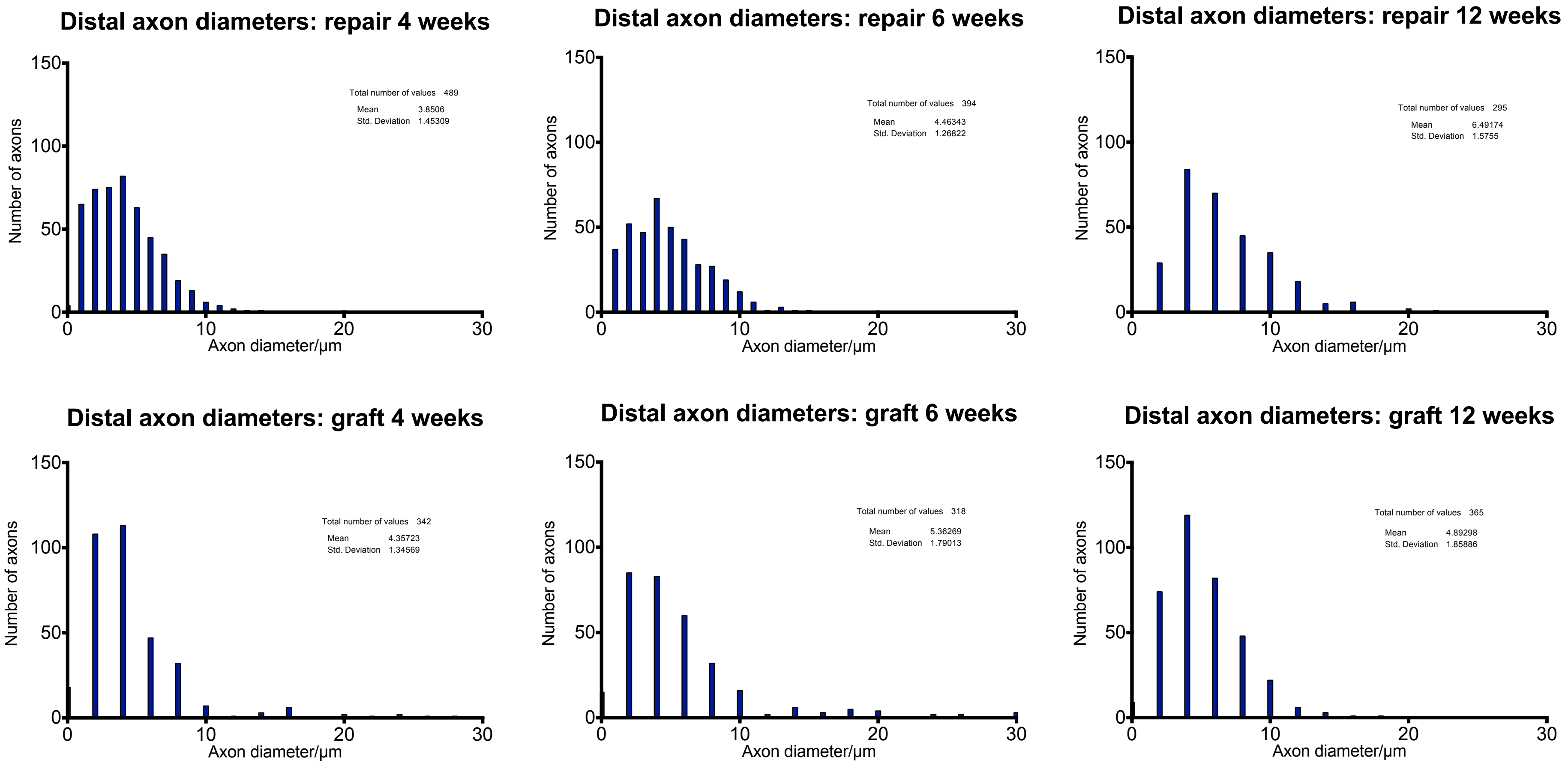

In controls there is an even, unimodal distribution of axon diameters around a mean of 7.7μm. In both interventional groups there are a large number of much smaller axons and the histograms are skewed towards the small calibre fibres. In both repairs and grafts the diameters increase but they remain small and skewed towards the left.

The diameters of control axons ranged from 3.1µm - 17.7µm proximally and 2.1µm - 14.8µm distally. At 4 weeks after repair or graft there was a large population of axons with diameters less than 2.5µm. This population was apparent both proximally and distally. Histograms of axon diameter were skewed to the left with very few axons greater than 8µm in diameter. The population of small axons diminished over time and the means of both the interventional groups increased between four and twelve weeks (Fig 40). In the grafted group there was a small number of axons at four and six weeks with large diameters (20-30µm) that were not present at twelve weeks. These large axons were not present in the repair group at any time.

The total cross section of all the axons innervating the muscle gives a measure of the innervating capacity of the nerve independently of whether the axons are individuals or sub-branches. In both intervention groups, at all time periods, the total area of proximal axons remained smaller than controls (Fig 41). Two way ANOVA was not significant (p=0.611), however the difference between the intervention groups was (p<0.001). Tukey's test shows the total axon surface area was larger than both repairs (p=0.008) and grafts (p<0.001) and that grafts were smaller than repairs (p=0.011). The total area of axons in the repair group initially fell between 4 and 6 weeks then increased again at 12 weeks. In the grafted group there was a steady increase from 4 to 12 weeks but the areas always remained smaller than the repair group, and the controls.

Distally there was no difference (two way ANOVA) in total axon area between controls and either repairs or grafts at any time period (p=0.557). The total areas appeared more stable than the proximal sampling point (Fig 42). The repair groups did show a very slight increase over time whilst the graft group increased between 4 and 6 weeks and decreased again towards 12 weeks.

Figure 41

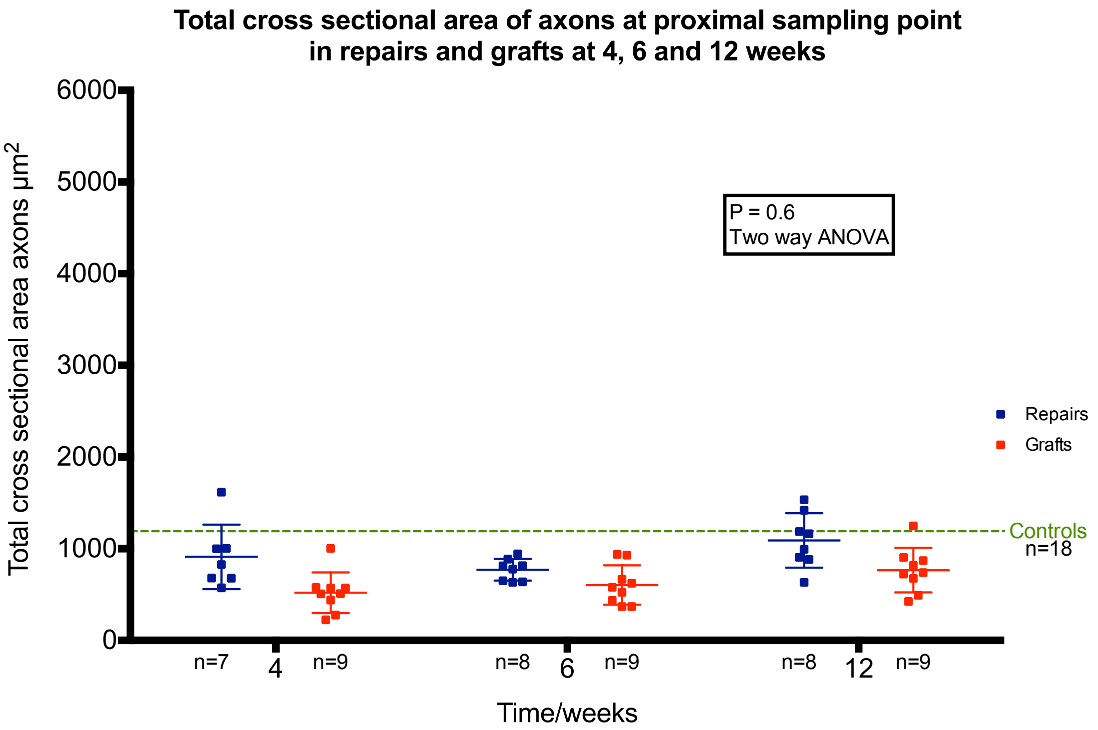

Figure 42

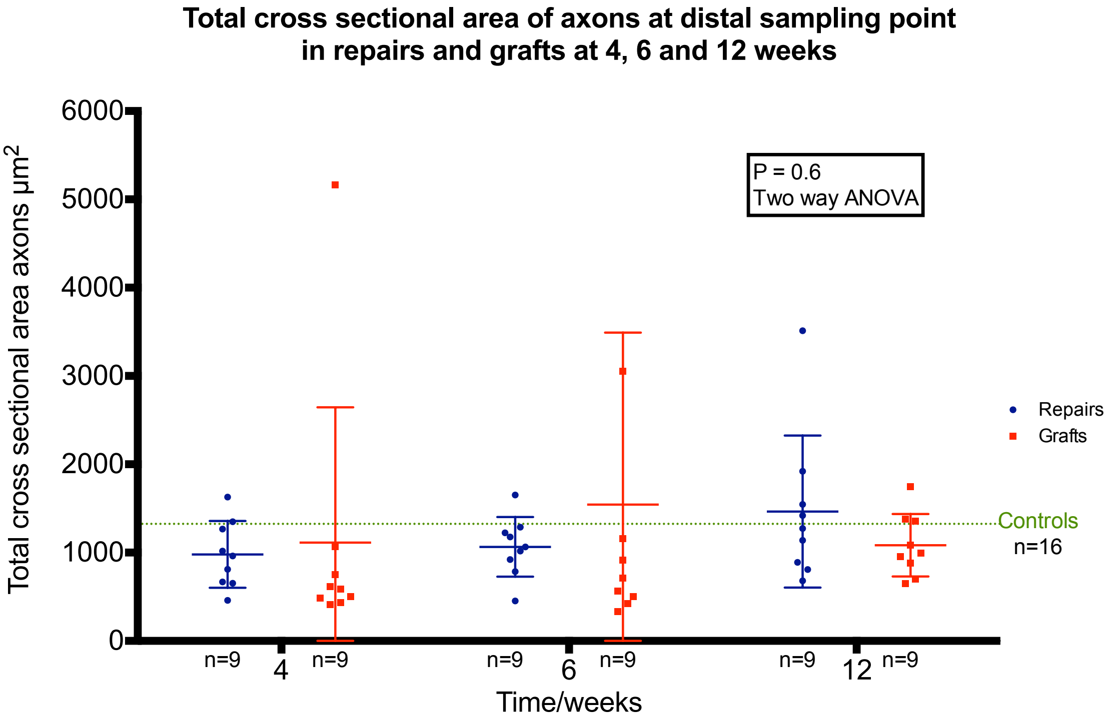

Two way ANOVA of total axon cross sectional area of repairs, grafts and controls was not significant at either the proximal (fig 41) or distal (fig 42) sampling points over time. However, Tukey's test showed that proximally the difference between both controls and either repairs ($p=0.08$) or grafts ($p<0.001$) was significant, and that grafts were smaller than repairs ($p=0.01$).

In the control specimens the total cross sectional area of axons increased by 11% proximal to distal whereas the number of axons increased by 19.7% (Table 14). The increase in axon number was greater than the increase in cross sectional area suggesting that each axon divides and tapers towards the muscle. This relationship was also seen in the repair group at four weeks. There was a large increase in axons but minimal increase in area. By six weeks this was reversed and the increase in area was larger than the increase in axon number, a trend that was even more apparent at twelve weeks. This suggests that the axons were increasing in size towards the target organ and smaller axons were being pruned. In the graft group the increase in diameter was also greater than the increase in axon number over time. However, the trend is the reverse of the repair group over time. At four and six weeks the increase in cross sectional area was far larger than the degree of branching. At twelve weeks the degree of branching had increased (to a percentage similar to that in repairs at four weeks) and the increase in cross sectional area had lessened. Neither group (repair or graft) achieved the proportions identified in the control group. This ongoing change may represent remodeling and pruning of axons. However, the timescale for remodeling is not clear. The total cross sectional area seems stable in the repair group from six weeks whilst it continues to change in the graft group. In both groups the percentage change in axon numbers is still evolving at twelve weeks.

Table 14.

Percentage change in total cross sectional area and axon number from proximal to distal in repairs and grafts at four, six, and twelve weeks, and controls.

	Controls		Repairs		Grafts	
	CSA	Axon No.	CSA	Axon No.	CSA	Axon No.
Controls	11.3%	19.7%				
4 Weeks			7.5%	49.0%	114.0%	27.5%
6 Weeks			38.3%	33.5%	115.7%	36.3%
12 Weeks			34.5%	3.9%	41.4%	40.3%

Mean motor unit size was calculated by dividing the number of neuromuscular junctions by the proximal number of axons. There was branching between the proximal and distal ends of the terminal nerve so using the proximal axon number as the denominator gives an accurate representation of motor unit size than the distal number. Two way ANOVA comparing intervention groups with controls was not significant (p=0.568) for both intervention and time. The mean motor unit sizes in both intervention groups (Repairs 8.9 ± 2.8 junctions/axon; Grafts 10.4 ± 4.7 junctions/axon) were significantly smaller than the control group (14 ± 2.5 junctions/axon; p<0.001). However, there was no significant difference between the two intervention groups (p=0.217). This suggests that each axon innervates a smaller number of junctions in the intervention groups than in the control group. In the repair group the size of the motor units increased over time (Fig 43). The graft group showed an initial increase followed by a decrease but the trend was one of motor unit size reducing in size (Table 15).

Table 15.

Mean motor unit sizes for both intervention groups at four, six and twelve weeks and controls. Mean ± Standard Deviation (n)

Time/Groups	Repairs junctions/axon	Grafts junctions/axon
4 weeks	7.8 ± 1.7 (7)	10.8 ± 5.7 (9)
6 weeks	9.4 ± 2.5 (8)	11.5 ± 5.3 (9)
12 weeks	9.3 ± 3.7 (8)	9.0 ± 2.9 (9)

Figure 43

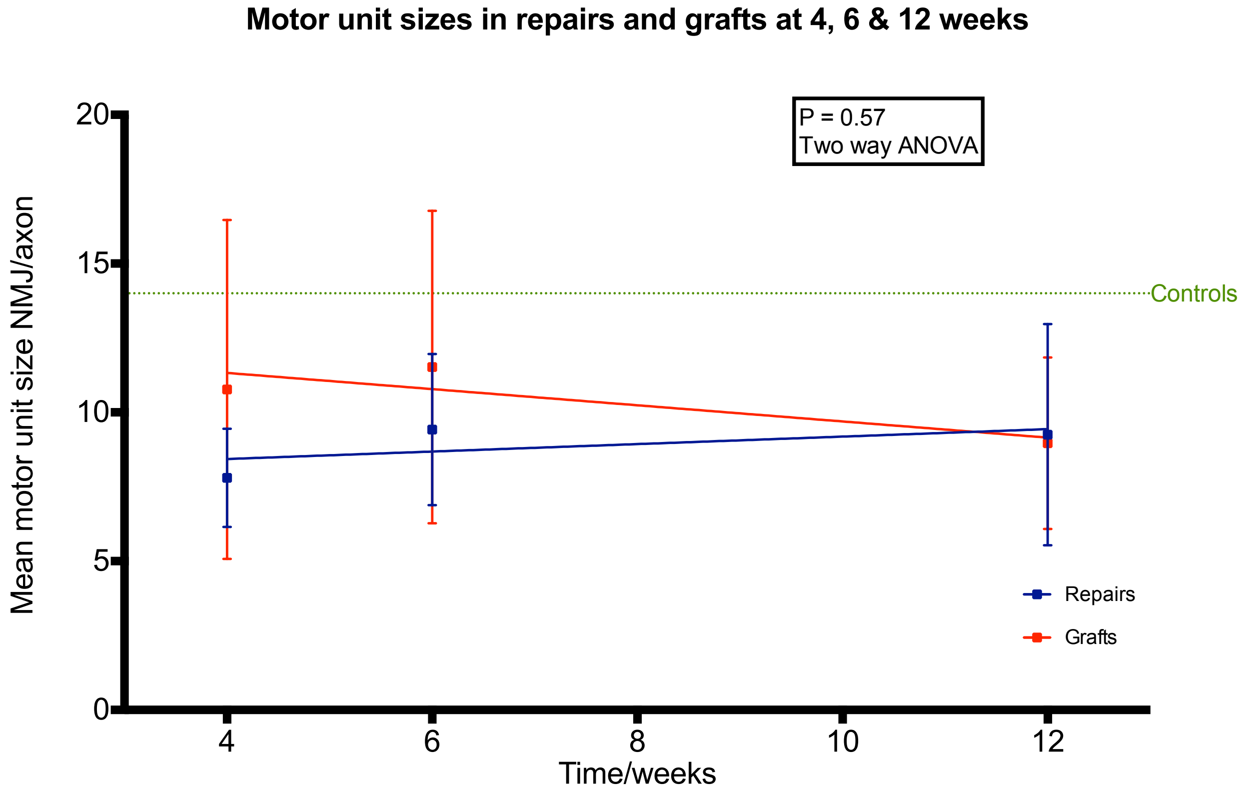

Two way ANOVA showed no difference between the mean motor unit size in controls and either intervention group. However, the mean motor unit sizes were smaller than controls for both interventions at all time points. The trend over time shows the number of motor units increasing in the repair group and decreasing in the graft group.

Labeling of myelin basic protein was identified around all axons in both the repair and graft groups at twelve weeks. In most specimens there were some empty myelin tubes that had not been reoccupied by regenerating axons (Fig 44). In a few cases where several small axons were very close together it was not possible to achieve sufficient resolution to elucidate whether they were in separate sheaths. In one animal the connective tissue fluorescence (*vide supra*) in some control specimens was present. In this case several small axons were shown occupying a single myelin sheath (Fig 45). This is consistent with the literature and probably represents multiple branches of a common axon within a single sheath (301).

Figure 44.

Confocal microscope images of myelin basic protein immunofluorescence in nerve repair and nerve graft mice

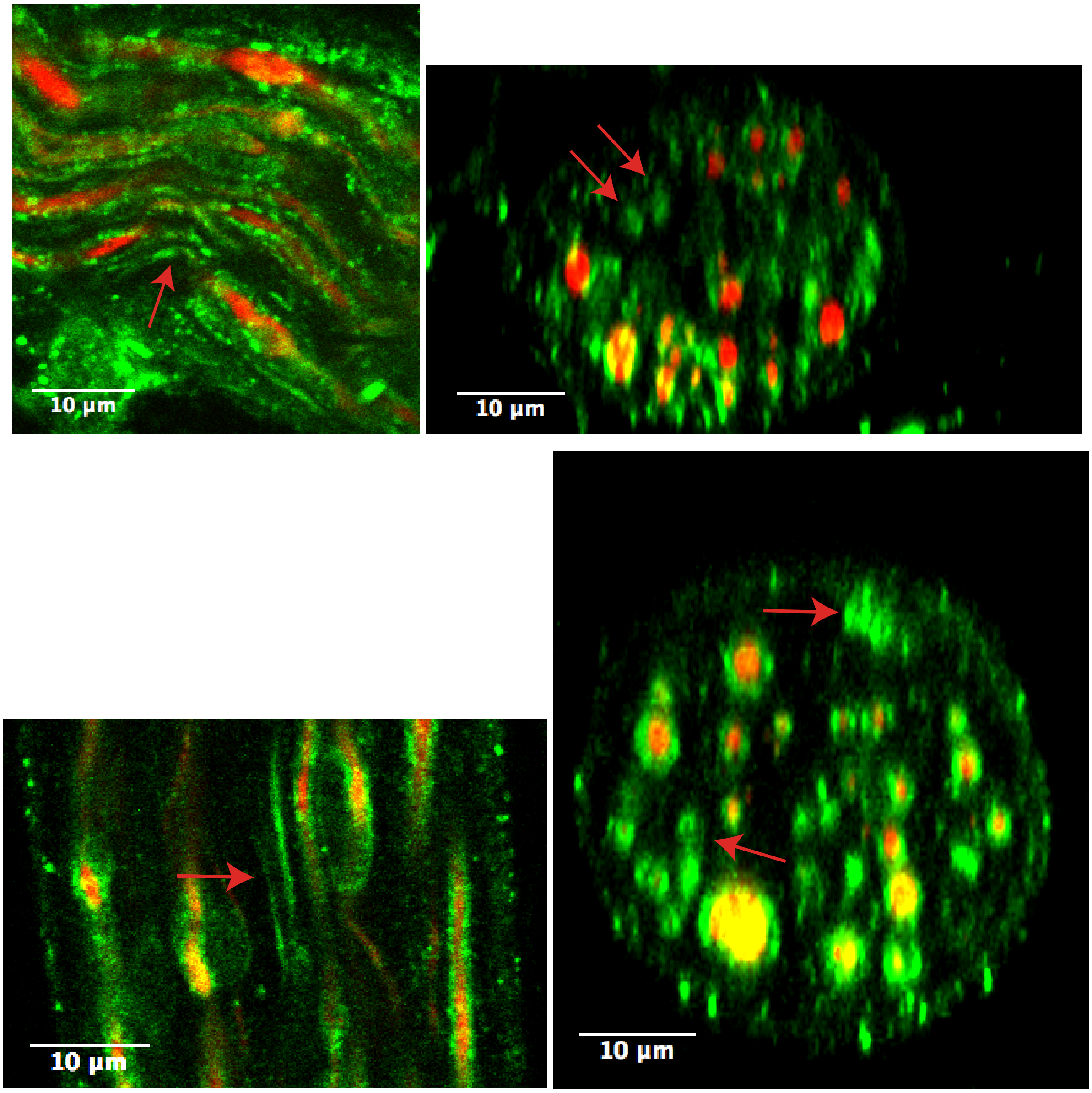

In these double-labeled confocal images (X60) axons are represented in red (YFP) and myelin in green (myelin basic protein antibody). The upper two images are from a nerve repair specimen at twelve weeks post intervention. The lower two images from a nerve graft specimen at twelve weeks post intervention. In both cases all axons are surrounded by a myelin sheath. The red arrows illustrate empty myelin sheaths.

Figure 45.

Two photon microscope images showing multiple axons in single myelin sheaths and empty sheaths.

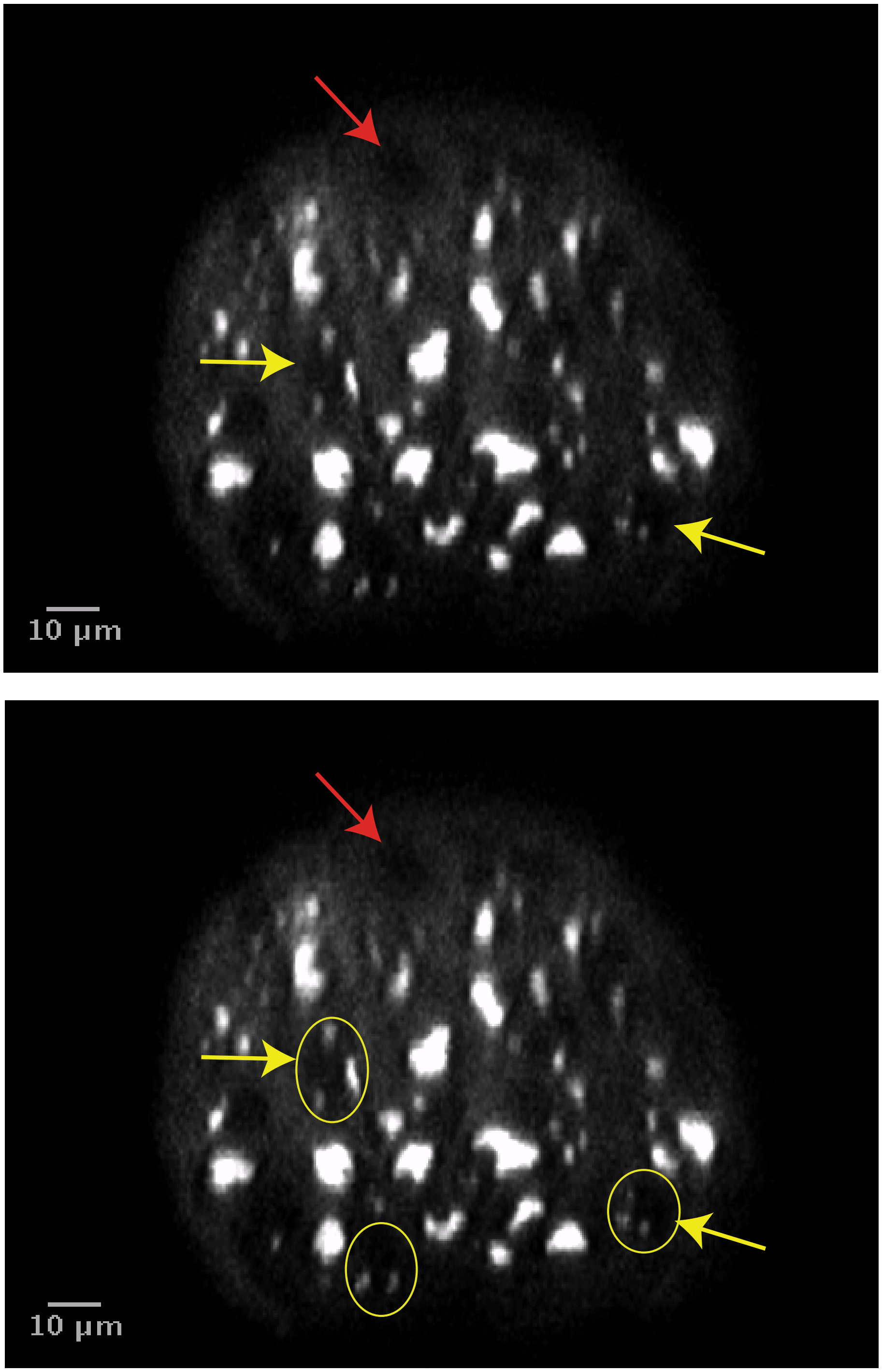

This is a single-channel, two-photon image of a nerve repair specimen at six weeks. Axons have a bright signal and connective tissue is faint. The black spaces are Büngner's bands. It is not possible to ascertain the presence of myelin in this image. The red arrow indicates an unoccupied sheath. The yellow arrows indicate multiple axons within a single sheath. The yellow circles highlight these sheaths in the lower image.

5.3 Summary

After nerve repair and graft, axons re-innervate the end-plate arbor within the muscle. The number of neuromuscular junctions remained constant across both intervention groups and controls. The number of axons that regenerate in the intervention groups appeared to be greater than those present in the control group. However, these axons are a mixed population with some large fibres and many smaller fibres. In the repair group the number of axons falls over time. This process was not identified in the graft population.

The literature supports the notion that regenerating axons undergo branching and subsequent remodeling over time. However, estimates of the number of new fibres per original axon vary widely (106,302-304). The patterns of reinnervation and motor unit size influence the characteristics of the muscle. The proximal number of axons is a more accurate representation of the true number of regenerating axons but still includes a mixture of axons and sub-branches from divisions that have occurred more proximally. Two techniques were employed to unravel this issue. The first was to analyse more closely the characteristics of the regenerating axons. The second was to use a different transgenic, the YFP-H, which is sparsely labeled to better visualize the patterns in the regenerating axons (see chapter 7).

6.

Characterisation of the changes in motor unit size by controlling for axon size in YFP-16 mice

6.1 Introduciton

The cross sections of the nerves show that the populations of axons between the intervention and control groups appear different. The controls exhibit an homogenous collection of axons that appear similar in size. The axons in the repair and graft groups are heterogeneous with a few large fibres and multiple smaller ones (Fig 46). One possible reason for this change is that each axon is giving off multiple branches. Each division could be symmetrical producing equal smaller neurites, or asymmetrical retaining some larger and some smaller branches. Studies of YFP-H specimens suggest that both scenarios are possible (Fig 47).

In the same way that branching occurs between the proximal and distal ends of the terminal nerve to the muscle, it is likely that branching occurs between the site of surgical intervention and the start of the terminal nerve. This is supported by previous studies that show axons branching both before and after a site of injury (104,305-308). Tracing the sparse labeled YFP-H mice also showed this to be possible (Fig 48). It can be assumed that not all of the axons counted at the proximal site originate from different cell bodies; some are likely to be branches of individual axons. To get an accurate estimation of motor unit size it is crucial to know which of the axons entering the muscle are true individuals and which are branches.

Figure 46.

Two photon microscope image of cross sections of the terminal nerve to interscutularis in a control, a nerve repair and a nerve graft mouse

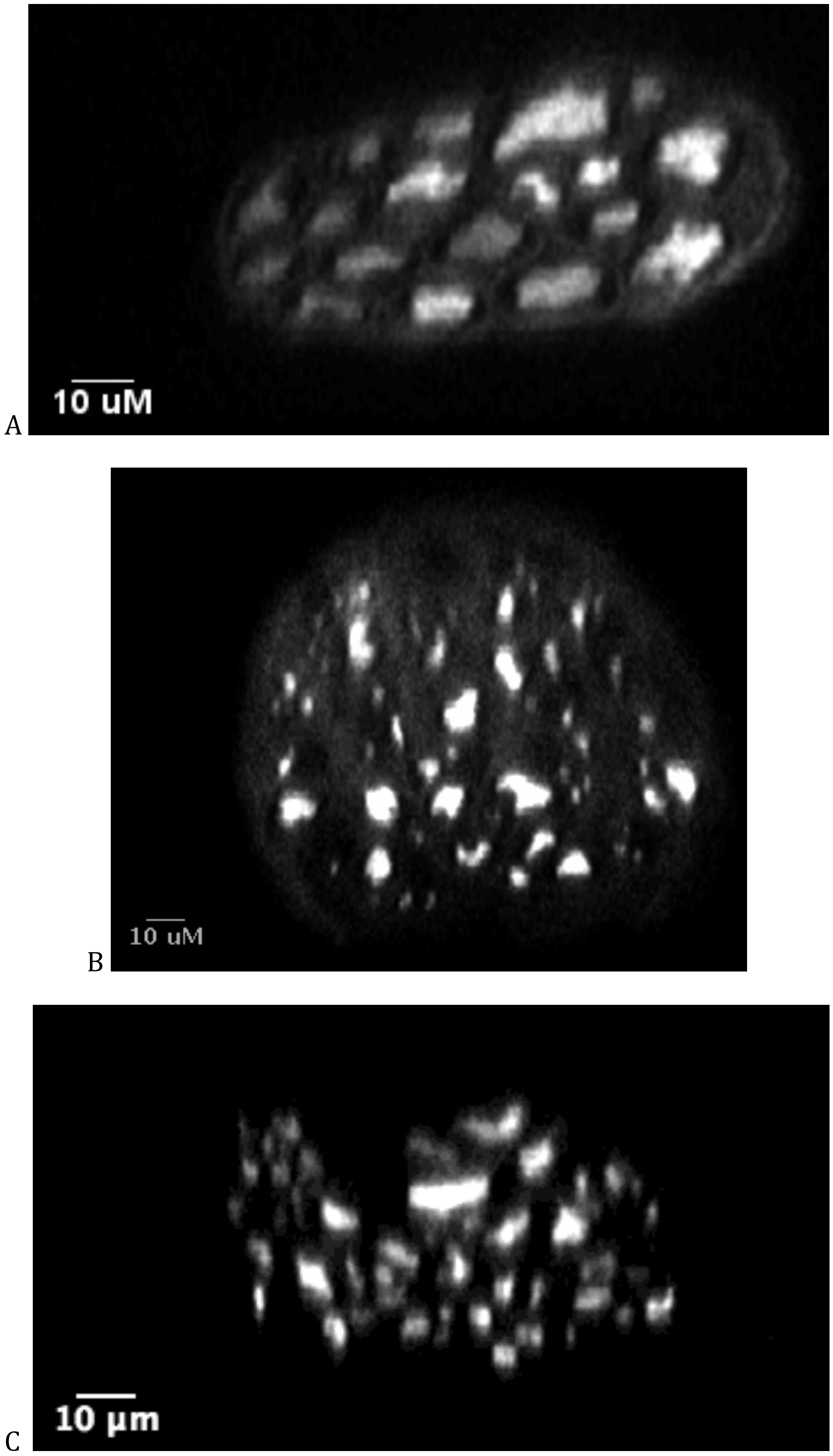

The single channel images are digital cross sections of image stacks taken in a two-photon microscope (63X). They show distal nerves at the junction with the muscle: A = control, B = repair at twelve weeks, C = graft at twelve weeks. The populations of axons in the intervention groups are more heterogeneous than the controls with a wide variation in their calibre and cross sectional outline.

Figure 47.

Two photon miscroscope image showing an axonal branch point in a YFP-H mouse after nerve graft

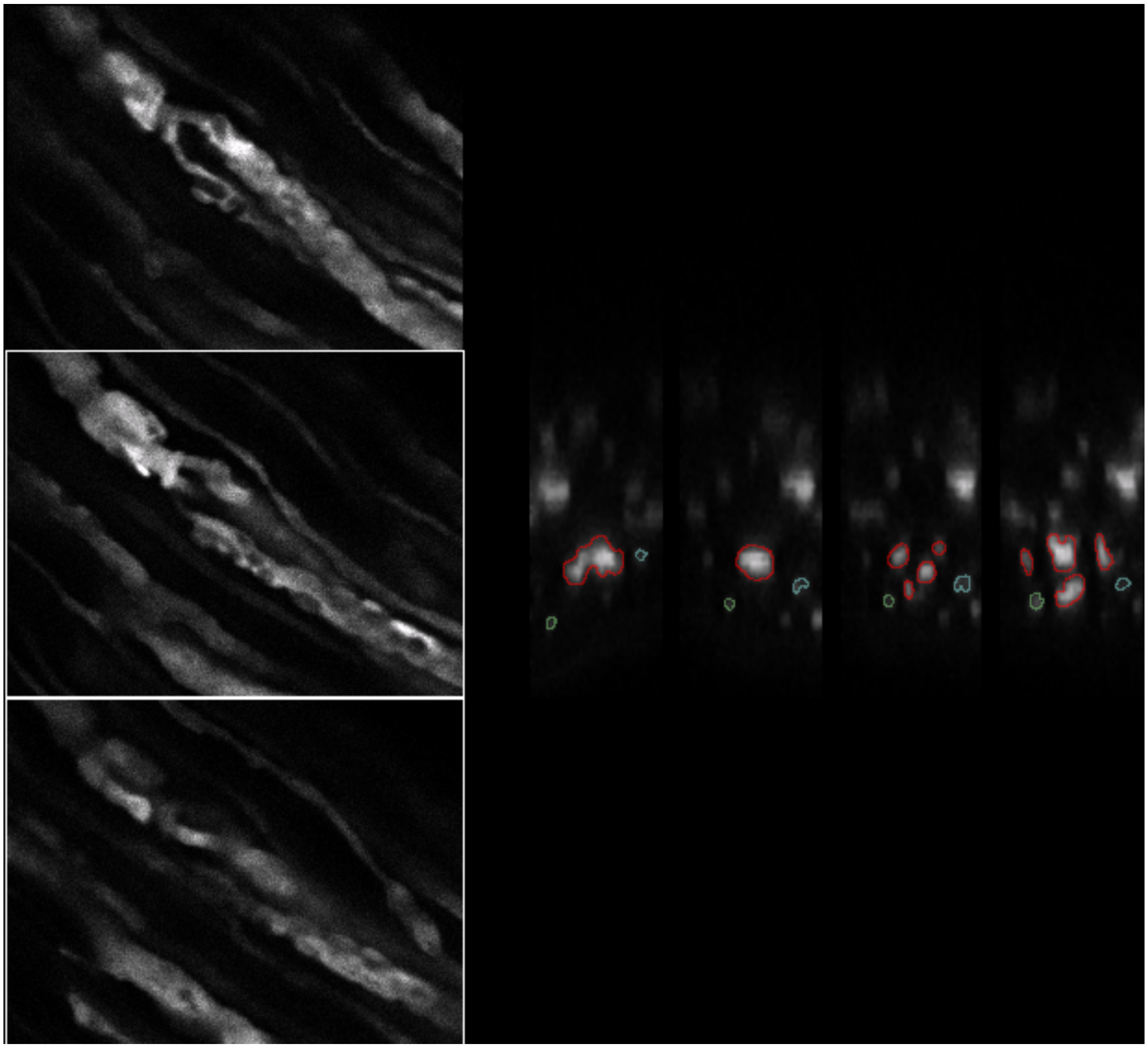

This shows an axonal branching point within a nerve. The images on the left show the irregularity of the axonal outline alternating between pinch points and bulges. It is easy to see how these could be mistaken for branch points without the benefit of 3 dimensional stacks of images. The images on the right show where serial cross sections have been taken to follow and analyse sub-branches of a single axon (red outline). The branches are not equal in calibre.

Figure 48.

Two photon microscope montages of YFP-H mice after nerve repair and traced axons illustrating branching patterns

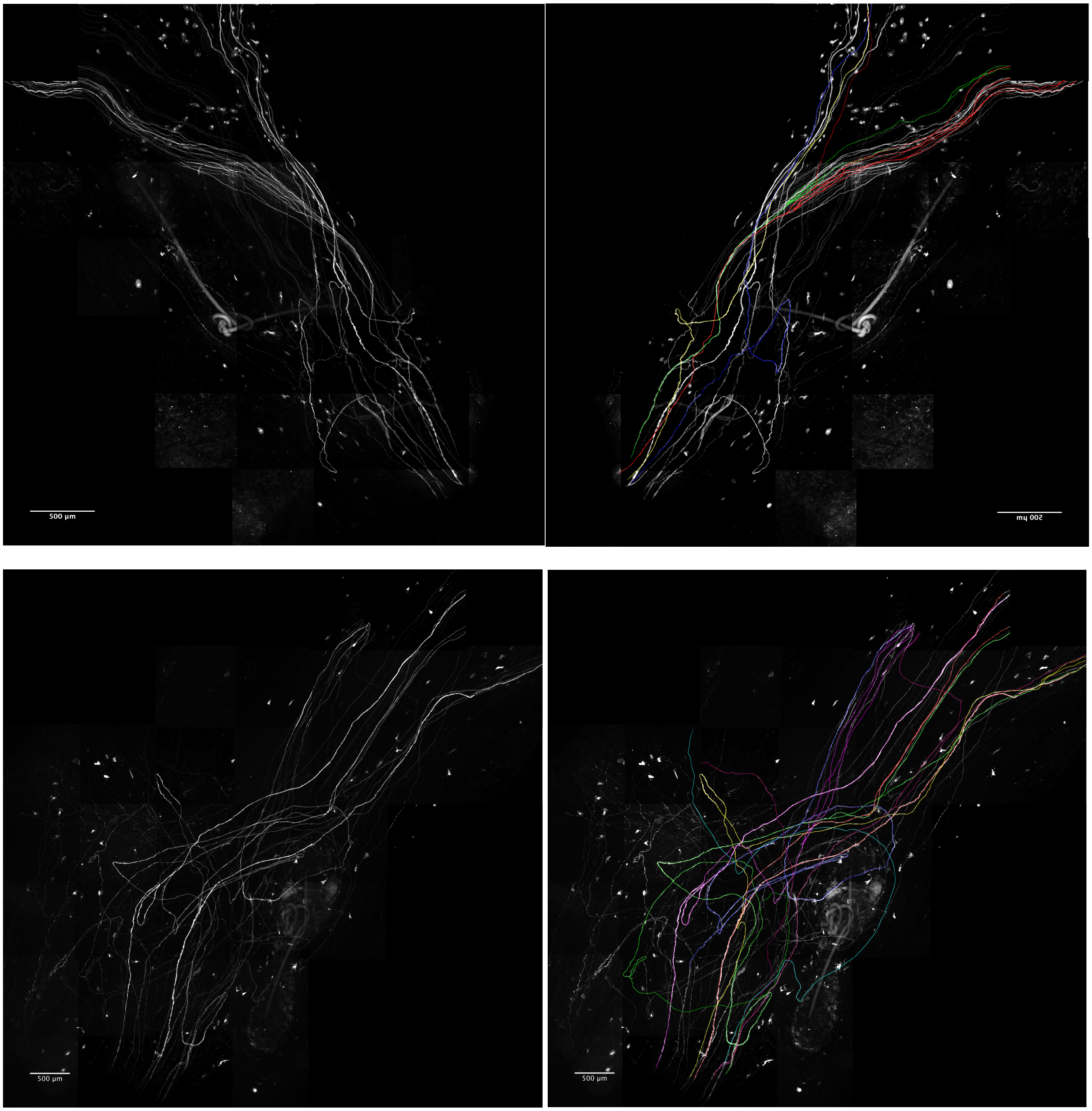

These are single channel two photon images of YFP-H sparse labeled specimens. Each is an example of a neuroma (left) which has been traced with each axon represented with a separate colour (right). The interesting features are the lack of branching at the point of the neuroma itself, with several axons subsequently branching in the distal nerves. In the upper image the red axon and the magenta axon in the lower image distribute of branches of individual axons into separate terminal nerves. This is physical evidence for synkinesis, with a single axon innervating different muscles.

The diameters of the axon populations vary significantly between the control and intervention groups. Some of the axons in the intervention groups are similar to those of controls, but many are smaller. These may represent sub-branches, which is supported by the reduction in axon numbers with remodeling. Some resemble be sensory or sympathetic fibres (Fig 49), neither of which would contribute to motor reinnervation. The original nerve to interscutularis contains only motor fibres (263). These could be fibres from other branches of the posterior auricular nerve that have entered the terminal nerve to interscutularis inappropriately.

The traditional method for estimating the number of regenerating axons is to biopsy the distal end of the nerve or nerve graft. The biopsy is then stained with thionin and acridine orange, sectioned and imaged. The number of myelinated and unmyelinated fibres are counted (309). However, there are limitations to this technique. It cannot distinguish branches from true individual axons. This can create confusion even over short distances. In the present method a stack of digital cross sections runs over several microns. The morphology of an axon includes outpouchings that run alongside the main fibre for multiple slices. In traditional cross sections these would appear to be separate axons (Fig 50). Scrolling through a stack and tracing the outline of an axon minimizes the chance of these sampling errors occurring. This improves the accuracy but it was not practicable to create a digital stack that encompassed all axons from proximal to the repair site to the level of the neuromuscular junction. Lu managed a precise wiring diagram for the interscutularis in a small number of uninjured muscles, but only over a distance of approximately 5mm of the terminal nerve (252). It would not be feasible with current tracing algorithms to follow axons across the distance from the site of intervention to every junction in the muscle in a sufficient number of specimens to generate statistical power to comment on the difference between repairs and grafts.

Figure 49.

Confocal microscope image the end plate zone in a nerve cut mouse showing aberrant reinnervation

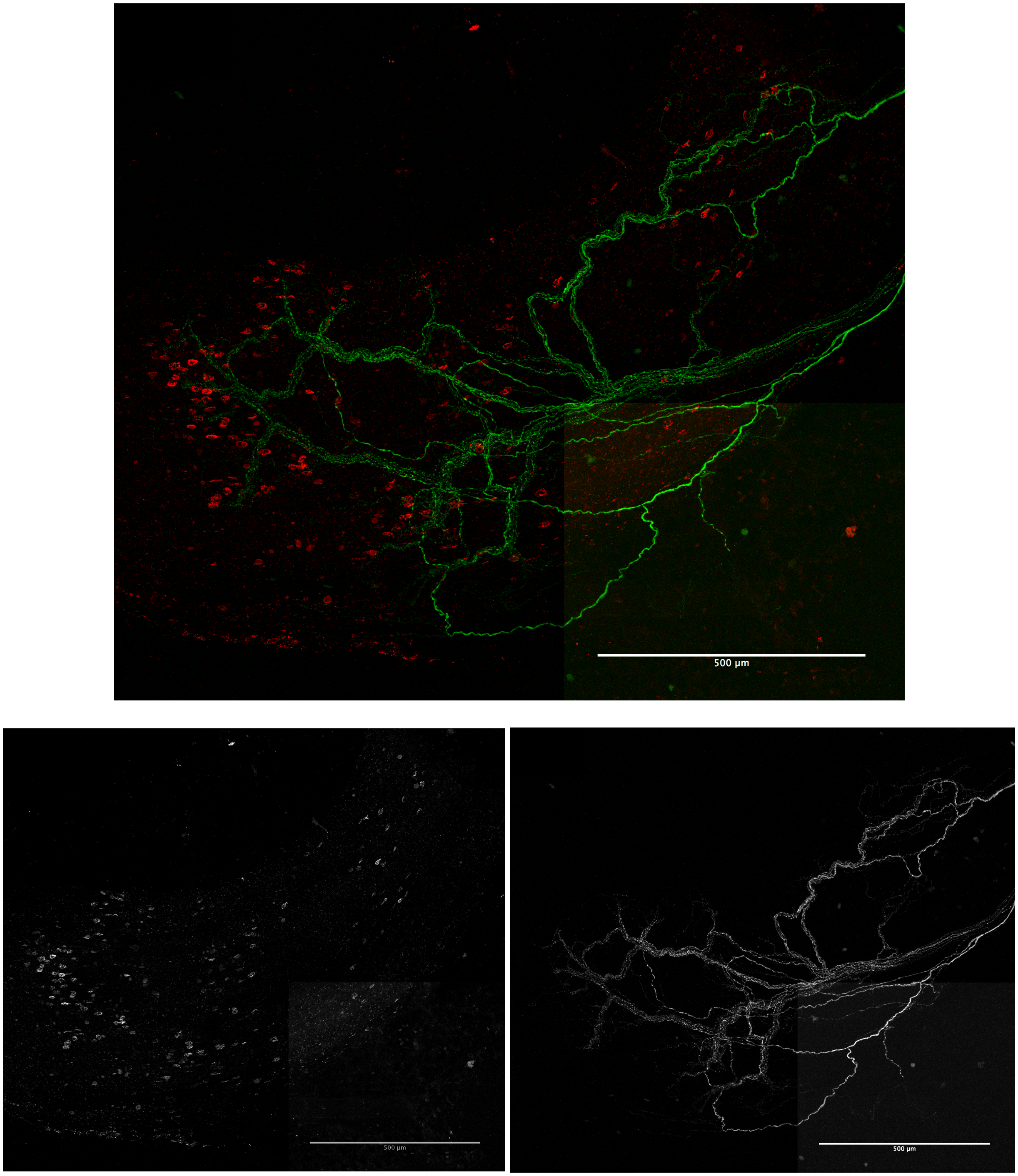

In this nerve cut specimen the neural arbor has been reoccupied by YFP axons. The axons have not re-established connections, or made de novo neuromuscular junctions, with the muscle, despite the presence of unoccupied junctions on the muscle surface. These YFP axons are still labeled with fluorophore, but have a very different morphology from the motor axons normally encountered innervating the interscutularis. They are of smaller calibre and have a characteristic wavy course that resembles sympathetic axons (personal communication with JW Lichtman).

Figure 50a.

Stack of two photon images showing details of axonal morphology at a node and possible branch point

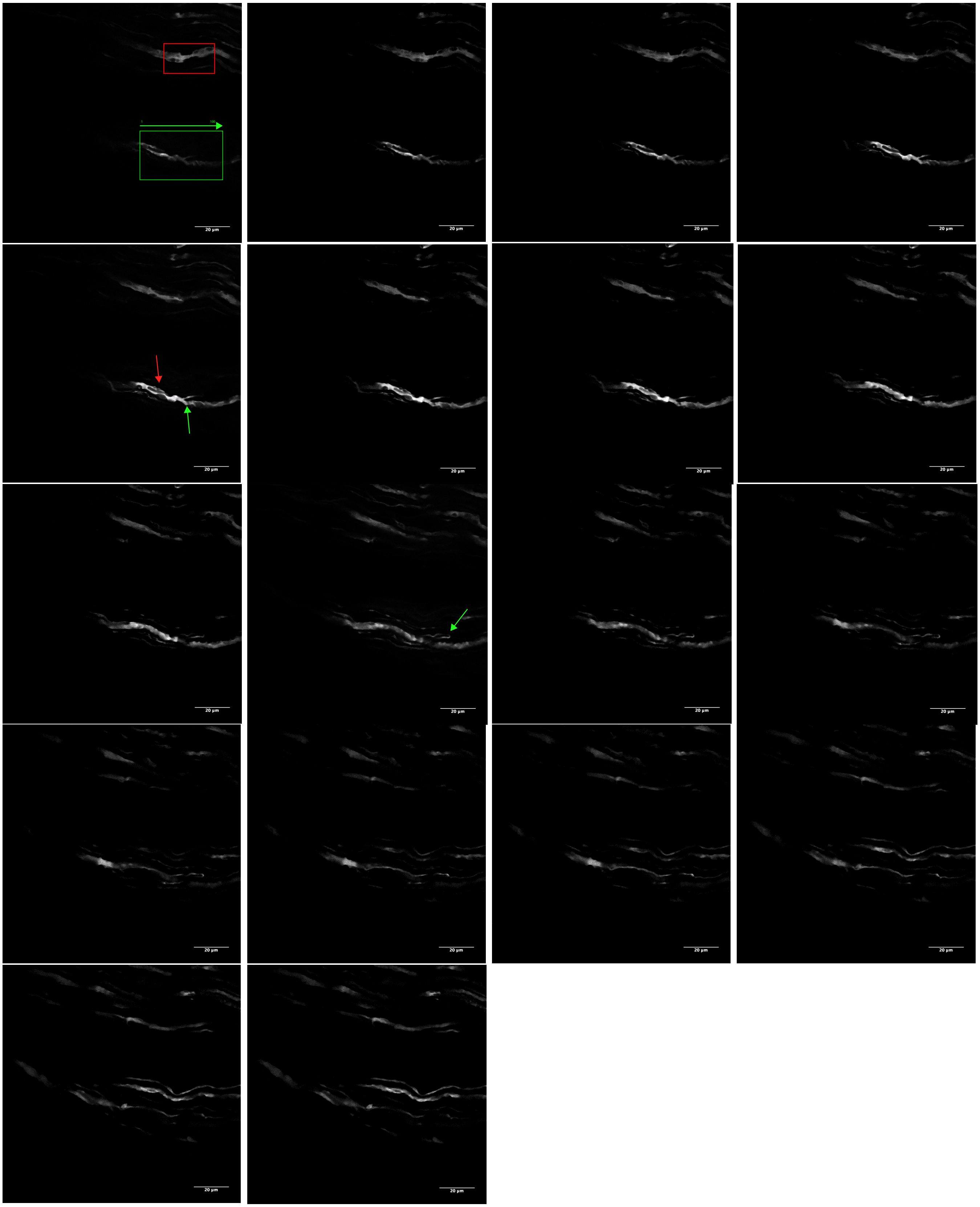

Figure 50b.

Stack of two photon images showing cross sections of the images from Fig 52a

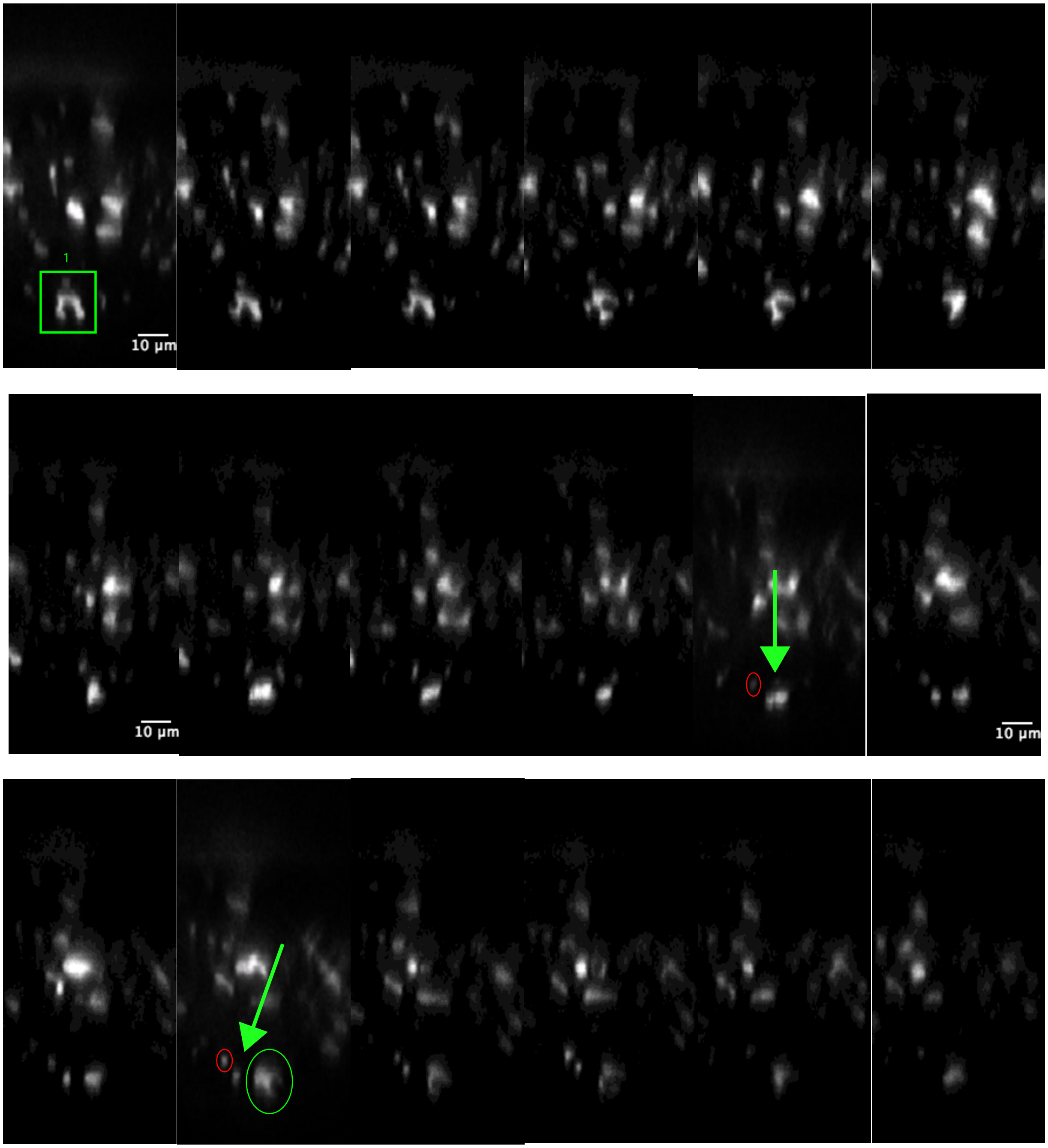

These are two-photon images of regenerating axons in a YFP-16 mouse six weeks after a nerve graft. The sequential series of images in figure 50a are part of a stack. In the first image of the sequence there are two axons in boxes. The red box shows the outline of an axon at the site of a node of Ranvier. This demonstrates the potential variation in axon calibre if sampled through a node. The axon in the green box has been digitally cross-sectioned in the direction of the arrow. Those cross sections are the sequence in figure 50b. In subsequent images from the stack the irregularities of the outline of this axon are demonstrated by the red arrow and a branching point by the green arrow. The sub-branch doubles back on itself (second green arrow). Figure 50b is the sequential series of digital cross sections. In the green box (section 1) the irregular outline indicated by the red arrow in figure 50a can be seen in cross section. These complex longitudinal bulges can easily be mistaken for branching points if a section were taken in isolation. Scrolling though the 3-dimensional stack enabled these sampling errors to be excluded. The green arrow indicates the point where the axon does branch. The red circle indicates where the sub-branch has doubled back and is travelling in the opposite direction. The point at which it doubles-back is in the last image.

The disparity between the control and intervention groups suggest that axon diameter could be used as a tool to estimate true axon numbers more accurately. A model motor axon population was calculated from two standard deviations of the mean diameter of the proximal axons in controls. This produced a minimum threshold axon diameter of 5.5µm. All axons with smaller diameters were excluded and the axon populations re-examined (Fig 51).

6.2 Results

The mean number of distal axons per specimen in the control group is 23.1 ± 5.8 (n=16). Thresholding reduced this to 20 ± 5.1 (n=16). The difference between the number of proximal axons and the number of *thresholded* distal axons was 2% (p=0.8, paired t-test, Fig 52). In the non-thresholded group there was an increase of 19.7% over the length of the terminal nerve. This supports the notion that sub-branches were excluded from the data and only true individual axons were retained.

In both intervention groups the number of proximal axons included within the threshold increased over time (Table 16). The repair group was stable at approximately 11 axons at weeks four and six but rose to 15 axons by week twelve. Conversely the graft group initially rose from 7 axons to 10 axons between weeks four and six but then remained stable between six and twelve weeks. These trends do not match those seen in the non-thresholded axon numbers (Fig 53). In the non-thresholded data the number of proximal axons falls in the repair group over time from 34.7 axons at four weeks to 27.6 axons at twelve weeks. In the graft group it remained stable at approximately 29 axons throughout (see Chapter 5).

Figure 51.

Cross section of a two photon stack of the terminal nerve illustrating thresholding of axons according to their calibre.

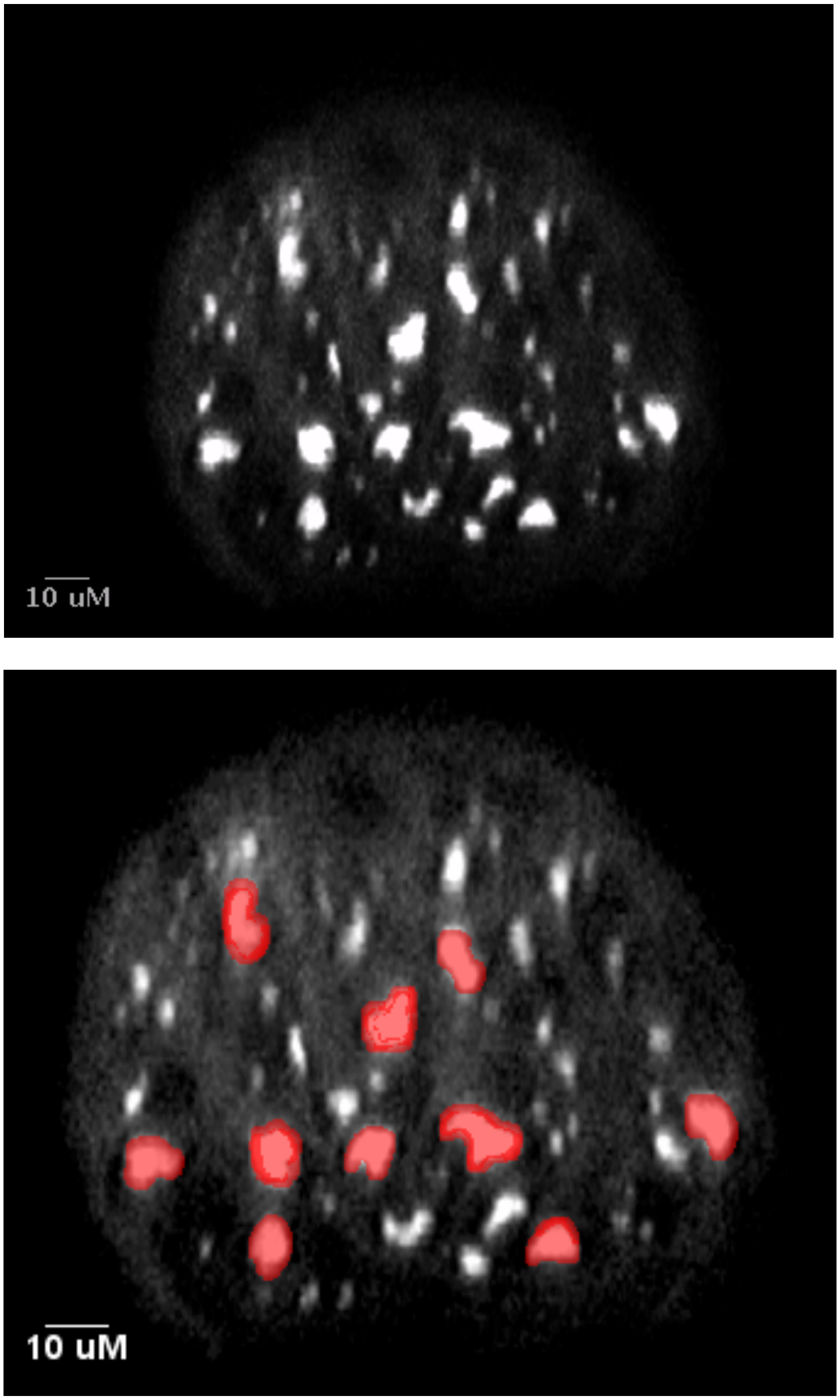

This is a digital cross section taken from a two-photon stack of images of a nerve in a YFP-16 mouse 6 weeks after nerve graft. The axons that are within two standard deviations have been highlighted in red.

Table 16.

Mean axon numbers after thresholding to exclude axons with a diameter less than 5.5µm. Mean ± Standard deviation (n)

	Weeks	Proximal Axon Number Mean (S.D., n)	Distal Axon Number Mean (S.D., n)
Controls		**19.6 ± 4.6 (16)**	23.1 ± 5.8 (16)
Repair	4	**11.9 ± 2.3 (**7)	13.1 ± 6.8 (7)
	6	**10.8 ± 1.3** (8)	16.6 ± 4.1 (8)
	12	**15.4 ± 5.2** (8)	**16.0 ± 5.6** (8)
Graft	4	**7.1 ± 3.3** (9)	9.9 ± 3.9 (9)
	6	**10.0 ± 4.0** (9)	12.9 ± 6.6 (9)
	12	**11.1 ± 3.3** (9)	**16.4 ± 6.0** (9)

The number of thresholded distal axons increased over time in both intervention groups, though the trend is the reverse of what was identified proximally. The repair group initially increased and then plateaued from six weeks. The graft group steadily increased throughout the time points. Both groups (repair and graft) converge at approximately 16 axons distally.

Comparing the change in number of axons proximal-to-distal in both groups over time between the thresholded and non-thresholded data it was apparent that these trends remained the same. In the repair group there was evidence of a remodeling process occurring. Over time the amount of branching levels off. This trend was not observed in the graft group and numbers steadily increased over time.

Figure 52

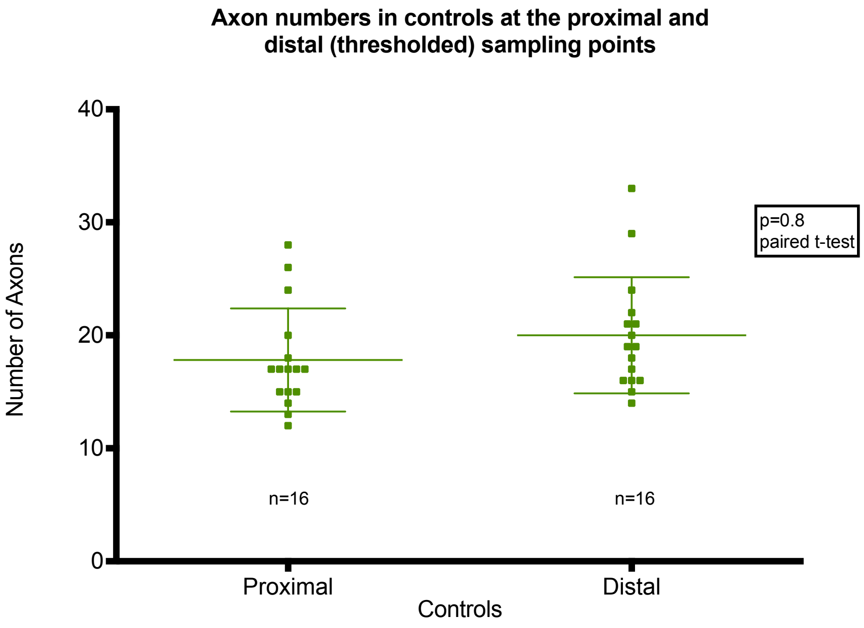

Figure 53

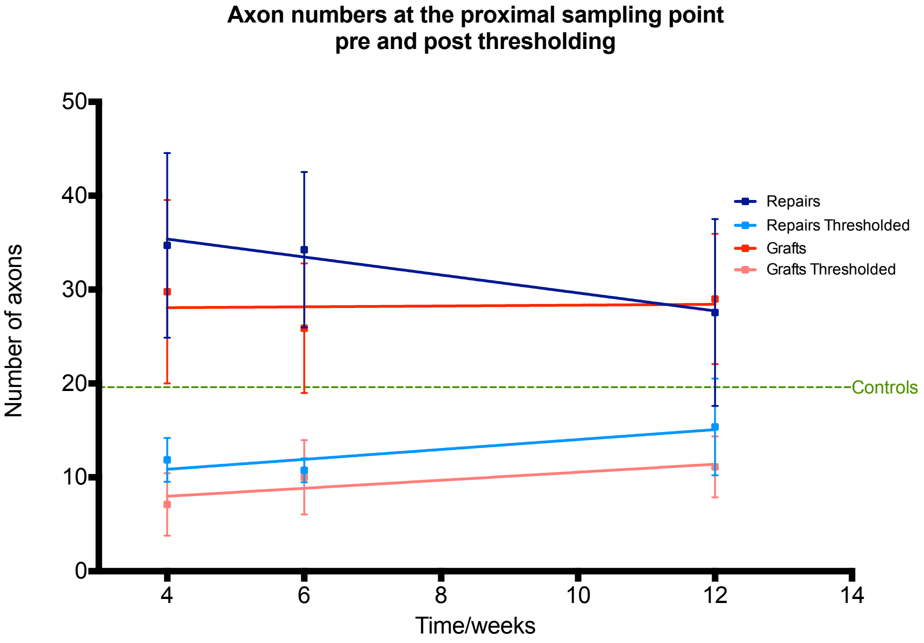

Figure 52 illustrates how thresholding axons in control specimens according to their diameters (2 s.d. of mean) removes the branches seen in the terminal nerve to interscutularis. There is no significant difference in axon numbers between the proximal and distal sampling points. In figure 53 thresholding at the proximal sampling point in the intervention groups reduces the number of axons to fewer than the controls at all time points. The trend over time is also reversed with both intervention groups now increasing the number of axons over time. Neither repairs of grafts achieve the same proportions as controls.

The mean axon diameters of each intervention, at each time period, were significantly smaller than controls (see Chapter 5). Once the diameters had been thresholded, the mean axon diameters of the intervention groups resembled the control population more closely (Table 17). However, they were still skewed towards smaller axons, and had fewer larger axons greater than 10μm in diameter than the controls populations (Fig 54).

Despite thresholding, the mean axon diameters of the intervention groups at the proximal sampling point were still not identical to controls. Whilst there was no statistical significance comparing intervention and time ($p=0.703$), the difference between the intervention groups was found to be significant ($p=0.008$). The mean axon diameters of the control group were significantly larger than the thresholded graft group ($p=0.007$), but the difference between the thresholded repair group and either the thresholded grafts, or the controls was not significant.

At the distally sampling point there was no significant difference in the diameter of the axons between either thresholded intervention and control groups ($p=0.371$) or between repair and graft ($p=0.714$) or at any time point ($p=0.435$).

Figure 54

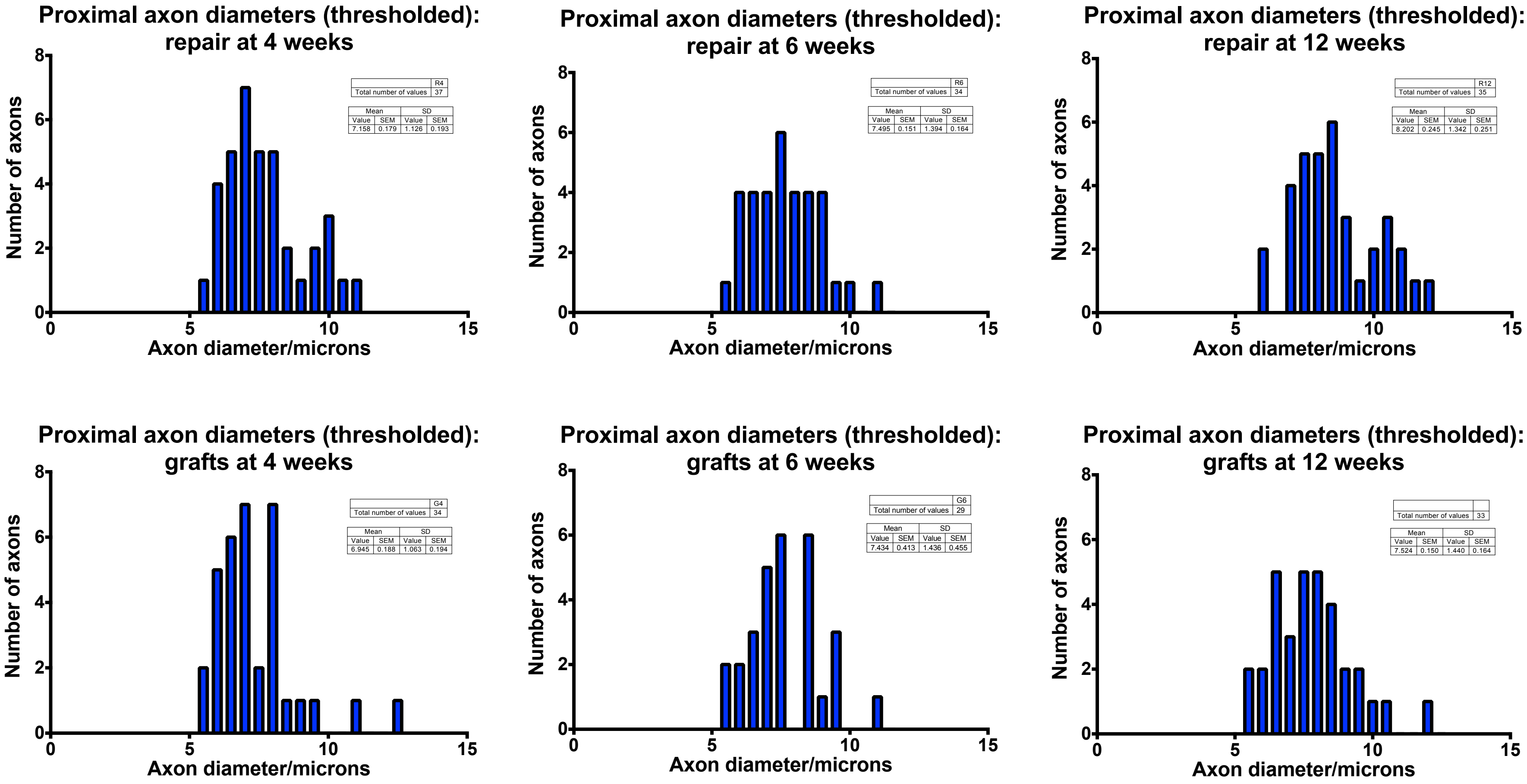

After thresholding the histograms of axon diameters for both intervention groups at the proximal sampling point resemble the control axon population much more closely. Two way ANOVA is not significant however, multi variant analysis shows the grafted axons to be significantly smaller than the controls (p=0.007). In both interventions the axon diameters are still skewed to the left and there are fewer axons greater than 10µm than in controls.

Table 17.

Axon Diameters (proximally and distally) in thresholded repairs and grafts compared to controls. Mean ± Standard deviation (n)

	Weeks	Proximal Diameter µm Mean (S.D., n)	Distal Diameter µm Mean (S.D., n)
Control		**8.0 ± 1.2** (313)	**7.7 ± 1.2** (393)
Repair	4	7.7 ± 1.3 (83)	7.3 ± 1.1 (137)
	6	7.7 ± 1.2 (87)	7.7 ± 1.2 (142)
	12	**8.5 ± 1.4** (123)	**9.0 ± 2.4** (167)
Graft	4	7.4 ± 1.4 (64)	7.0 ± 1.0 (89)
	6	7.7 ± 1.3 (90)	9.8 ± 3.1 (117)
	12	**7.8 ± 1.5** (100)	**7.7 ± 1.4** (148)

The motor unit size in the control group was 14.0 ± 2.5 junctions/axon (n=16). If thresholding data does give a more accurate count of the axons regenerating after repair or graft, by removing branches then it suggests that fewer axons re-occupy the neuromuscular arbor. This would increase the size of the motor units. Recalculating the motor unit sizes using these thresholded axon populations in each of the intervention groups both proximally and distally the mean motor unit size for repairs was 24.9 ± 10.76 junctions/axon (n=24) proximally and 20.0 ± 8.4 junctions/axon (n=27) distally. The graft group were 35.6 ± 24.3 junctions/axon (n=27) proximally and 26.2 ± 17.6 junctions/axon (n=27) distally. These motor units were larger (each axon innervates more junctions) than the control group. This contrasts with the non-thresholded data where they were smaller. They were also reducing in size over time for both repairs and grafts(Table 18, Fig 55). Since the number of neuromuscular junctions remained stable (*vide* *supra*) this indicates an increase in the number of axons included in the thresholding. This could indicate the growth in the size of true axons as sub-branches are trimmed due to remodeling.

Two way ANOVA of intervention and time illustrated that there was not a significant difference in the size of the motor units between the control and thresholded intervention groups (p=0.068). However, the difference between the groups was significant (p=0.012). The difference between the four and twelve week data sets also showing significance (p=0.016) as the axon populations are remodeled.

Table 18.
Motor unit size after axon diameter thresholding to exclude axons with a diameter less than 5.5µm. Mean ± Sandard deviation (n)

	Weeks	Proximal Motor Unit Size Mean (S.D., n)	Distal Motor Unit Size Mean (S.D., n)
Controls		**14.0 ± 2.5 (16)**	
Repair	4	**23.0 ± 7.3** (7)	22.0 ± 9.4 (7)
	6	**28.7 ± 3.5** (8)	21.0 ± 7.5 (8)
	12	**18.0 ± 5.7** (8)	**16.9 ± 8.2** (8)
Graft	4	**51.5 ± 33.6** (9)	32.5 ± 14.9 (9)
	6	**32.5 ± 17.5** (9)	30.1 ± 24.3 (9)
	12	**22.7 ± 3.2** (9)	**16.0** ± 4.0 (9)

Figure 55.

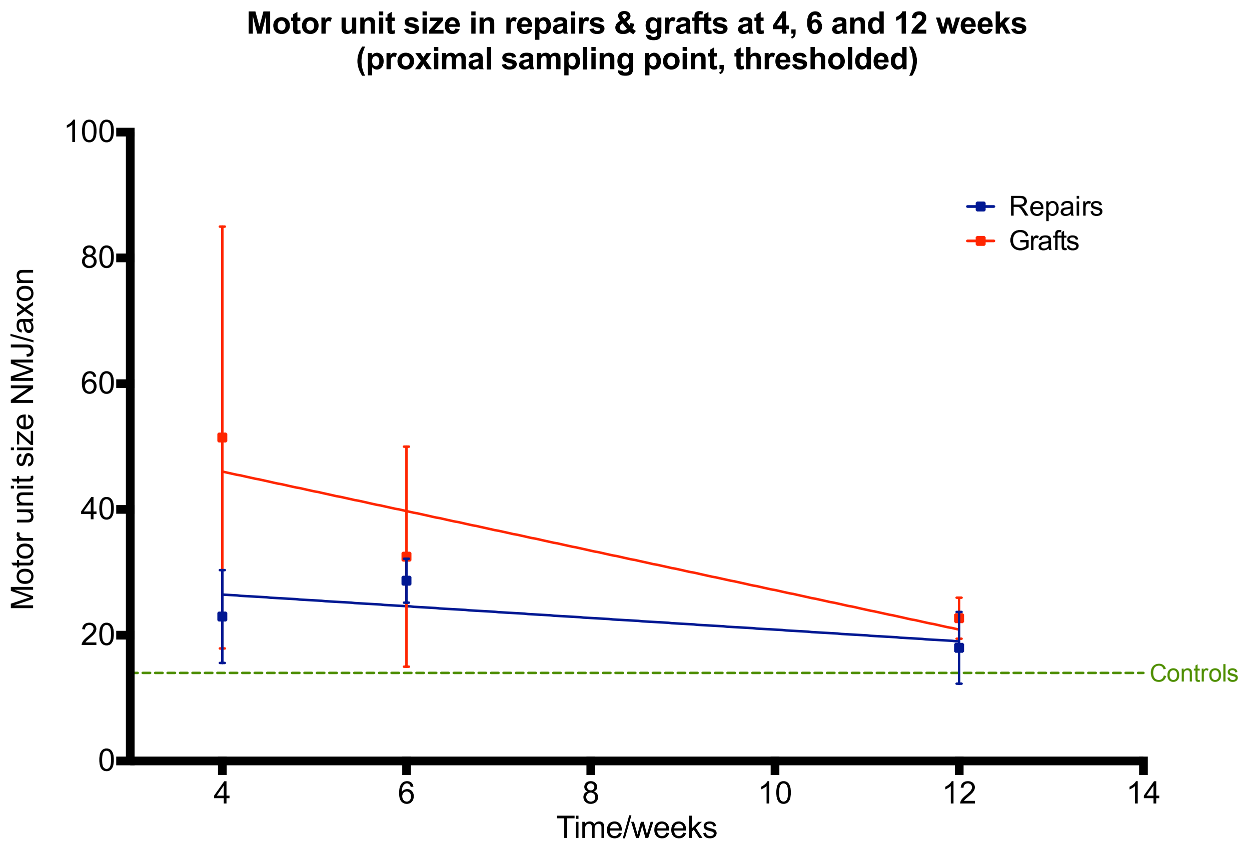

Motor unit size in repairs & grafts at 4, 6 and 12 weeks (proximal sampling point, thresholded)

This figure illustrates how the mean motor unit sizes in both intervention groups are much larger than controls when the axon numbers have been thresholded according to diameter. In addition the trend for the mean motor unit size to fall over time in both intervention groups. Previously this was seen only in the grafted group.

6.3 Summary

The smallest axonal fibres with diameters less than 2 standard deviations of the control population of motor axons are unlikely to contribute to motor reinnervation. If they are included in the calculation of motor unit size the motor units appear to be small. This would suggest that there are fewer muscle fibres per axon which would confer increased fine motor control. Over time the size of the motor units in this non-thresholded data increased as axons are remodeled and pruned. If these small axons are excluded the motor unit sizes of the intervention groups are larger than controls. This would imply that there are fewer individual axons regenerating to occupy the same number of junctions and muscle fibres which is consistent with approximately 40% of axons regenerating across a repair site (310). The number of thresholded axons at the proximal point increases over time in both interventional groups. This would be consistent with a gradual increase in diameter of some small axons (that are initially filtered out) as they take over the territories of less successful smaller sub-branches and get more of a foothold in the reinnervated muscle (298,311-315).

7.

Grapes, sprouts, bundles and branches: A qualitative characterisation of the intra- and extra-muscular changes seen after reinnervation in YFP-H and YFP-16 mice

7.1 Introduction

In the preceding chapters we have set out a quantitative evaluation of the patterns of reinnervation after nerve repair or nerve graft. An advantage of transgenic animals that express fluorescent proteins in their peripheral axons is that it makes it possible to image the entire arbor of that regenerating nerve. The regenerated axons are displayed almost as a time-lapse of the process of reinnervation. In addition to the statistical analysis it is useful to review the overall patterns of the reinnervation, more specifically focusing on the changes in the morphology of the axons and junctions that are not adequately communicated in a quantitative manner.

YFP is sparsely expressed in the YFP-H line with only 5-10% of axons labeled with the protein. This allowed us to view single axons without the distraction of the entire population. In a similar way to Cajal's silver staining, this allowed analysis of the patterns of regeneration taken by individual axons in the reinnervation of the muscle. Observing axons at twelve weeks, after remodeling has occurred, shows the branching patterns of successful axons that have made connections with NMJ in the muscle.

7.2 Results

There are several interesting results from this group. Some axons undergo multiple divisions at several distinct branching points to produce a myriad of sub-branches. Other axons have no branches at all. Some axons have sub-branches that enter different terminal nerves that supply different end-organ muscle targets. This is direct evidence of synkinesis. Some axons perform several loops at the site of the neuroma before entering the distal nerve, whilst others travel across the site of repair directly unhindered (Fig 48)

The data above has shown that there is no change in the number of junctions, but that the reinnervated junctions, in both repair and graft, are smaller than the control group. The junctions gradually increase in size over time but do not recover their original cross sectional areas, as demonstrated by the control junction population. In addition, there are changes in the junctional morphology that are harder to quantify. Many junctions lose their distinctive "pretzel-like" quality and the end-plate gutter becomes thinner and more fragmented. In a few cases the junction resembles a bunch of grapes with small beaded areas of double-labeled end plate receptors that are strung out and discontinuous. It is not possible to tell if these more disrupted junctions are single junctions that have disintegrated or areas of new junction forming *de novo* on denervated muscle fibres. There is a spectrum of junctional morphology in reinnervated muscles that ranges from normal through to strings of tiny bead-like receptor zones (Figs 56 and

57). These changes are present at junctions in all reinnervated muscles and whilst they are more prevalent in the specimens at four weeks they appear to persist over time. There is evidence of grapes and beads in muscles at twelve weeks following both nerve repair and nerve graft. Several of the graft muscles at four and six weeks have what appear to be much smaller junctions than normal. Reviewing the mean surface area for these specimens shows that they have the smallest mean junction sizes in their time groups. These junctions resemble those seen in the nerve cut group at four weeks, but are double-labeled showing that the end-plates have been re-occupied by regenerating axons. This might indicate a delay in the process of axon regeneration.

Figure 56.
Confocal microscope images of morphological changes at NMJ four weeks after a nerve repair

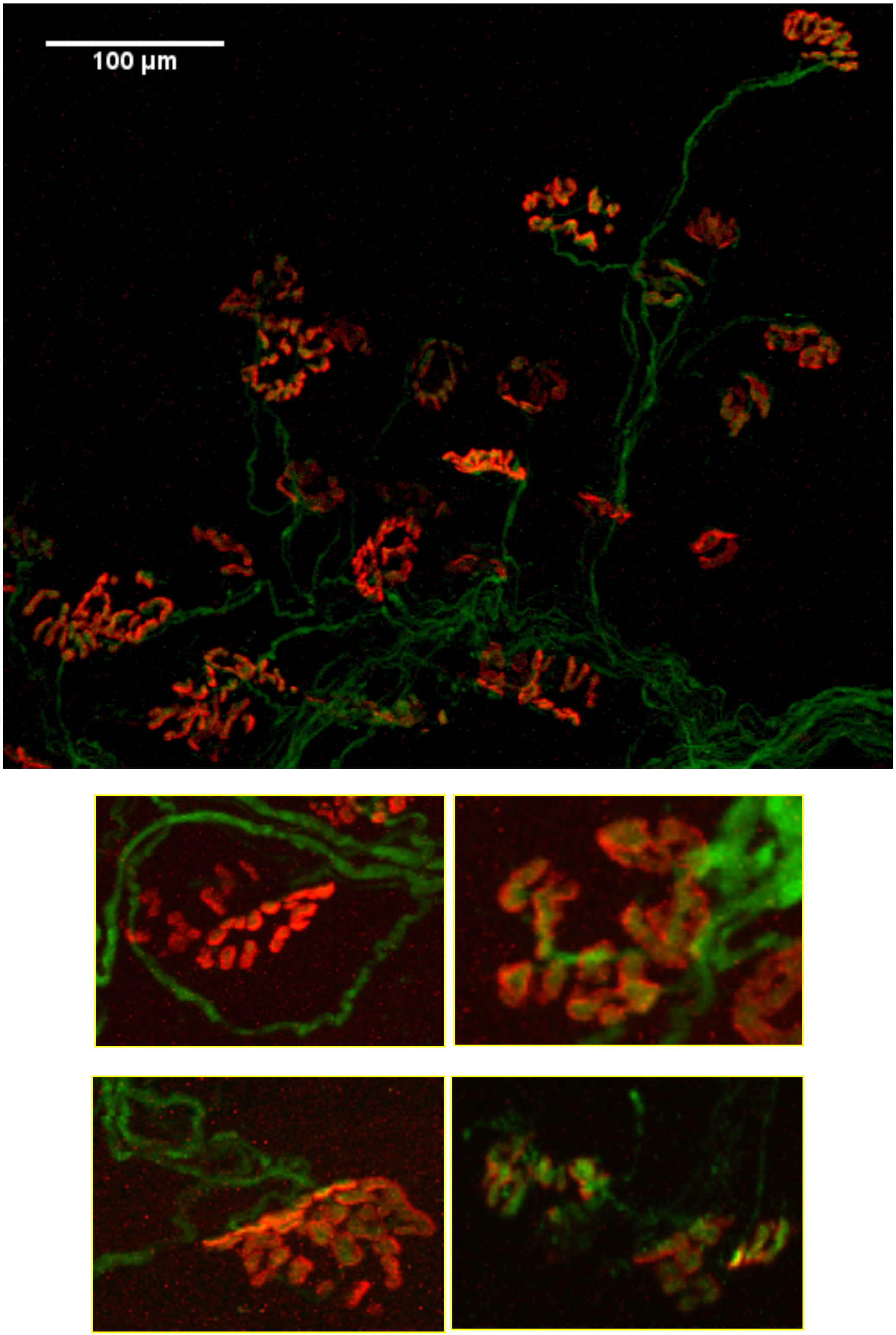

These double-labeled images are of a nerve repair specimen four weeks after intervention. The receptor gutters of the junctions have lost some of their continuity, loosing the ‘pretzel’ shape of the control junctions. The green axons are disordered and more loosely fasciculated than normal, and some have put out some terminal sprouts from occupied junctions.

In conjunction with the changes noted in the end-plates there is also a change in the intramuscular axons. The most immediately obvious change being a looseness to the main axon bundles, the trunk and main boughs, to follow the arbor analogy. In the control specimens these are closely fasciculated with axons tightly packed together. In the reinnervated muscles these main bundles are less constrained and the individual axons are more loosely bound together. Again this appears to persist over time. At the junctions the axons exhibit several features not seen in the control group. As mentioned above the extent of reinnervation as measured by re-occupation of junctions could be considered complete. The number of double-labeled junctions was no different in interventions or controls. There were only four muscles that showed any completely denervated junctions, two nerve repair specimens, one at four and one at six weeks, and two nerve graft specimens, again at four and six weeks. In each case it was a small number of junctions (R4=3/343; R6=30/308; G4=5/330; G6=4/318) and the junctions were of normal architecture (Fig 57). Partial innervation, where the junction was only partially covered by an axon, was also a rare occurrence (Fig 57). Two repairs at six weeks had 4 (of 319) and 5 (of 308) partially innervated junctions respectively, and one graft at four weeks had 7 (of 318) partially innervated junctions. In two muscles, a repair and a graft each at twelve weeks appeared to show a single junction that was poly-innervated by two separate axons (Fig 58). Four grafted muscles at 6 weeks showed junctions innervated in series where an axon occupied one junction and then continued via a terminal sprout to occupy another junction (Fig 59). Whilst the number of junctions innervated in this way was low the presence of terminal axonal sprouts was much more prevalent. All reinnervated muscles at all time frames showed some evidence of terminal sprouting. The degree of terminal sprouting was subjectively greatest at earlier time frames and in the grafted muscles. In both repairs and grafts it reduced with time but did not totally resolve. The terminal sprouts were not uniform in character. They varied from thin spidery tendrils

Figure 57. Confocal microscope image of denervated NMJ in a reinnervated muscle.

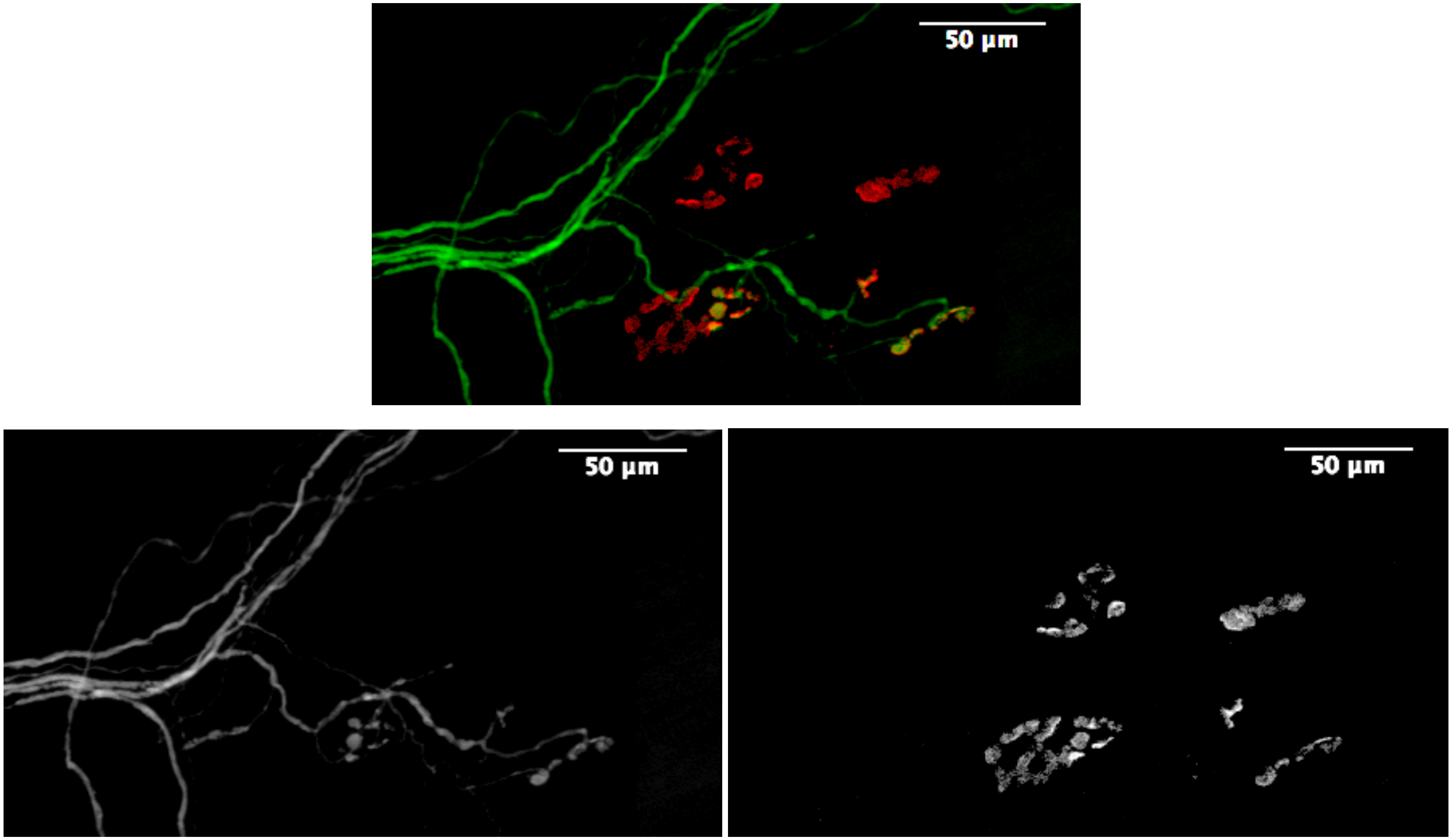

In this nerve repair specimen at six weeks there is an example of both a partially reinnervated neuromuscular junction, and two junctions that has not been reinnervated. The upper image is double labeled with axons in green and junctions in red. The lower left image shows only the green channel (axons). One branch overlies three junctions, innervated in series. The gutter of the first junction is only partially occupied. The second and third junctions have atrophied, but the remaining gutter is completely occupied. The lower right image shows the red channel (NMJ) which demonstrates five junctions. Two of these have not been reinnervated at all.

Figure 58.
Confocal microscope image of polyinnevated NMJ in a reinnervated muscle

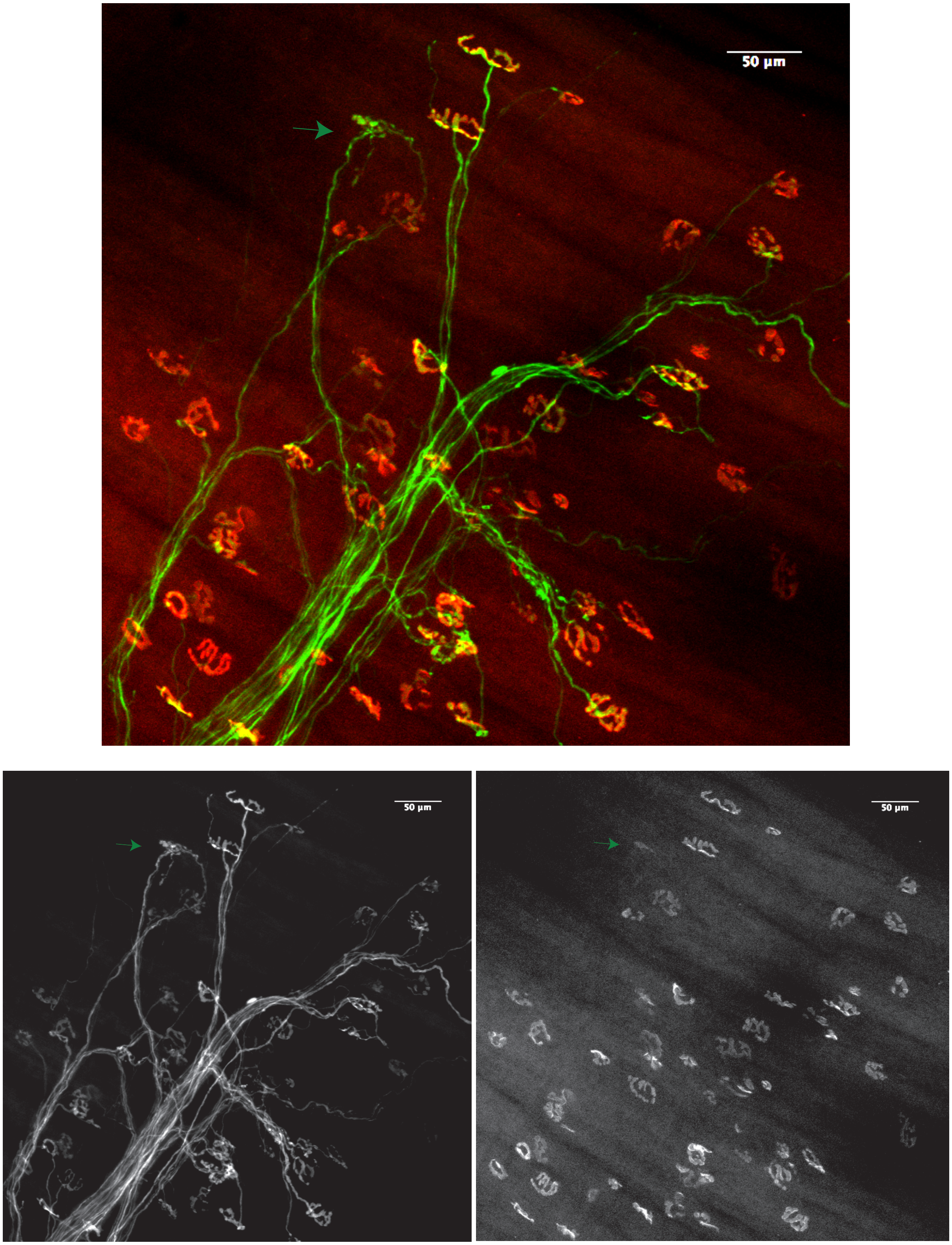

This double-labeled image is a nerve repair specimen four weeks after intervention. The green arrow indicates a neuromuscular junction that receives polyinnervation from two axons. One of these is itself a terminal branch from an adjacent junction.

Figure 59.
Confocal microscope image of terminal sprouting

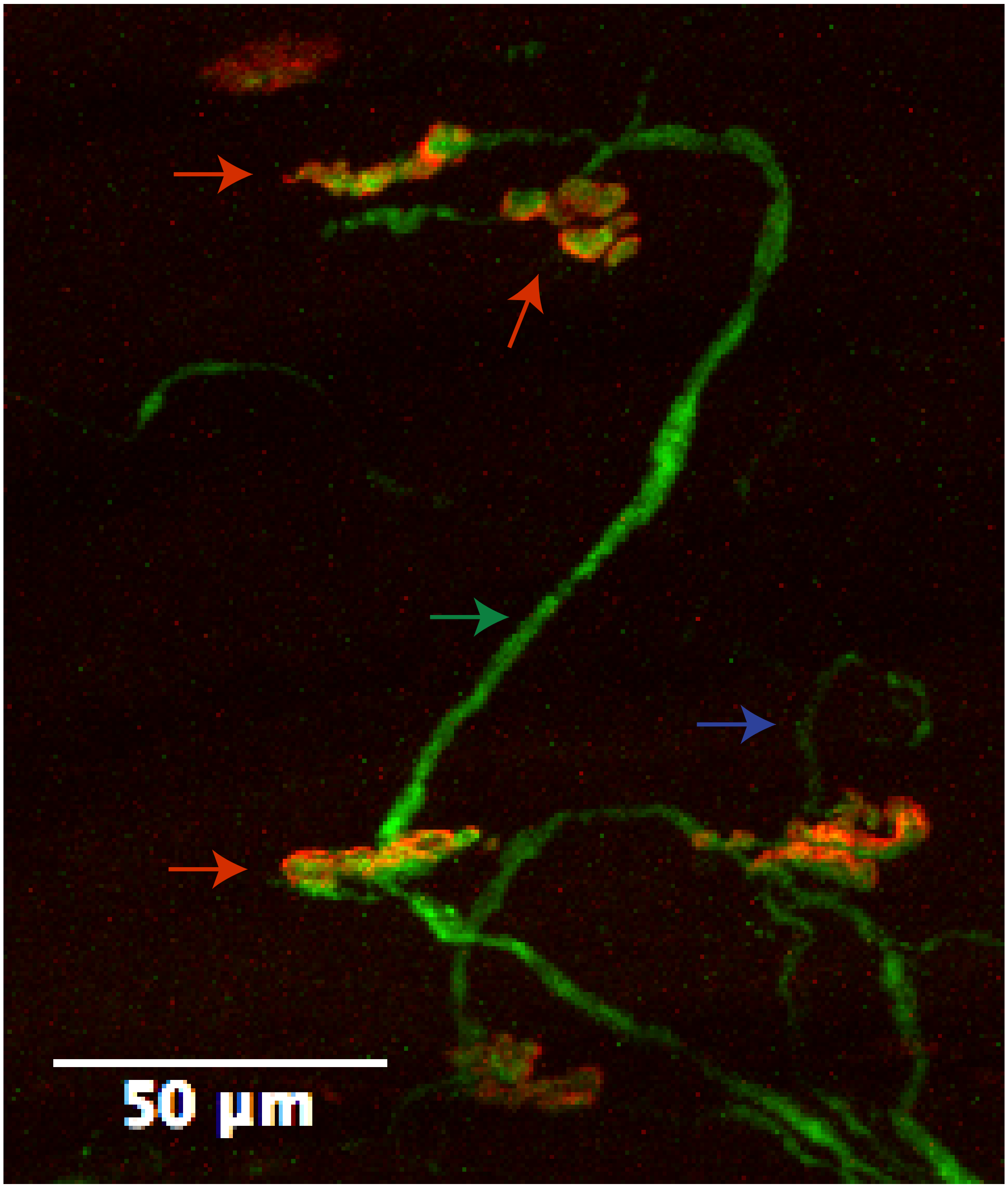

This double-labeled image is from a nerve graft specimen, six weeks after intervention. An axon (green arrow) innervates three neuromuscular junctions (red arrows) in series. Having occupied the first junction, a terminal branch proceeds to two further junctions. In addition a further terminal branch (blue arrow) is visible extending from a separate junction.

Figure 60. Confocal microscope image showing sprouts, webs and tendrils in reinnervated muscle

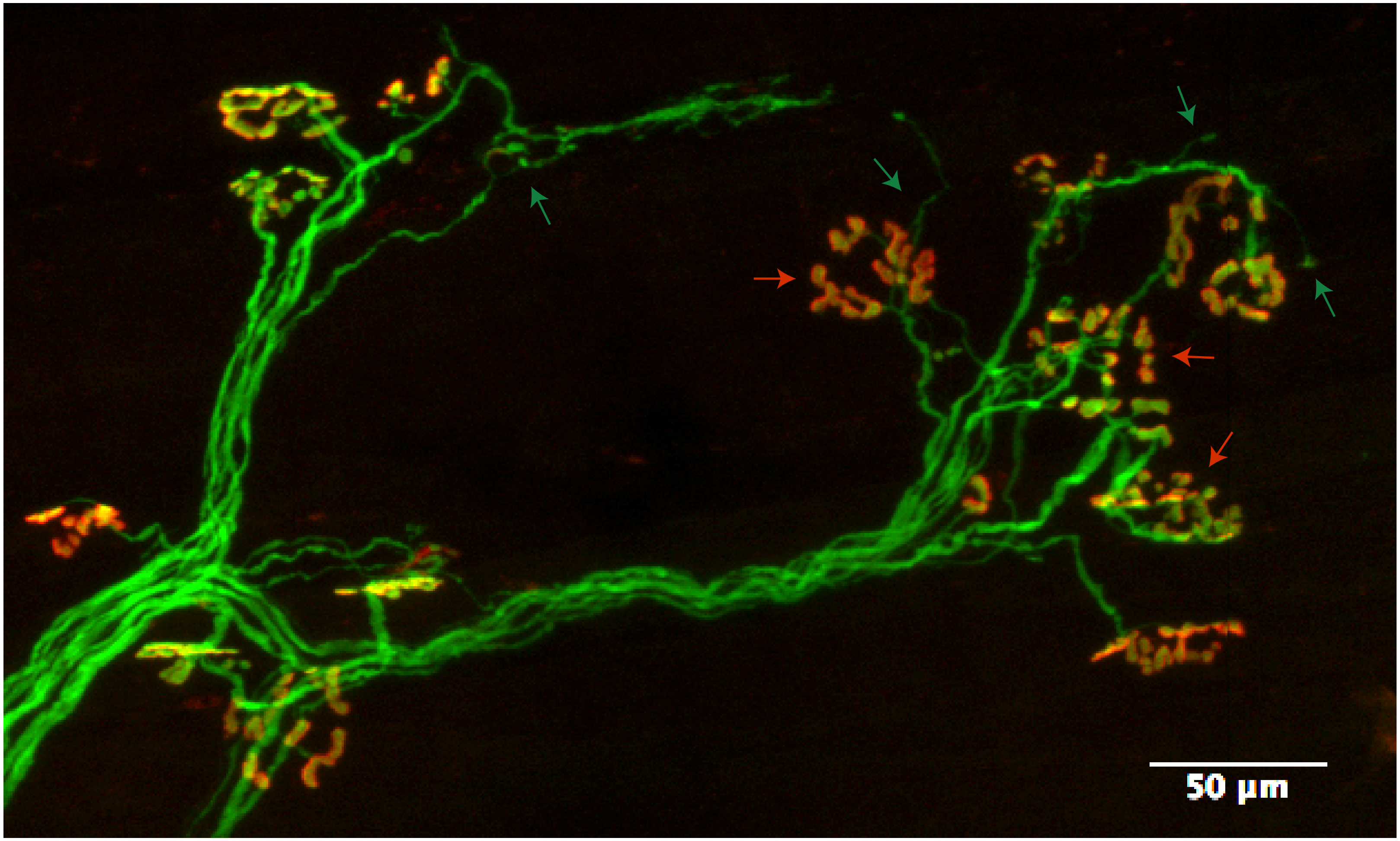

This double-labeled image of a nerve graft specimen at six weeks post intervention shows a number of changes in both axons and neuromuscular junctions. The junctions (red arrows) have loss of gutter continuity, resembling ‘bunches of grapes’ rather than the normal ‘pretzel’. The axons show numerous terminal sprouts and terminal branches (green arrows).

spreading out with minimal alteration in vector, to confused webs of matted fibres with blebs and condensations (Fig 60). Where these terminal sprouts were most prevalent they were often associated with bunches of grape-like junctional end-plates. Occasionally an axon appears to enter the arbor and not make any connections with junctions (Fig 49). These axons have a characteristic wavy appearance that resembles sympathetic fibres (personal communication with JW Lichtman).

8.

Discussion

8.1 Overview of Reinnervation

The overwhelming impression when looking at the muscles in this study is that there has been a remarkable degree of reinnervation. This is the case with both nerve repair and nerve graft at each of the three time periods studied. The neural arbor is reoccupied and the neuromuscular junctions are present with the normal "pretzel" appearance seen in control animals. This in itself is a testament to the reinnervation process. The purpose of this study was to examine the changes in both the muscle and the nerve after reinnervation. The aim was to correlate these changes with possible causes of reduced function in the clinical scenario of free-functional muscle transfer for facial reanimation. To reconstruct facial palsy a muscle is transferred to the face and reinnervated by a branch of a cranial nerve, either via a direct repair or through a nerve graft. In this study we focused on a branch of the facial nerve and assessed the differences in reinnervation between two possible interventions: nerve repair (R) and nerve graft (G). There are twenty seven animals per intervention divided equally between three time periods: four, six and twelve weeks. By observing the changes that occur over time, as the returning axons reoccupy the distal nerve stump and neuromuscular junctions, we hope to assess how the relationship between the nerve and muscle matures. By comparing the results twelve weeks after surgical intervention we hope to assess longer-term differences between the two interventions and the control group. The choice of twelve weeks is a compromise, to balance the differences seen from maturation of reinnervation and remodeling of the arbor, with the degenerative changes associated with ageing (316,317).

Initial pilot studies in YFP mice suggested that a regenerating nerve that has been damaged in the lateral neck arrives at the denervated muscle two to four days after a nerve crush, and approximately two weeks after a nerve repair or graft. Several parameters were measured to assess the regenerating nerve and the reinnervated muscle. To assess the nerve the number and calibre of the axons were measured at two locations within the nerve: at the start of the terminal nerve branch to the muscle (i.e. where the only target organ remaining is the interscutularis muscle) and just before the nerve enters the muscle (i.e. its most distal extra-muscular point). Immunohistochemical labeling was used to identify the presence of a myelin sheath around the axons. The muscle was imaged to identify the neuromuscular junctions that were double-labeled for bungarotoxin (acetylcholine receptors) and axons (YFP), indicating that they had been reinnervated. The number and area of those neuromuscular junctions was measured.

The total number of neuromuscular junctions remains stable in both the nerve repair and nerve graft groups with respect to controls at each of the time periods. This suggests that the number of muscle fibres is also stable, since only one mature junction forms per fibre. Images from the nerve cut controls show that the disintegration of the end-plates is a gradual process. Almost all of the junctions retain a normal contour four weeks after denervation. Over time the number of normal junctions declines. By six weeks there are still junctions that are recognisable as end plates despite being small, although most junctions have totally degenerated and disappeared. By twelve weeks there are scattered fragments that label with alpha-bungarotoxin, but no recognizable junctions (Fig 34). It was initially surprising to see any junctions with normal architecture six weeks after denervation. However, this finding supports the idea that rapid junction turnover occurs during reinnervation and is related to asynchronous innervation (318-320). In the total absence of synaptic activity there is a gradual shrinking of the junction with atrophy of the muscle fibre, but no impetus for rapid resorption (287,321).

At four weeks after nerve repair or nerve graft most of the junctions have a normal morphology but are smaller than normal NMJ. The reduction in the size of the junctions probably reflects some muscle fibre atrophy that occurred during the period of denervation that is not yet restored (322). The junctions in the nerve cut controls demonstrate the gradual shrinkage seen with denervation. Comparing the size of the junctions from the two intervention groups with those of the nerve cut controls, we see that the repair group is larger by four weeks, whilst the graft group is slightly smaller. This is biased by the reduction in numbers of junctions that are still measureable in the nerve cut controls, which may represent junctions that were larger than the mean prior to denervation. It does suggest that there has been some return to function and a reversal of muscle fibre atrophy resulting in a recovery of junction size in the repair group by four weeks. Over time the junctions in both intervention groups continue to increase in size but plateau between six and twelve weeks. The repair group recovered 94% of the mean size of control junctions by twelve weeks, whilst the graft group achieved 77%. However the total surface area of reoccupied junctions was less, with repairs reaching 77% and grafts 61% of controls. The junctions recovered more than the 20% safety factor required for function (323). Given that the number of junctions did not change, this indicates that each muscle fibre, and hence junction, increased in size as it regained function over time, but that the recovery of the muscle was globally reduced. This might be as a result of chronic changes in the muscle fibres after a period of total denervation, or perhaps reflects a reduced capacity of the returning axons to restore the full complement of junctions to their original state.

There are morphological changes exhibited by some of the junctions. There are several examples of junctions where the receptor gutters loose continuity and appear thinner and more fragmented (Figs 58-62). The receptor areas are only partially occupied or inaccurately covered by the nerve. Where this occurs it is often accompanied by changes in the appearance of the axons in the peri-junctional area. Some axons are very thin and show peri-terminal blebbing, and occasionally there will be polyinnervation of a single site by several different axons (Figs 57 & 59). These are all features akin to the signs of ageing at the neuromuscular junction identified by Valdez (Fig 61) (5). The degree of poly-innervation however, was rare and observed in only two junctions across two muscles. This is in agreement with the long term outcomes described by Luff (223). These changes are seen in specimens at all time periods in both intervention groups, and do not resolve with remodeling of the arbor. Comparison of the junctions from a nerve repair or nerve graft specimen with those of its contralateral control muscle show that these junctions remain altered when directly controlled for age. It would be interesting to ascertain if these changes were initiated by the axons, or by the junctions. It is possible that these altered junctions are associated with a particular population of axons, perhaps those with very enlarged motor units that are over-stretched. There is no impression from the YFP-16 specimens that all the “aged” junctions are associated with a particular axon (i.e. a single motor unit) and they are too numerous to attribute to identified axons. This change in morphology may have an impact on the muscle characteristics after reinnervation in a similar way to age related deterioration, with reduced coordination and power of contraction. This would have consequences for all free-functional muscle transfers, be they for facial reanimation or brachial plexus reconstruction. Muscles with aged junctions have been shown to contract less effectively than controls (324).

Figure 61.
Valdez's images of age related change in NMJ (2010)

Age-related changes in the neuromuscular system. (A) Tibialis anterior muscle in a young adult mouse that expressed YFP in motor axons. In the region shown, two nerve bundles (yellow) innervated individual muscle fibers. AChRs were labeled with Alexa-594-BTX (red). Complete apposition between nerve terminals and AChRs is typical in young animals. (B) Tibialis anterior muscle in a 24-mo-old mouse. Denervated (arrows) and partially vacated AChR sites as well as prominent axonal swellings (arrowheads) are common. Young adult (C) and aged (D–J) NMJs are shown at higher magnification. Age-related alterations included complete denervation of the postsynaptic AChR site (D), fragmentation and faintly labeled patches of receptors (E), and receptors that are only partially covered by the nerve terminal (E–F). In some cases the innervating axons are very thin (G), bear large swellings proximal to the nerve terminal (H), multiply innervate one NMJ (I), or extend processes beyond the receptor area (J). [Scale bars: 50 μm (A–B) and 10 μm (C–J.)

Images of age related changes in axons and neuromuscular junctions from Valdez *et al* in PNAS 2010 (5). Many of these morphological changes are reminiscent of the changes we have observed after reinnervation.

The nerve cut group demonstrated some interesting changes in this regard. As previously mentioned the surgical protocol in the nerve cut group was revised once initial results showed that, despite excision of a 1cm segment of nerve, some specimens were showing reoccupation of the arbor. Examination of the site of the excision revealed a large, uncoordinated neuroma in continuity. The axons form a loose helical structure as they cross the unsupported area between the nerve ends (Fig 7). To prevent this the parotid gland was mobilized and interposed between the cut ends of the nerve as a barrier. However, there were a number of specimens from the original protocol examined at four, six and twelve weeks, that demonstrated unusual features that are worth discussion. In one muscle at four weeks, one at six weeks, and two at twelve weeks, the familiar arbor has been reoccupied by YFP axons, but the nerves do not make any connections with the neuromuscular junctions. The axons have a different appearance from the normal motor axons, they are thin and often blebbed and perhaps represent sensory or sympathetic fibres (Fig 49). In one specimen, six weeks after nerve cut, the junctions have been reoccupied but the neuromuscular junctions exhibit an extreme version of the changes noted above in some of the nerve repair and nerve graft specimens. The end-plates are ill-defined and fragmented (Fig 62). There is excessive terminal sprouting with numerous junctions innervated in series as opposed to parallel. These changes are presumably due to a longer delay in reinnervation caused by the time it took the axons to cross the gap between the cut ends unsupported by bands of Büngner. It is interesting that in the repair and graft group the changes, whilst more subtle, are seen in specimens at four, six and twelve weeks. This suggests that these changes in junctional morphology are not restored with time, and that any degradation of the junction associated with a delay in reinnervation may be a permanent feature.

Figure 62. Confocal microscope montage of NMJ in late reinnervation (nerve cut)

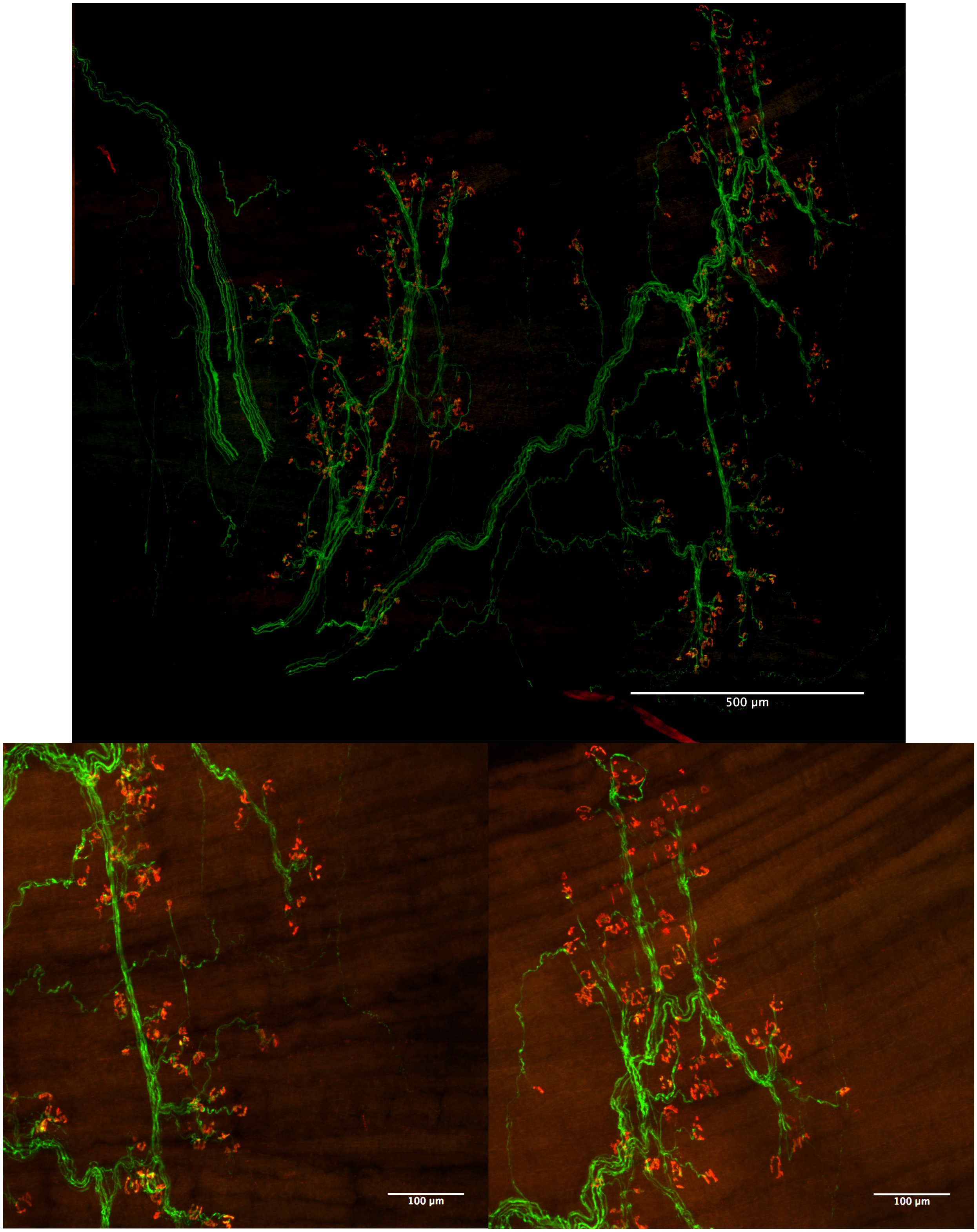

This specimen six weeks after a nerve cut (original protocol) shows changes in the neuromuscular junctions. They are double-labeled and thus reinnervated, however the junctions are small and fragmented. This may reflect the delay in reinnervation as the axons traversed the un-repaired nerve division.

One strategy to increase the ultimate power of contraction of the transferred muscle in facial reanimation has been to transfer a larger-than-required muscle to allow for the atrophy that occurs in the lag time before reinnervation, whilst the nerve regenerates. Animal studies have shown that a transfered muscle will atrophy by as much as 50% before it is reinnervated, but retain sufficient numbers of fibres to provide adequate power and excursion once functional (325-327). Fu demonstrated that where muscles were reinnervated after a six month period of chronic denervation, they regenerated approximately 50% of functional muscle fibres (226). Human nerves regenerate at approximately 1mm per day. A six month period of denervation therefore correlates with a growth distance of 150-180mm, approximately the distance a cross-facial nerve graft has to span in a classical two-stage facial reanimation procedure. Performing facial reanimation in two stages enables axons to be present at the distal end of the graft, reducing the distance the axons subsequently have to regenerate at the time of muscle transfer. This minimizes the period of time the muscle is denervated and thus the extent of its atrophy. However, this strategy does mean that the axons of the cross-facial nerve graft are deprived of a distal target for a significant period of time, whilst they are growing across the face.

Henneman proposed the size principle for the activation of motor units, which is key to the coordinated function of a muscle (111). Smaller units, where an axon innervates only a few muscle fibres, contract first and larger units are activated as more force is required. The number and ratio of small and large motor units within any muscle are related to the tasks it performs. A disruption in this balance would alter the normal sequence of recruitment and affect a muscle's ability to perform those tasks. In reinnervation the number of axons that regenerate and the number of junctions that are successfully reoccupied, determines the size of the recovered motor units. We believe that disruption of these motor unit proportions is key to the variability in the success of free-functional muscle transfers. Urso-Baiarda postulated the bottle neck theory of reinnervation, suggesting that there are two potential culprits that can disrupt the motor unit ratios and lead to poor function (328). If there are insufficient available muscle fibres due to atrophy the muscle becomes the bottleneck. In this case harmony can be restored by remodeling of the regenerated axons. If there are insufficient regenerating axons the nerve becomes the bottleneck. The regenerating axons are overstretched in their attempt to innervate the available muscle fibres. Remodeling of axons cannot restore the size principle and contractions will be disorganized (Fig 63).

Jacobs and MacQuillan have suggested that the number of axons regenerating to the distal end of the nerve graft is equal to or surpasses that of the normal nerve (81,288). This would suggest that the cause of the bottleneck is therefore the muscle, and support the theory that transferring a larger muscle could improve results. However, Mussini and Schmalbruch have shown that muscle atrophy after denervation is not, in itself, the only cause of poor reinnervation, and that muscle fibres that have been denervated for several months can still regenerate once a stimulus is restored (217,218). In addition axons that have been chronically deprived of a target have a reduced ability to effectively re-innervate a muscle (219,329,330). Similarly Scwhann cells become less able to nourish axons after long periods without their trophic support (226,330). This suggests that the focus on reducing the period of denervation of the muscle may be misguided. It might be that the ratio between the number of muscle fibres and the number of axons, at the moment when the nerve reoccupies the neuromuscular arbor, is vital to its reinnervation characteristics.

Figure 63.
Cartoon of the Bottleneck theory of reinnervation

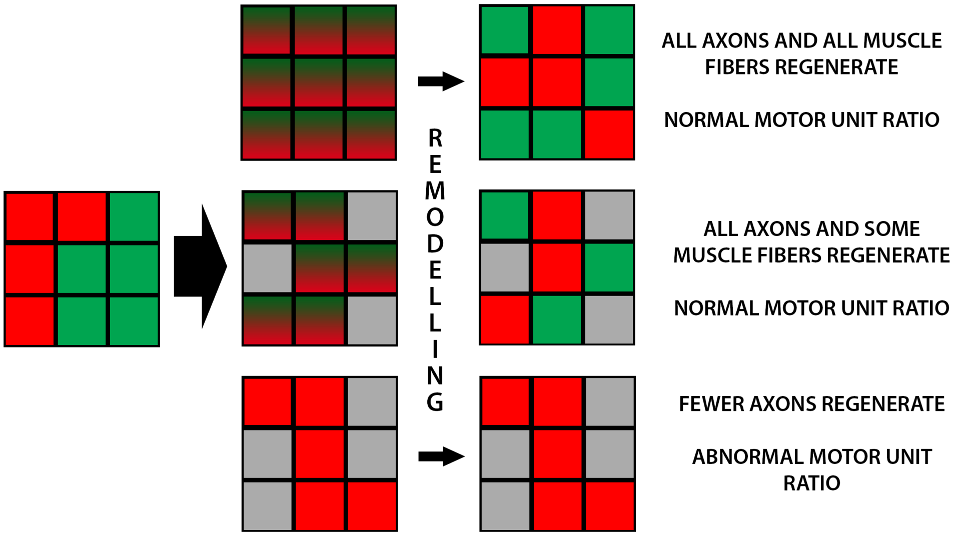

Remodeling of motor units according to the bottleneck theory. Restoration of the motor unit proportions is dependent of the number of regenerating axons.

Unlike Jacobs and MacQuillan, Frey and Terzis have reported a reduced number of axons at the distal extent of the cross-facial nerve graft (83,84). If the nerve is the bottleneck then a large number of muscle fibres might exceed the capacity of the regenerating axons to increase the size of their motor units. Perhaps we should turn our attention to the quality of the regenerating axons. Terzis has shown a correlation between a greater number of axons in a donor nerve, and improved functional and aesthetic outcome in facial reanimation (84). We have shown that the number of neuromuscular junctions remains the same after nerve repair or graft. If the number of junctions remains the same, the size and nature of the motor units becomes dependent on the number of axons that re-innervate the muscle. If the number of axons also remains the same, the mean motor unit size should stay constant. If it changes it will affect the number of muscle fibres each axon controls. Axons have been shown to be able to increase their sphere of influence 4-6 fold (221,222). However motor units greater than 6 times normal size are not stable and those axons are no longer capable of sustaining tetanic force (222-225,324). This suggests that there is an upper limit of the amount of work each axon can sustain. In addition, the amount axons are able to expand their influence is also reduced in older axons (331-333).

Larger axons have larger motor units. Lu has shown that there is a direct relationship between the calibre of an axon and its motor unit size, with the increase in cross sectional area scaled to the square of the motor unit size (252). It is not clear whether an axon that enlarges the size of its motor unit can match the output of an axon that would normally innervate that many muscle fibres. After a nerve crush there is accurate reoccupation of the normal arbor and restoration of original motor units (103). However after more significant nerve injury this pattern is disrupted. Nguyen has shown that the proportion of junctions reinnervated by their original axons falls from over 95% with a nerve crush to less than 5% after a nerve division. In a nerve repair the picture is more akin to the nerve division group, in that there is a discontinuity between the proximal and distal nerve stumps and complete disruption of the glial architecture. The physical approximation of the cut ends cannot restore the undamaged state. It serves to reduce the size of the gap between the ends and to make the loss of axons into the surrounding tissues less likely. Even if 100% of axons entered the distal stump, there is little chance that they would re-enter their original tubes and therefore their original arbors. In a nerve graft axons have to cross two repair sites, which further reduces axon numbers in the distal stump, and the chances of an accurate re-wiring of the circuit. In these scenarios disruption of the normal motor unit sizes and ratios seems inevitable. In free functional muscle transfer these patterns are further complicated by the pairing of a nerve and muscle that would not normally interact. The returning nerve has to navigate a foreign arbor.

In the YFP animals we can trace the nerve from the point where it enters the muscle, back towards the site of nerve repair or nerve graft. The axons look well ordered within the terminal branch but there is variability in axon diameter that is not seen in the normal controls. At the site of neurorraphy there is a considerable change in the nerve. The ordered axons appear to break free and tumble over one another. This is a neuroma, and in the YFP-16 animals there is a disordered whorl of axons that seem to form numerous tight loops (Fig 12). Even here though, it is astonishing to see how quickly order is restored once the axons enter the distal stump. Within the space of a few microns they recover the gross appearance of the normal nerve. In the case of the graft there is a second neuroma, much the same as the first. Here again it is remarkable how much order there is in the substance of the graft, with axons tightly restrained for the section of transferred nerve between the two neuromas (Fig 35). It is an anatomical necessity of this methodology that the graft is quite short, and it is possible to see a few axons that have found the distal stumps despite bypassing the graft. These results suggest that once axons escape the proximal stump they undertake a searching pattern to seek the distal stump. This process is provoked by neurotropic mediators and is powerful enough to entice axons over considerable distances. This is especially apparent in some of the pilot specimens in the nerve cut control groups. Here the neuroma continues to grow, forming a helical structure until the axons find the distal stump over 10 mm away. Once the distal Schwann cell tubes were occupied order was again restored and the muscle arbor reoccupied (Fig 7). This necessitated a change in the surgical protocol for the nerve cut group. Rather than a simple excision of a segment of nerve, the parotid gland was interposed as a barrier between the cut ends to prevent reinnervation by the original nerve.

In two early nerve cut specimens, prior to the change in protocol mentioned above, the arbor appears to be restored but the junctions are not reoccupied (i.e. not double-labeled with YFP and alpha bungarotoxin) and resemble those of the other nerve cut samples (Fig 49). The axons are small and wavy with numerous small branching points. These axons could be sensory or autonomic in nature. Once the Büngner's bands have been occupied it may be physically difficult for more axons to enter and displace those already there. It is unresolved whether the capacity of the Schwann cell tube can limit the eventual size of the regenerating axons. If the arbor is reoccupied by inappropriate sensory axons, it may reduce or prevent the ability of the returning motor axons to displace them and therefore result in a weakened or functionless muscle.

The YFP-H animals, where there is fluorescent expression in only a small percentage of the axons, provide a tool for examining the patterns of axonal regeneration at the site of the repair, and the distal nerve, in more detail. The neuroma in the YFP-16 specimens appears to be a maelstrom of axons with each axon, and possibly multiple branches, making several turns and contributing to the chaos. It is clear from the YFP-H specimens that each axon makes a small contribution to the overall picture. Some pass directly through the repair with almost no deviation. Others make one, or two rotations of 360 degrees before passing into the distal stump. Some axons appear to form multiple loops and never enter the distal nerve. Some of the three dimensional information is lost as the neuroma is squashed in the Z plane during imaging. It is possible that these axons have left the site of repair and are lost to the surrounding connective tissue. Branching within the repair site is rare and tends to occur once the axons are within the distal Schwann cell tubes (Fig 50). Intuitively it would seem advantageous to divide early and often, producing multiple ‘daughter’ branches each with an opportunity to find the distal stump. It may be the case in our specimens that the unsuccessful branches have already been retracted and remodeled. However, an alternative view could be that multiple branches may exact too large a metabolic demand on the axon, since they will all continue to grow until at least one finds a target. Once an axon is within a Schwann cell tube it not only receives some support from the glial cells, but it also has a much higher chance of finding a target that will provide trophic support, since the empty bands of Büngner are likely to lead to a distal target. In this scenario it would be advantageous to support a single growth cone until contact is made with empty Schwann cell tubes. Subsequent branching to fill adjacent empty tubes would be more likely to maximize the chances of finding an empty end target.

Poor results are a common feature of facial nerve axotomy (334,335). In a simple repair of the main nerve abnormal movements, or synkinesis, of the various muscle groups supplied by the 5 main terminal branches of the facial nerve are considered inevitable (336-338). It is thought that a major contributing factor to the synkinesis is the misdirection of axons (339,340) or their collaterals (202,304,341) into inappropriate final pathways resulting in polyneuronal innervation

(197,342,343). Guntinas-Lichius studied the effects of reducing collateral branching, on reinnervation of normally independent muscle groups innervated by separate terminal branches of the facial nerve (344). The number of collaterals at the point of repair was inhibited by antibodies to nerve growth factor, and the results analysed with retrograde labeling of each of the muscle groups. With a simple repair the total number of cell bodies labeled was greatly increased, which he assigns to 'hyperinnervation' by collaterals from previously unlabeled neural pools. In the antibody groups the number of cell bodies per muscle group is much more akin to the controls, albeit with some double- and triple-labeling. However, there is no change in the functional outcome between the repair and antibody-blocked groups.

The YFP-H transgenic line offers an interesting tool with which to examine axonal regeneration. In the YFP-16, fully-labeled line images of regenerating nerves as they pass through the point of the repair become confused by the density of labeling. Whilst it is possible to trace out a wiring diagram in the normal control muscle, following an individual axon through this maelstrom is not feasible (252). The YFP-H line is sparsely labeled with only 5-10% of axons expressing the yellow fluorophore. Images of the site of a repair and the distal nerve provide a history of the route taken by a small number of regenerating axons. It provides a time-lapse snap-shot of the axons' passage through the neuroma, and each of the subsequent branching points. Once the axon has made a connection with the distal muscle it can remodel its synaptic connections, but it cannot alter the path it took to get to the target. These tools show that individual axons respond very differently to the challenge of reinnervation.

Most axons form searching loops at the point of the repair. The fixing process and the subsequent flattening as the nerves have been mounted on slides prevents us from commenting on the direction of those loops and whether they are all in the same direction (i.e. right or left spirals). Individual axons might perform multiple or single loops, a very small number navigate across the repair site directly. Some, but not all, of the axons in the distal tubes do undergo branching. The degree of branching is very variable. Some axons produce no branches, others divide once or twice, and a few produce in excess of ten. Most branches remain in a single terminal nerve, however some enter different terminal nerves (Fig 48). This is direct evidence for the presence of synkinesis where a single axon innervates multiple muscles. In a mixed nerve it is possible for the distal targets to be trophically different (eg cutaneous sensory versus motor). This allows for remodeling to correct for aberrant wiring, provided an axon reaches both targets. An axon that only reaches appropriate targets would not have the differential signaling required to remodel its connections (296,345,346). The facial nerve is almost exclusively motor, supplying multiple muscle targets. Axons that reach more than one motor target would receive appropriate trophic support from all targets and therefore no impetus to undergo remodeling.

There is some branching between proximal and distal ends of the normal terminal nerve to interscutularis which represents a 19.7% increase in the number of axons. This is greater than that found by Lu. This difference may result from a methodological disparity in the location of the proximal sample between the two studies. We have sampled the entire length of the terminal nerve, whilst he stopped 5mm from the muscle edge. There is less branching seen in the terminal nerve in YFP-H specimens than in the YFP-16 controls. In the YFP-H specimens the percentage of axons that express fluorophore increases with age. We have seen in our specimens that there is a gradation of intensity of expression across axons (Fig 64). It has been suggested that the intensity may be related to the size of the axon or to accumulation of fluorescent protein over time (personal correspondence with JWL). Lu has demonstrated that larger axons have larger motor units (252). This may explain the larger motor unit sizes seen in YFP-H controls versus YFP-16 controls. The reduced levels of branching seen in the YFP-H animals may reflect less actual branching, or less branching in this subset of axons with larger motor units. Where an axon has branched its terminal arbors tend to avoid overlap (347). Though the muscle preparations have been flattened in the Z plane, this relationship is largely preserved in the interscutularis, since it is a flat muscle *in vivo*. In the arbors of the normal YFP-H control specimens the axons tend not to overlap, suggesting that they are individual axons rather than branches that occurred proximal to the terminal nerve. In the intervention groups this is no longer the case. This supports the case that not all regenerating axons are individuals, some are sub-branches that will tolerate overlapping arbors (Fig 65).

The percentage change in the number of axons (i.e. branching) that occurs in the terminal nerve is not significantly greater in the intervention groups than in controls. However the total number of axons is significantly greater in both intervention groups, proximally and distally, than in controls. This suggests that either many more axons are being diverted into this terminal nerve, or that these axons have already branched several times prior to entering the terminal nerve. The percentage change in the neve repair group reduces over time until, by twelve weeks, it is less

Figure 64. Confocal microscope montage illustrating the gradation in intensity across a YFP-H arbor

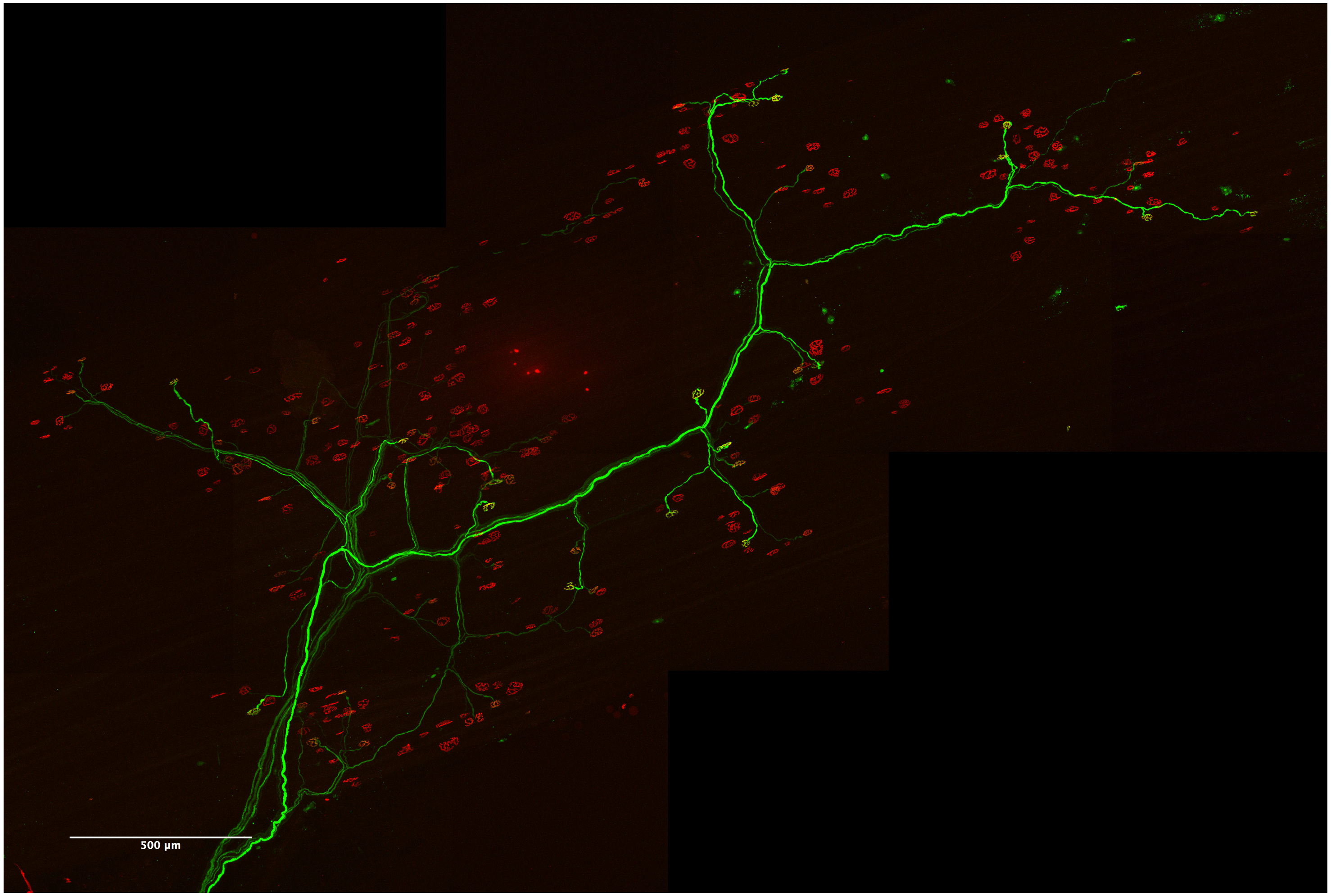

This is a double-labeled image of a YFP-H control specimen. Six axons are labeled with fluorophore, one of which is brighter than the rest. It is possible to elucidate the entire motor unit of this axon from the weaker signal of the remaining axons.

Figure 65. Confocal microscope montage illustrating overlapping arbors after reinnervation

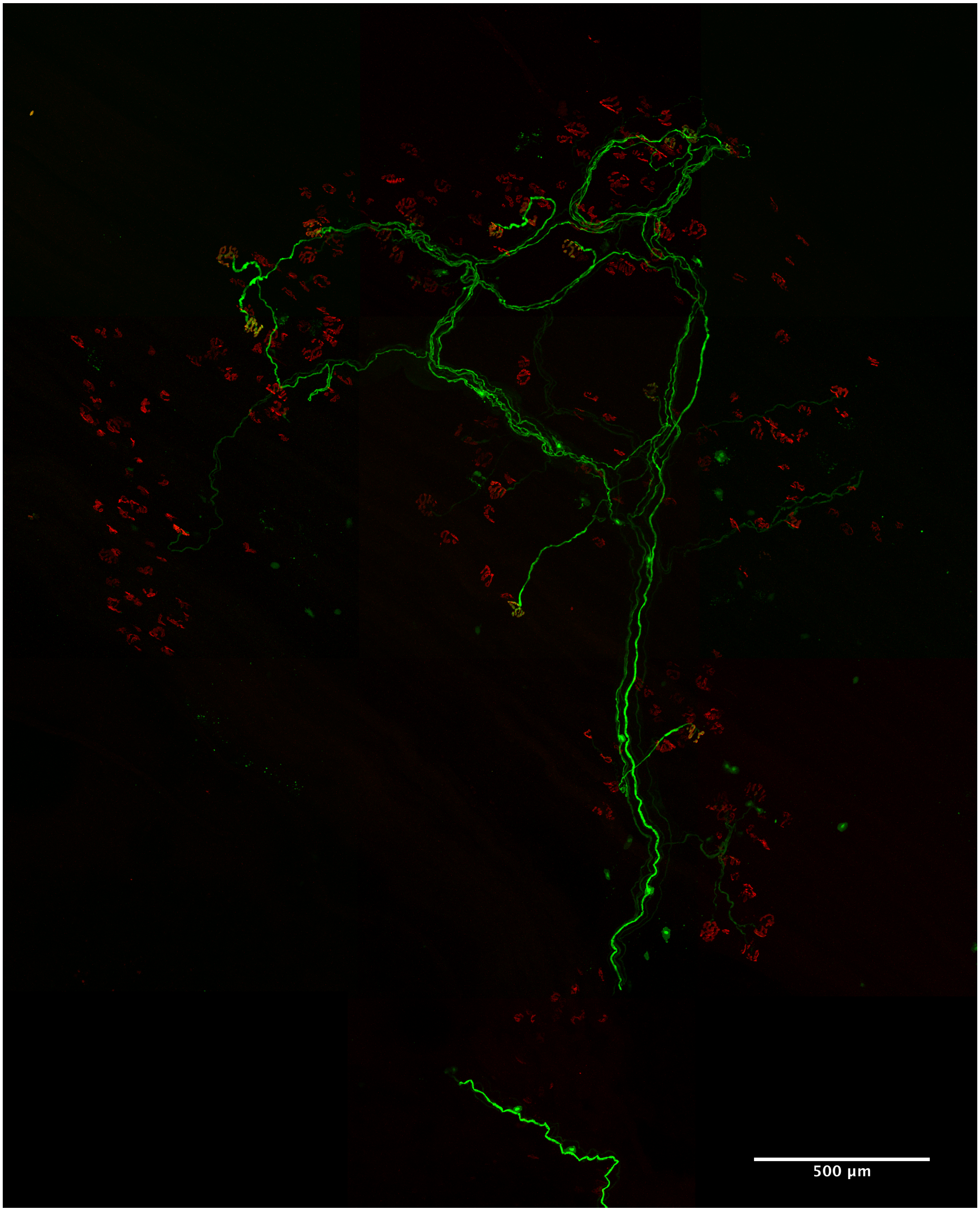

This is a double-labeled image of a YFP-H nerve graft specimen that has reinnervated its arbor. In comparison with the spaced motor units of the individual axons in the YFP-H control specimen (Fig 66), these axons are overlapping.

than in control specimens. This is primarily as a result of a reduction in the number of distal axons, indicating that sub-branches have been remodeled. This change does not occur in the nerve grafted group where the percentage change remains constant throughout. The process of axon remodeling in the nerve repair group is not occurring in the nerve graft group.

The trend observed in the nerve repair group pattern is consistent with the literature whereby regenerating peripheral axons undergo an initial period of branching, with subsequent pruning of redundant axons and branches over time. In the 1950s Shawe performed an elegant series of experiments to try and elucidate and quantify this phenomenon (304). Earlier reports had suggested each original axon produced something between three and fifty or more new fibres (106,302,303,348). Shawe examined regenerating nerves in a rabbit model, by taking multiple sections above and below the site of nerve injury (crush or repair). These were stained by two different methods, and he accepts that there was only an 81% concordance between them, with particular difficulty in identifying fibres less than 0.5µm accurately. He performed a nerve crush or a nerve repair on two nerves: the mixed motor and sensory nerve to medial gastrocnemius, and the purely sensory sural nerve. After the crush injury in the mixed nerve, Shawe noted a rapid increase in the number of fibres around the site of injury, which extended both proximally and distally. Counts at the site of the crush indicate that each original axon gave rise to 3 branches by day twenty five post injury. Of these only two thirds grew 1 cm by day fifty, giving a fibre count of double the original (the maximum achieved). This then reduced over the next fifty days, and then remained stable at 140% of the original until two hundred and twenty five days, when the experiment ceased. Myelination of fibres took longer, but by one hundred days, 80% of the fibres were encased (still greater than 100% of the original number). The figures with the repaired nerve were very similar with the only difference being a greater increase in the number of fibres initially seen proximal to the lesion. Shawe suggested this was aberrant recurrent growth. In the sural (sensory) nerve crush Shawe found a slightly different picture with slower initial growth and fewer branches. By thirty five days post injury there was a 37% increase in fibre numbers, suggesting that approximately 20% of original fibres had formed branches, roughly equivalent to the number of large, myelinated fibres in the original nerve. Shawe suggests that branching may be dependent on the size of the fibre, with large axons being capable of supporting more divisions, and that there may be a difference between sensory and motor neurons (304).

This work exposes a contradiction in nerve regeneration theories. Shawe's work, and that of Jenq and Coggeshall after him, suggest that there should be more fibres distal to a site of nerve injury, whether it is a crush or a repaired division (349). In contrast groups such as Chor, Gutman and Sanders proposed that approximately a third of axons will escape the site of a repair, and become a neuroma instead of entering the distal bands of Büngner (203,350). More recently Mackinnon performed experiments to follow the distal progress of sciatic nerves regenerating after nerve repair in a rat model over one to twenty four months (351). Repaired nerves were harvested and sectioned at the repair site and 1cm proximal and distal. Axon fibres were counted and their diameters estimated by taking the smallest diameter for each fibre in each section. The axon numbers increased significantly in comparison to controls in the months following repair, almost doubling in number at three months. This figure steadily fell, but remained significantly greater than controls at one year. By two years there was no longer a statistical difference between repaired and control nerves. In contrast the change in mean axon diameter (4.7µm) remained significantly less than controls (6.5µm) across the entire time frame, and did not change at all between one and two years . Mackinnon suggests that the number of axons only returned to a stable state after two years, by which time the numbers were not significantly different from controls. The reduction in axon fibres to a non-significant level only occurred after a delay of a year. Mackinnon hypothesizes that this is due to pruning back of fibres that were unsuccessful in innervating a target connection. It is not clear why this process would take a year. This late reduction could also reflect age related loss as opposed to remodeling. Valdez has shown that in the absence of nerve injury, the number of myelinated motor axons can fall by 30% over an equivalent time frame of two years (5).

It has been noted that in partial denervation a muscle recovers almost complete pre-injury tension after a few weeks, even if there is no regeneration of the severed axons (352-354). What is fascinating is that there appears to be no loss of muscle fibres in this process (355,356). The denervated muscle fibres are reinnervated by sprouts from the remaining axons, either through nodal or terminal sprouting (357-361). Nodal sprouts are branches that occur at a node of Ranvier, where an axonal offshoot follows an empty perineural sheath to an unoccupied junction. Terminal sprouts originate from axons at neuromuscular junctions, and re-occupy the empty gutter of a denervated adjacent junction.

Burkel has shown that several myelinated axons can reside in a single perineural sheath with no intervening septa (362). Although there is a basement membrane surrounding Schwann cells, this leaves open the possibility of communication between axons at nodes of Ranvier in a common perineural sheath. These nodal sprouts only occur at nodes that are in proximity of a branch point in an adjacent denervated sheath (361). The sprouts seem to occur at the node closest to the empty branch point. It has been suggested that nodal sprouting only occurs intramuscularly (357). Hoffman reported that he saw fine processes extramuscularly, but Brown thinks that these were elements from denervated Schwann cells (343,363). In this study it is hard to establish the presence of nodal sprouting intramuscularly, but there is evidence for branching occurring at extramuscular nodes and multiple sub-branches existing within a single myelin sheath (Figs 50 & 45). Strictly speaking this is classified as branching, as it is occurring outside of the muscle but the process looks very similar. Interestingly this is occurring far from the empty end plates and may indicate that there is a branching stimulus coming from the empty Schwann cell tubes.

Terminal sprouts emanate from occupied neuromuscular junctions. Their paths across the surface of muscle fibres are erratic and resemble 'escaped' axons, outside of the directed growth exhibited by regenerating axons or nodal sprouts within the confines of a perineural or Schwann cell tube (203). Schwann cell processes probably accompany these terminal sprouts as they grow towards vacant end-plates (364). In my results there is some evidence of terminal sprouting, though it is not as prevalent as extramuscular branching (Fig 59). Both nodal and terminal sprouts mature and eventually myelinate (343,359). There is a watershed diameter of between 1 and 2 μm at which all axons become myelinated (209). My immunohistochemical data shows that all the axons in this study were encased in myelin sheaths, and that there are instances of myelin sheaths that are unoccupied. There are a number of examples where there are several axons within a single myelin sheath (Fig 45). This evidence is supported by a few specimens where the autofluorescence of the connective tissue demonstrates the Büngner’s bands, and the several axons are visible in a single tube. The resolution of the immunohistochemical labeling is not fine enough to determine whether the axons are individually ensheathed within this outer layer. If not this arrangement would be detrimental to the propagation of an action potential in any single axon.

8.2 *Thresholding of Axon Populations*

In this study we have shown that the population of axons that reinnervates a muscle after nerve repair or nerve graft is different from controls. Axon calibres fluctuate and can vary considerably along their length especially where they are pinched at the nodes of Ranvier. Overall they tend to taper more distally. Our method of tracing axons for 5 digital slices (1.9µm) provides both a total axonal count and accurate mean diameters. In addition, by being able to scroll through a digital cross section over several hundred cross sections (even though only 5 are traced and averaged), avoids two possible sampling errors: mistaking an aberrant axonal outline for a branch point and sampling through a node (Fig 50).

Axons in control nerves are relatively homogeneous in size, with an average diameter of 8.0µm. The diameters of axons in the both the intervention groups are much more heterogeneous. They are characterised by a few larger axons, with a similar calibre to those in the normal controls, and numerous smaller fibres with a diameter less than 2.5µm. This population of very small axons is initially predominant in both groups, with the histogram of axon diameters skewed to the left. In both groups the number of larger fibres increases over time and the population of small fibres dwindles but never disappears. The mean axon diameters remain significantly smaller than the controls, with the repairs being slightly larger than the grafts throughout. We know that remodeling of axons occurs after successful reoccupation of motor end plates, with those axons unable to establish connections retracting (197). The increase in axon diameter probably indicates the growth of the successful axons that are receiving trophic support from their motor unit. Lu has shown that the diameter of an axon does correlate with the size of its motor unit (252). Measuring the diameters of axon branches at a site of division in YFP-H animals shows that there can be considerable variation in size. All branches are smaller than the original axon but not all branches are of equal size (Fig 47).

Bray's study of regenerating, unmyelinated fibres in the crushed cervical sympathetic trunk, showed some similarities to our study (301). Distal to the injury there was a four-fold increase in axon number at one month post injury, and each Schwann cell tube contained many small axons. At one month the median axon diameter was less than 0.4µm and this left shift was persistent at six months, despite a small number of the axons increasing in size to near normal, and the proportion of axons greater than 0.9µm increasing from 1% to 10%. This supports the idea of an initial period of intense sprouting, which produces very small calibre fibres that are subsequently remodeled, with those that presumably don't reach distal targets atrophying, and those that do increasing in diameter. This may help to explain Jacobs's results, where a series of cross facial nerve grafts were biopsied at their distal extent six months after the first stage of a reanimation procedure (at the time of the second stage) (81). He found large numbers of small unmyelinated axons, but relatively few larger myelinated axons at the distal end of the nerve graft. Without a distal muscle target the regenerating axons would have no trophic stimulus to mature and remodel the multiple branches. Without this process of remodeling it is impossible to be certain how many of these fibres represent individual axons. My results confirm this increase in axon numbers distal to the site of intervention, with multiple very small axons and fewer axons of a diameter equivalent to controls. Subsequent remodeling over time with pruning of the number of axons is observed in the nerve repair group. This is most apparent in the change in distal axon numbers. In the nerve repair group a trend is noticeable between four and six weeks and the percentage change continues to fall between six and twelve weeks. This trend is not apparent in the nerve graft group. There is no fall in distal axon numbers over time and the percentage change in axon numbers remains stable from four to twelve weeks. This suggests that the second repair site encountered by regenerating axons in the grafted group has an impact on their ability to reinnervate the muscle, and that the process of remodeling is either slower or not occurring in this group.

As each axon produces successful sub-branches that innervate vacant end plates, its motor unit size increases. Regardless of the initial size of an axon's motor unit, there seems to be a maximum amount it can increase in size, of four to five-fold (365-367). Unfortunately our data doesn't allow us to know how many of the axons at the proximal sampling point are already branches themselves. This prevents us from calculating an accurate mean motor unit size from this data alone. In both interventional groups the number of axons at the proximal sample point is greater than the control specimens at all time points. Over time the change in axon numbers with remodeling is reflected in the motor unit sizes. The motor unit size in nerve repairs trends toward that of controls, whilst in the nerve grafted group it remains static. However both are consistently smaller. At face value this suggests that the motor units are smaller after intervention, and that each axon now innervates fewer muscle fibres than in controls. This is not impossible, as some axons that would ordinarily have innervated other muscles, may now be included in the branch to interscutularis. However it is unlikely that the branch to interscutularis would consistently have significantly more axons in it than before. In addition, the loss of the homogeneity in axon diameter seen in the control group suggests that not all the axons in the intervention groups are the same.

We re-evaluated the data using diameter as a proxy measure, to indicate which axons were true axons and which were branches. The mean diameter of the axons in the control groups is 8.0μm.

Lu has shown that the interscutularis is only innervated by motor axons so this population of axons can be used to define a typical motor axons (252). Two standard deviations from this value gives a diameter range of 5.5μm to 10.5μm (mean 8.6μm). We used the smaller value as a cut off, assuming that axons smaller than this value were unlikely to be making a significant contribution to muscle contraction, and were most likely to be either motor axon sub-branches undergoing remodeling, or sensory axons that had been misdirected into the terminal nerve. This thresholded data exposed changes in the trends seen in axon remodeling.

Thresholding of the control data excluded 23 of 278 axons that were smaller than 2 standard deviations. These axons ranged from 3.01μm to 5.41μm. The difference in the intervention groups is much more dramatic, but brought the distribution of axon diameters into line with the control group. After thresholding there is no significant difference in the overall axon diameter distribution between the groups. The change in axon diameter over time is more subtle, though there is still a disparity between the two groups. The nerve repair group steadily increases in mean diameter from 7.3μm at four weeks, to 7.5μm at six weeks, and 8.1μm by twelve weeks. This compares with a control mean both before (8.0μm) and after thresholding (8.6μm). The nerve graft group increases from 7.0μm at four weeks, to 7.4μm at six weeks, and 7.6μm at twelve weeks. It is possible that this represents a delay in the time it takes the graft group to remodel, which would fit with the anatomical reality of two repair sites, and a devascularised segment of graft tissue.

Given that ninety percent of nerve repairs leave a deficit, it seems unlikely that the motor units would be smaller after nerve repair or nerve graft (368). The number of thresholded axons at the proximal point increases over time in both interventional groups. This would be consistent with a gradual increase in diameter of some smaller axons (that are initially filtered out by thresholding), as they take over the territories of less successful smaller sub-branches, and get more of a foothold in the reinnervated muscle (298,311-315). The mean motor unit was re-calculated using only thresholded axons. In contrast to the unfiltered results, these motor unit sizes are significantly larger than controls (P=0.0002, One-way ANOVA). This is more consistent with Ashur's estimate of approximately 40% of axons crossing a neurorraphy. They get smaller over time which is consistent with remodeling where successful axons get larger and unsuccessful axon branches are pruned (310). Using thresholded data the size of the mean motor unit twelve weeks after intervention was significantly larger in both nerve repairs (18.0 ± 5.7) and nerve grafts (22.7 ± 3.2) compared to controls [14.0 ± 2.5 (P<0.0001, One-way ANOVA)].

Individual axons have been shown to be capable of increasing the number of muscle fibres they innervate, and hence their motor unit size, in response to partial denervation (221,222). However, their capacity to increase their influence is not limitless. A four to six fold increase in motor unit size is unsustainable, and tetanic force cannot be maintained. In our experimental model this degree of increase is not seen, but this model uses a small muscle and its original nerve. In facial reanimation a small buccal branch is used to power a large skeletal muscle. It is much more likely that the donor nerve will be over-stretched. Unfortunately there is very little data in the literature regarding the axon counts in humans, in either the donor nerves or muscles used in facial reanimation. Jacobs suggested that the buccal branch contains approximately 5500 axons of which 1700 are myelinated (81). Happak peformed an elegant study looking at the muscle fibres in a variety of facial muscles, but unfortunately did not investigate the axonal loads of their innervating nerves (369). Our unit is currently revisiting the subject to elucidate this matter more clearly. If the donor nerve is over stretched it is the bottleneck, the rate-limiting factor affecting outcomes. This suggests that we should turn the focus of our reconstructive planning towards the donor nerve, trying to tailor the muscle transfer to its re-innervating capacity. A smaller muscle that is well innervated would be more physiologically sound than a larger, poorly innervated one.

9. Conclusion

We can conclude that both the first and second null hypotheses are upheld with respect to the neuromuscular junctions. There is no difference in the number of neuromuscular junctions between either the repairs or grafts and the control populations. After reinnervation individual junctions, and the total receptor surface area, are smaller than controls, regardless of whether the nerves were repaired or grafted. The reinnervated junctions after nerve graft are also smaller than those after nerve repair, but in both groups they reached an adequate size to be consistent with normal function (299). There is no difference in the neuromuscular junction characteristics between the control group and either the nerve repair of nerve graft group.

The picture with respect to the regenerating axons is more complicated. At first glance it would seem that the first null hypothesis is rejected whilst the second is upheld. There are more axons in the reinnervated specimens than in controls, but there is no difference between the repaired or grafted nerves. However, the regenerating axons are a heterogeneous and evolving population of axons. Whilst the regenerating axons from the nerve graft group remain significantly different from the controls over time, the nerve repair group start to resemble the controls. However, the difference between the repair and grafts never becomes significant. The first null hypothesis can be rejected in part (i.e. there is a difference between grafts and controls) but the second is retained.

When analyzing for both intervention and time with respect to motor unit size the first null hypothesis is retained. However, looking at intervention alone it is rejected (the motor units were significantly smaller in the intervention groups than controls), whilst the second is retained (there was no difference between nerve repairs and nerve grafts). However, closer examination of the regenerating axons shows large numbers of very small fibres and fewer large axons that resemble the homogenous control samples. Once the axon populations are controlled for calibre the picture changes. The first null hypothesis is retained, as the axon populations in the nerve repair and nerve graft group are remodeled to more closely resemble the controls. However, there is significant difference between the two intervention groups, rejecting the second null hypothesis.

The use of transgenic mice that express yellow fluorescent protein in their axons has provided us with an extraordinary tool with which to examine the entire wiring system of a muscle after nerve repair and nerve graft. This has pertinent clinical relevance by increasing our understanding of how this interaction is affected. The medical profession accepts that we rarely manage to return an injured body to its pre-injured state, but through greater understanding we reduce the size of the deficit. Our dealings with the nervous system are still in their infancy, and currently we often have to accept poorer outcomes than we are comfortable with. The advent of microsurgery has changed radically how we intervene in nerve injuries, but there is still room for improvement. As we understand more we can adapt our techniques to strive for improvements whilst, or perhaps by, embracing our limitations.

In the scenarios we are concerned with in this thesis, the biology seems to be trying to overcome the obstacles in its path by expanding the influence of each axon, in an attempt to fill the empty arbor in the muscle. The nerve is thus the bottleneck and the reduced number of axons reinnervating the muscle leads to changes in the proportions of the motor units that cannot be subsequently remodeled. There is however a limit to that expansion. Perhaps we would be better off matching the muscular arbor to the capabilities of the donor nerve, using a smaller muscle that can be more efficiently reinnervated. In addition the branching of the regenerating axons into terminal nerves that lead to different target muscles means that synkinesis is almost inevitable. This aberrant wiring is beyond the ability of biological remodeling to correct. The changes at the neuromuscular junction, stable over all time frames, perhaps indicate that complete denervation prematurely ages the muscle. This is a problem to which we have no solution at present, other than the encouraging work in the field of ageing that suggests that some of this change could be reversible with calorific restriction or exercise (5).

10. Bibliography

1. Harrison DH, Grobbelaar AO. Pectoralis minor muscle transfer for unilateral facial palsy reanimation: An experience of 35 years and 637 cases. J Plast Reconstr Aesthet Surg 2012, Jul;65(7):845-50.

2. Gray H. Gray's anatomy: With original illustrations by henry carter. Arcturus Publishing; 2009.

3. Green EC. Anatomy of the rat. New York and London Hafner Publishing Company 1968:128-70.

4. Green EC. Anatomy of the rat. New York and London Hafner Publishing Company 1968:128-70.

5. Valdez G, Tapia JC, Kang H, Clemenson GD, Gage FH, Lichtman JW, Sanes JR. Attenuation of age-related changes in mouse neuromuscular synapses by caloric restriction and exercise. Proc Natl Acad Sci U S A 2010;107(33):14863.

6. Peitersen. Bell's palsy: The spontaneous course of 2,500 peripheral facial nerve palsies of different etiologies. Acta Otolaryngol 2002;Suppl 549:4-30.

7. Resende LAL, Weber S. Peripheral facial palsy in the past: Contributions from avicenna, nicolaus friedreich and charles bell. Arq Neuropsiquiatr 2008;66:765-9.

8. May M, Barnes L. Pathologic considerations in facial nerve disorders: Clinicopathologic correlations. The Facial Nerve 2000:153.

9. Schaitkin BM, May M, Klein SR. Office evaluation of the patient with facial palsy: Differential diagnosis and prognosis. In: May, Schaitkin, editors. The Facial Nerve 2nd Ed. New York: Thieme; 2000.

10. Bird TD. Nicolaus A. Friedreich's description of peripheral facial nerve paralysis in 1798. J Neurol Neurosurg Psychiatry 1979;42(1):56.

11. Cawthorne T. The pathology and surgical treatment of bell's palsy. Proc R Soc Med 1951, Jul;44(7):565-72.

12. Jonkees LB. Some observations on children with defective hearing. Medicamundi 1957;3(3):73-7.

13. McGovern FH, Konigsmark BW, Sydnor JB. An immunological concept for bell's palsy: Experimental study. Laryngoscope 1972, Sep;82(9):1594-601.

14. McCormick DP. Herpes-simplex virus as a cause of bell's palsy. Lancet 1972, Apr 29;1(7757):937-9.

15. Murakami S, Mizobuchi M, Nakashiro Y, Doi T, Hato N, Yanagihara N. Bell palsy and herpes simplex virus: Identification of viral DNA in endoneurial fluid and muscle. Ann Intern Med 1996, Jan 1;124(1 Pt 1):27-30.

16. Cocchiarella L, Andersson G, Association AM. Guides to the evaluation of permanent impairment. 5, illustrated, reprint ed. Chicago]: American Medical Association; 2001.

17. Bell C. On the nerves; giving an account of some experiments on their structure and functions, which lead to a new arrangement of the system. Philosophical Transactions of the Royal Society of London 1821;111:398-424.

18. Tomasch J. On the number and size of cells in the nuclei of motor cranial nerves in man. Z Mikrosk Anat Forsch 1963;70:298-314.

19. Vraa-Jensen GF, Aagesen E. The motor nucleus of the facial nerve: With a survey of the efferent innervation of the facial muscules: A normal-anatomical study. Ejnar Munksgaard; 1942.

20. Courville J. The nucleus of the facial nerve; the relation between cellular groups and peripheral branches of the nerve. Brain Res 1966;1(4):338-54.

21. Brodal A. Neurological anatomy in relation to clinical medicine. Oxford University Press New York; 1969.

22. Van Buskirk C. The seventh nerve complex. J Comp Neurol 1945;82(3):303-33.

23. Feinstein B, Lindegard B, Nyman E, Wohlfart G. Studies on action potentials in normal human muscles. Acta Psychiatr Neurol Scand 1954;29(2):189-95.

24. Voss H. [Number and arrangement of muscle spindels in the upper hyoid bone muscle, in the trapezius and latissimus dorsi muscles]. Anat Anz 1956, Dec 28;103(21-24):443-6.

25. Bruesch SR. The distribution of myelinated afferent fibers in the branches of the cat's facial nerve. J Comp Neurol 1944;81(2):169-91.

26. Huber E. Evolution of facial musculature and cutaneous field of trigeminus. Part II. Q Rev Biol 1930;5(4):389-437.

27. Camicheal EA, Woollard HH. Some observations on the fifth and seventh cranial nerves. Brain 1933;56(2):109-25.

28. Foley JO, DuBois FS. An experimental study of the facial nerve. J Comp Neurol 1943;79(1):79-105.

29. Kitai ST, Tanaka T, Tsukahara N, Yu H. The facial nucleus of cat: Antidromic and synaptic activation and peripheral nerve representation. Exp Brain Res 1972;16(2):161-83.

30. Woodburne RT. A phylogenetic consideration of the primary and secondary centers and connections of the trigeminal complex in a series of vertebrates. Journal of Comparative Neurology 1936;65(1):403-501.

31. Kimmel DL. Development of the afferent components of the facial, glossopharyngeal and vagus nerves in the rabbit embryo. Journal of Comparative Neurology 1941;74(3):447-71.

32. Torvik A. Afferent connections to the sensory trigeminal nuclei, the nucleus of the solitary tract and adjacent structures; an experimental study in the rat. J Comp Neurol 1956, Nov;106(1):51-141.

33. Kunc Z. [Relation of afferent fibers of facial, glossopharyngeal and vagus nerves to spinal tract of trigeminal nerve]. Cesk Neurol 1957, Jun;20(4):225-32.

34. Kerr FW. Facial, vagal and glossopharyngeal nerves in the cat. Afferent connections. Arch Neurol 1962, Apr;6:264-81.

35. Rhoton AL, O'Leary JL, Ferguson JP. The trigeminal, facial, vagal, and glossopharyngeal nerves in the monkey. Afferent connections. Arch Neurol 1966, May;14(5):530-40.

36. Willer JC, Lamour Y. Electrophysiological evidence for a facio-facial reflex in the facial muscles in man. Brain Res 1977, Jan 7;119(2):459-64.

37. Verzijl HT, van der Zwaag B, Cruysberg JR, Padberg GW. Möbius syndrome redefined: A syndrome of rhombencephalic maldevelopment. Neurology 2003, Aug 12;61(3):327-33.

38. Bonnet RM. Causes of facial palsies. In: Beurskens, editors. The Facial Palsies, complementary approaches. Utrecht: Lemma Publishers; 2005.

39. Peitersen. Bell's palsy: The spontaneous course of 2,500 peripheral facial nerve palsies of different etiologies. Acta Otolaryngol 2002;Suppl 549:4-30.

40. Coker NJ, Kendall KA, Jenkins HA, Alford BR. Traumatic intratemporal facial nerve injury: Management rationale for preservation of function. Otolaryngol Head Neck Surg 1987, Sep;97(3):262-9.

41. Ghali S, MacQuillan A, Grobbelaar AO. Reanimation of the middle and lower face in facial paralysis: Review of the literature and personal approach. J Plast Reconstr Aesthet Surg 2011, Apr;64(4):423-31.

42. Tamai S, Komatsu S, Sakamoto H, Sano S, Sasauchi N. Free muscle transplants in dogs, with microsurgical neurovascular anastomoses. Plast Reconstr Surg 1970, Sep;46(3):219-25.

43. Mathes SJ, Nahai F. Classification of the vascular anatomy of muscles: Experimental and clinical correlation. Plast Reconstr Surg 1981, Feb;67(2):177-87.

44. Taylor GI, Palmer JH. The vascular territories (angiosomes) of the body: Experimental study and clinical applications. Br J Plast Surg 1987, Mar;40(2):113-41.

45. Cormack GC, Lamberty BG. A classification of fascio-cutaneous flaps according to their patterns of vascularisation. Br J Plast Surg 1984, Jan;37(1):80-7.

46. Harii K, Ohmori K, Torii S. Free gracilis muscle transplantation, with microneurovascular anastomoses for the treatment of facial paralysis: A preliminary report. Plast Reconstr Surg 1976;57(2):133.

47. Harrison DH. The pectoralis minor vascularized muscle graft for the treatment of unilateral facial palsy. Plast Reconstr Surg 1985, Feb;75(2):206-16.

48. Terzis JK. Pectoralis minor: A unique muscle for correction of facial palsy. Plast Reconstr Surg 1989;83(5):767.

49. Manktelow RT, Tomat LR, Zuker RM, Chang M. Smile reconstruction in adults with free muscle transfer innervated by the masseter motor nerve: Effectiveness and cerebral adaptation. Plast Reconstr Surg 2006, Sep 15;118(4):885-99.

50. Frey M, Giovanoli P. The three-stage concept to optimize the results of microsurgical reanimation of the paralyzed face. Clin Plast Surg 2002, Oct;29(4):461-82.

51. Craniofacial Muscles. Springer; 2013.

52. Zuker RM, Manktelow RT. Functioning free muscle transfers. Hand Clin 2007, Feb;23(1):57-72.

53. Zuker RM, Bezuhly M, Manktelow RT. Selective fascicular coaptation of free functioning gracilis transfer for restoration of independent thumb and finger flexion following volkmann ischemic contracture. J Reconstr Microsurg 2011, Sep;27(7):439-44.

54. Harrison DH, Grobbelaar AO. Pectoralis minor muscle transfer for unilateral facial palsy reanimation: An experience of 35 years and 637 cases. J Plast Reconstr Aesthet Surg 2012, Jul;65(7):845-50.

55. Woollard AC, Harrison DH, Grobbelaar AO. An approach to bilateral facial paralysis. J Plast Reconstr Aesthet Surg 2010, Mar 4;63(9):1557-60.

56. Terzis JK. Pectoralis minor: A unique muscle for correction of facial palsy. Plast Reconstr Surg 1989;83(5):767.

57. Frey M, Giovanoli P. The three-stage concept to optimize the results of microsurgical reanimation of the paralyzed face. Clin Plast Surg 2002, Oct;29(4):461-82.

58. O'Brien BM, Pederson WC, Khazanchi RK, Morrison WA, MacLeod AM, Kumar V. Results of management of facial palsy with microvascular free-muscle transfer. Plast Reconstr Surg 1990, Jul;86(1):12-22; discussion 23-4.

59. Terzis JK, Noah ME. Analysis of 100 cases of free-muscle transplantation for facial paralysis. Plast Reconstr Surg 1997, Jun;99(7):1905-21.

60. Frey M, Michaelidou M, Tzou CH, Pona I, Mittlböck M, Gerber H, Stüssi E. Three-dimensional video analysis of the paralyzed face reanimated by cross-face nerve grafting and free gracilis muscle

transplantation: Quantification of the functional outcome. Plast Reconstr Surg 2008, Dec;122(6):1709-22.

61. House JW. Facial nerve grading systems. Laryngoscope 1983, Aug;93(8):1056-69.

62. Ross BG, Fradet G, Nedzelski JM. Development of a sensitive clinical facial grading system. Otolaryngol Head Neck Surg 1996, Mar;114(3):380-6.

63. Hato N, Fujiwara T, Gyo K, Yanagihara N. Yanagihara facial nerve grading system as a prognostic tool in bell's palsy. Otol Neurotol 2014, Oct;35(9):1669-72.

64. Berg T, Jonsson L, Engström M. Agreement between the sunnybrook, house-brackmann, and yanagihara facial nerve grading systems in bells palsy. Otology & Neurotology 2004;25(6):1020-6.

65. Ho AL, Scott AM, Klassen AF, Cano SJ, Pusic AL, Van Laeken N. Measuring quality of life and patient satisfaction in facial paralysis patients: A systematic review of patient-reported outcome measures. Plast Reconstr Surg 2012, Jul;130(1):91-9.

66. O'Brien BM, Pederson WC, Khazanchi RK, Morrison WA, MacLeod AM, Kumar V. Results of management of facial palsy with microvascular free-muscle transfer. Plast Reconstr Surg 1990, Jul;86(1):12-22; discussion 23-4.

67. Hidalgo DA, Jones CS. The role of emergent exploration in free-tissue transfer: A review of 150 consecutive cases. Plast Reconstr Surg 1990;86(3):492.

68. Terzis JK, Anesti K. Experience with developmental facial paralysis: Part II. Outcomes of reconstruction. Plast Reconstr Surg 2012;129(1):66e.

69. Sunderland S. The anatomy and physiology of nerve injury. Muscle Nerve 1990, Sep;13(9):771-84.

70. Madison RD, Sofroniew MV, Robinson GA. Schwann cell influence on motor neuron regeneration accuracy. Neuroscience 2009;163(1):213-21.

71. Zeineh LL, Wilhelmi BJ, Zook EG. Managing acute nerve injuries in extremities. Operative Techniques in Plastic and Reconstructive Surgery 2002;9(3):111-6.

72. Ashur H, Vilner Y, Finsterbush A, Rousso M, Weinberg H, Devor M. Extent of fiber regeneration after peripheral nerve repair: Silicone splint vs. Suture, gap repair vs. Graft. Exp Neurol 1987, Aug;97(2):365-74.

73. Flores AJ, Lavernia CJ, Owens PW. Anatomy and physiology of peripheral nerve injury and repair. Am J Orthop (Belle Mead NJ) 2000, Mar;29(3):167-73.

74. Deal DN, Griffin JW, Hogan MV. Nerve conduits for nerve repair or reconstruction. Journal of the American Academy of Orthopaedic Surgeons 2012;20(2):63-8.

75. Griffin JW, Hogan MV, Chhabra AB, Deal DN. Peripheral nerve repair and reconstruction. The Journal of Bone & Joint Surgery 2013;95(23):2144-51.

76. MacQuillan AHF, Grobbelaar AO. Functional muscle transfer and the variance of reinnervating axonal load: Part II. Peripheral nerves. Plast Reconstr Surg 2008;121(5):1708.

77. MacQuillan AHF, Grobbelaar AO. Functional muscle transfer and the variance of reinnervating axonal load: Part I. The facial nerve. Plast Reconstr Surg 2008;121(5):1570.

78. Fuglevand AJ. Mechanical properties and neural control of human hand motor units. J Physiol 2011, Dec 1;589(Pt 23):5595-602.

79. Aszmann OC, Rab M, Kamolz L, Frey M. The anatomy of the pectoral nerves and their significance in brachial plexus reconstruction. J Hand Surg Am 2000, Sep;25(5):942-7.

80. Terzis JK, Wang W, Zhao Y. Effect of axonal load on the functional and aesthetic outcomes of the cross-facial nerve graft procedure for facial reanimation. Plast Reconstr Surg 2009, Nov;124(5):1499-512.

81. Jacobs JM, Laing JHE, Harrison DH. Regeneration through a long nerve graft used in the correction of facial palsy: A qualitative and quantitative study. Brain 1996;119(1):271.

82. Aitken JT, Sharman M, Young JZ. Maturation of regenerating nerve fibres with various peripheral connexions. J Anat 1947, Jan;81(1):1-22.

83. Frey M, Happak W, Girsch W, Bittner RE, Gruber H. Histomorphometric studies in patients with facial palsy treated by functional muscle transplantation: New aspects for the surgical concept. Ann Plast Surg 1991, Apr;26(4):370-9.

84. Terzis JK, Wang W, Zhao Y. Effect of axonal load on the functional and aesthetic outcomes of the cross-facial nerve graft procedure for facial reanimation. Plast Reconstr Surg 2009, Nov;124(5):1499-512.

85. Langley JN, Anderson HK. The union of different kinds of nerve fibres. J Physiol 1904, Aug 22;31(5):365-91.

86. Erlanger J, Schoepfle GM. A study of nerve degeneration and regeneration. Am J Physiol 1946, Nov;147(3):550-81.

87. Berry CM, Grundfest H, Hinsey JC. The electrical activity of regenerating nerves in the cat. J Neurophysiol 1944;7(2):103-15.

88. Bernstein JJ, Guth L. Nonselectivity in establishment of neuromuscular connections following nerve regeneration in the rat. Exp Neurol 1961, Sep;4:262-75.

89. Miledi R, Stefani E. Non-selective re-innervation of slow and fast muscle fibres in the rat. Nature 1969, May 10;222(5193):569-71.

90. Schmalbruch H. The morphology of regeneration of skeletal muscles in the rat. Tissue Cell 1976;8(4):673-92.

91. Carlson BM, Gutmann E. Regeneration in free grafts of normal and denervated muscles in the rat: Morphology and histochemistry. Anat Rec 1975;183(1):47-61.

92. Brushart TM, Henry EW, Mesulam MM. Reorganization of muscle afferent projections accompanies peripheral nerve regeneration. Neuroscience 1981;6(10):2053-61.

93. Brushart TM, Seiler WA. Selective reinnervation of distal motor stumps by peripheral motor axons. Exp Neurol 1987, Aug;97(2):289-300.

94. Brushart TM. Motor axons preferentially reinnervate motor pathways. J Neurosci 1993, Jun;13(6):2730-8.

95. Gordon T, Stein RB. Time course and extent of recovery in reinnervated motor units of cat triceps surae muscles. J Physiol 1982, Feb;323:307-23.

96. Gordon T, Gillespie J, Orozco R, Davis L. Axotomy-induced changes in rabbit hindlimb nerves and the effects of chronic electrical stimulation. J Neurosci 1991, Jul;11(7):2157-69.

97. Gorio A, Carmignoto G, Finesso M, Polato P, Nunzi MG. Muscle reinnervation--ii. Sprouting, synapse formation and repression. Neuroscience 1983;8(3):403-16.

98. Toft PB, Fugleholm K, Schmalbruch H. Axonal branching following crush lesions of peripheral nerves of rat. Muscle Nerve 1988, Aug;11(8):880-9.

99. Fu SY, Gordon T. Contributing factors to poor functional recovery after delayed nerve repair: Prolonged denervation. J Neurosci 1995, May;15(5 Pt 2):3886-95.

100. Fenrich K, Gordon T. Canadian association of neuroscience review: Axonal regeneration in the peripheral and central nervous systems--current issues and advances. Can J Neurol Sci 2004, May;31(2):142-56.

101. Ide C. Peripheral nerve regeneration. Neurosci Res 1996;25(2):101-21.

102. Boyd JG, Gordon T. Glial cell line-derived neurotrophic factor and brain-derived neurotrophic factor sustain the axonal regeneration of chronically axotomized motoneurons in vivo. Exp Neurol 2003, Oct;183(2):610-9.

103. Nguyen QT, Sanes JR, Lichtman JW. Pre-existing pathways promote precise projection patterns. Nat Neurosci 2002, Sep;5(9):861-7.

104. Sulaiman OAR, Boyd JG, Gordon T. 36. Axonal regeneration in the peripheral nervous system of mammals. Neuroglia 2004;1(9):454-67.

105. Lichtman JW, Smith SJ. Seeing circuits assemble. Neuron 2008, Nov 6;60(3):441-8.

106. y Cajal SR. Degeneration & regeneration of the nervous system. Oxford University Press, Humphrey Milford; 1928.

107. Harrison RG. The outgrowth of the nerve fiber as a mode of protoplasmic movement. J Exp Zool 1959;142:5-73.

108. Kandel ER, Schwartz JH, Jessell TM. Principles of neural science. McGraw-Hill New York; 2000.

109. Movement of sodium and potassium ions during nervous activity; Cold spring harbor symposia on quantitative biology. 1952.

110. Fuglevand AJ. Mechanical properties and neural control of human hand motor units. J Physiol 2011, Dec 1;589(Pt 23):5595-602.

111. Olson CB, Carpenter DO, Henneman E. Orderly recruitment of muscle action potentials. Arch Neurol 1968, Dec;19(6):591-7.

112. Milner-Brown HS, Stein RB, Yemm R. The orderly recruitment of human motor units during voluntary isometric contractions. J Physiol 1973, Apr;230(2):359-70.

113. y Cajal SR. Recollections of my life. The MIT Press; 1989.

114. Aguayo AJ, Vidal-Sanz M, Villegas-Perez MP, Bray GM. Growth and connectivity of axotomized retinal neurons in adult rats with optic nerves substituted by PNS grafts linking the eye and the midbraina. Ann N Y Acad Sci 1987;495(Cell and Tissue Transplantation into the Adult Brain):1-7.

115. Waller A. New method for the study of the nervous system. London Journal of Medicine 1852;2(43):609.

116. George EB, Glass JD, Griffin JW. Axotomy-induced axonal degeneration is mediated by calcium influx through ion-specific channels. J Neurosci 1995, Oct;15(10):6445-52.

117. Stoll G, Griffin JW, Li CY, Trapp BD. Wallerian degeneration in the peripheral nervous system: Participation of both schwann cells and macrophages in myelin degradation. J Neurocytol 1989, Oct;18(5):671-83.

118. Bulsara KR, Iskandar BJ, Villavicencio AT, Skene JH. A new millenium for spinal cord regeneration: Growth-associated genes. Spine (Phila Pa 1976) 2002, Sep 1;27(17):1946-9.

119. Kreutzberg GW. Microglia: A sensor for pathological events in the CNS. Trends Neurosci 1996, Aug;19(8):312-8.

120. Bomze HM, Bulsara KR, Iskandar BJ, Caroni P, Skene JH. Spinal axon regeneration evoked by replacing two growth cone proteins in adult neurons. Nat Neurosci 2001, Jan;4(1):38-43.

121. Strittmatter SM, Igarashi M, Fishman MC. GAP-43 amino terminal peptides modulate growth cone morphology and neurite outgrowth. J Neurosci 1994, Sep;14(9):5503-13.

122. Gordon T, Gillespie J, Orozco R, Davis L. Axotomy-induced changes in rabbit hindlimb nerves and the effects of chronic electrical stimulation. J Neurosci 1991, Jul;11(7):2157-69.

123. Tetzlaff W, Alexander SW, Miller FD, Bisby MA. Response of facial and rubrospinal neurons to axotomy: Changes in mrna expression for cytoskeletal proteins and GAP-43. J Neurosci 1991, Aug;11(8):2528-44.

124. LeBlanc AC, Poduslo JF. Axonal modulation of myelin gene expression in the peripheral nerve. J Neurosci Res 1990, Jul;26(3):317-26.

125. Fenrich K, Gordon T. Canadian association of neuroscience review: Axonal regeneration in the peripheral and central nervous systems--current issues and advances. Can J Neurol Sci 2004, May;31(2):142-56.

126. Boyd JG, Gordon T. Glial cell line-derived neurotrophic factor and brain-derived neurotrophic factor sustain the axonal regeneration of chronically axotomized motoneurons in vivo. Exp Neurol 2003, Oct;183(2):610-9.

127. LeBlanc AC, Poduslo JF. Axonal modulation of myelin gene expression in the peripheral nerve. J Neurosci Res 1990, Jul;26(3):317-26.

128. Stoll G, Trapp BD, Griffin JW. Macrophage function during wallerian degeneration of rat optic nerve: Clearance of degenerating myelin and ia expression. The Journal of Neuroscience 1989;9(7):2327.

129. Fenrich K, Gordon T. Canadian association of neuroscience review: Axonal regeneration in the peripheral and central nervous systems--current issues and advances. Can J Neurol Sci 2004, May;31(2):142-56.

130. Fu SY, Gordon T. The cellular and molecular basis of peripheral nerve regeneration. Mol Neurobiol 1997;14(1-2):67.

131. Anton ES, Weskamp G, Reichardt LF, Matthew WD. Nerve growth factor and its low-affinity receptor promote schwann cell migration. Proc Natl Acad Sci U S A 1994, Mar 29;91(7):2795-9.

132. Liu HM, Yang LH, Yang YJ. Schwann cell properties: 3. C-fos expression, bfgf production, phagocytosis and proliferation during wallerian degeneration. J Neuropathol Exp Neurol 1995, Jul;54(4):487-96.

133. Bungner O. Uber die degenerations und regenerationsvorgange am nerven nach verletzungen. Beitr. Pathol. Anat 1891;10:321-87.

134. Brück W. The role of macrophages in wallerian degeneration. Brain Pathol 1997, Apr;7(2):741-52.

135. Avellino AM, Hart D, Dailey AT, Mackinnon M, Ellegala D, Kliot M. Differential macrophage responses in the peripheral and central nervous system during wallerian degeneration of axons. Exp Neurol 1995;136(2):183-98.

136. Tang S, Woodhall RW, Shen YJ, deBellard ME, Saffell JL, Doherty P, et al. Soluble myelin-associated glycoprotein (MAG) found in vivo inhibits axonal regeneration. Mol Cell Neurosci 1997;9(5-6):333-46.

137. Filbin MT. Myelin-associated glycoprotein: A role in myelination and in the inhibition of axonal regeneration? Curr Opin Neurobiol 1995, Oct;5(5):588-95.

138. Filbin MT. The muddle with MAG. Mol Cell Neurosci 1996;8(2-3):84-92.

139. Hirata K, Kawabuchi M. Myelin phagocytosis by macrophages and nonmacrophages during wallerian degeneration. Microsc Res Tech 2002, Jun 15;57(6):541-7.

140. Landis SC. Neuronal growth cones. Annu Rev Physiol 1983;45:567-80.

141. Kater SB, Letourneau PC. Biology of the nerve growth cone. A. Liss; 1985.

142. Letourneau PC, Cypher C. Regulation of growth cone motility. Cell Motil Cytoskeleton 1991;20(4):267-71.

143. y Cajal SR. A quelle époque apparaissent les expansions des cellules nerveuses de la moëlle épinière du poulet? Gustav Fischer; 1890.

144. y Cajal SR. Recollections of my life. The MIT Press; 1989.

145. Harrison RG. The outgrowth of the nerve fiber as a mode of protoplasmic movement. J Exp Zool 1959;142:5-73.

146. Speidel CC. Adjustments of nerve endings: Harvey lecture, january 16, 1941. Bull N Y Acad Med 1942, Oct;18(10):625-53.

147. O'Connor TP, Duerr JS, Bentley D. Pioneer growth cone steering decisions mediated by single filopodial contacts in situ. J Neurosci 1990, Dec;10(12):3935-46.

148. Tosney KW, Landmesser LT. Growth cone morphology and trajectory in the lumbosacral region of the chick embryo. The Journal of Neuroscience 1985;5(9):2345.

149. Bovolenta P, Mason C. Growth cone morphology varies with position in the developing mouse visual pathway from retina to first targets. J Neurosci 1987, May;7(5):1447-60.

150. Halpern ME, Chiba A, Johansen J, Keshishian H. Growth cone behavior underlying the development of stereotypic synaptic connections in drosophila embryos. J Neurosci 1991, Oct;11(10):3227-38.

151. Hollenbeck PJ, Bray D. Rapidly transported organelles containing membrane and cytoskeletal components: Their relation to axonal growth. J Cell Biol 1987, Dec;105(6 Pt 1):2827-35.

152. Dai J, Sheetz MP. Axon membrane flows from the growth cone to the cell body. Cell 1995, Dec 1;83(5):693-701.

153. Reinsch SS, Mitchison TJ, Kirschner M. Microtubule polymer assembly and transport during axonal elongation. J Cell Biol 1991, Oct;115(2):365-79.

154. Bentley D, O'Connor TP. Cytoskeletal events in growth cone steering. Curr Opin Neurobiol 1994, Feb;4(1):43-8.

155. Heidemann SR, Lamoureux P, Buxbaum RE. Cytomechanics of axonal development. Cell Biochem Biophys 1995;27(3):135-55.

156. Heidemann SR, Lamoureux P, Buxbaum RE. Cytomechanics of axonal development. Cell Biochem Biophys 1995;27(3):135-55.

157. Letourneau PC. The cytoskeleton in nerve growth cone motility and axonal pathfinding. Perspect Dev Neurobiol 1996;4(2-3):111-23.

158. Sanes DH, Reh TA, Harris WA. Development of the nervous system. Academic Pr; 2011.

159. Bray D. Mechanical tension produced by nerve cells in tissue culture. J Cell Sci 1979, Jun;37:391-410.

160. Harris WA. Homing behaviour of axons in the embryonic vertebrate brain. 1986.

161. Letourneau PC. Cell-to-substratum adhesion and guidance of axonal elongation. Dev Biol 1975, May;44(1):92-101.

162. Hammarback JA, Palm SL, Furcht LT, Letourneau PC. Guidance of neurite outgrowth by pathways of substratum-adsorbed laminin. J Neurosci Res 1985;13(1-2):213-20.

163. Nardi JB. Neuronal pathfinding in developing wings of the moth manduca sexta. Dev Biol 1983, Jan;95(1):163-74.

164. Nardi JB, Vernon RA. Topographical features of the substratum for growth of pioneering neurons in the manduca wing disc. J Neurobiol 1990, Dec;21(8):1189-201.

165. Lemmon V, Burden SM, Payne HR, Elmslie GJ, Hlavin ML. Neurite growth on different substrates: Permissive versus instructive influences and the role of adhesive strength. J Neurosci 1992, Mar;12(3):818-26.

166. McKenna MP, Raper JA. Growth cone behavior on gradients of substratum bound laminin. Dev Biol 1988, Nov;130(1):232-6.

167. Bixby JL, Harris WA. Molecular mechanisms of axon growth and guidance. Annu Rev Cell Biol 1991;7:117-59.

168. McKerracher L, Chamoux M, Arregui CO. Role of laminin and integrin interactions in growth cone guidance. Mol Neurobiol 1996, Apr;12(2):95-116.

169. Cohen J, Johnson AR. Differential effects of laminin and merosin on neurite outgrowth by developing retinal ganglion cells. J Cell Sci Suppl 1991;15:1-7.

170. Walsh FS, Doherty P. Neural cell adhesion molecules of the immunoglobulin superfamily: Role in axon growth and guidance. Annu Rev Cell Dev Biol 1997;13:425-56.

171. Tang J, Rutishauser U, Landmesser L. Polysialic acid regulates growth cone behavior during sorting of motor axons in the plexus region. Neuron 1994, Aug;13(2):405-14.

172. Goodman CS, Raper JA, Chang S, Ho R. Grasshopper growth cones: Divergent choices and labeled pathways. Progress in Brain Research 1983;58:283-304.

173. Goodman CS, Bastiani MJ, Doe CQ, Du Lac S, Helfand SL, Kuwada JY, Thomas JB. Cell recognition during neuronal development. Science 1984;225(4668):1271-9.

174. Goodman CS. Mechanisms and molecules that control growth cone guidance. Annu Rev Neurosci 1996;19:341-77.

175. Bastiani MJ, Harrelson AL, Snow PM, Goodman CS. Expression of fasciclin I and II glycoproteins on subsets of axon pathways during neuronal development in the grasshopper. Cell 1987, Mar 13;48(5):745-55.

176. Harris WA. Local positional cues in the neuroepithelium guide retinal axons in embryonic xenopus brain. Nature 1989, May 18;339(6221):218-21.

177. Gundersen RW, Barrett JN. Neuronal chemotaxis: Chick dorsal-root axons turn toward high concentrations of nerve growth factor. Science 1979, Nov 30;206(4422):1079-80.

178. Lumsden AG, Davies AM. Chemotropic effect of specific target epithelium in the developing mammalian nervous system. Nature 1986;323(6088):538-9.

179. Colamarino SA, Tessier-Lavigne M. The axonal chemoattractant netrin-1 is also a chemorepellent for trochlear motor axons. Cell 1995, May 19;81(4):621-9.

180. Luo Y, Raible D, Raper JA. Collapsin: A protein in brain that induces the collapse and paralysis of neuronal growth cones. Cell 1993, Oct 22;75(2):217-27.

181. Kolodkin AL, Matthes DJ, Goodman CS. The semaphorin genes encode a family of transmembrane and secreted growth cone guidance molecules. Cell 1993, Dec 31;75(7):1389-99.

182. Fan J, Raper JA. Localized collapsing cues can steer growth cones without inducing their full collapse. Neuron 1995, Feb;14(2):263-74.

183. Kapfhammer JP, Raper JA. Interactions between growth cones and neurites growing from different neural tissues in culture. J Neurosci 1987, May;7(5):1595-600.

184. Silver J, Ogawa MY. Postnatally induced formation of the corpus callosum in acallosal mice on glia-coated cellulose bridges. Science 1983, Jun 3;220(4601):1067-9.

185. Sulaiman OAR, Boyd JG, Gordon T. 36. Axonal regeneration in the peripheral nervous system of mammals. Neuroglia 2004;1(9):454-67.

186. Ide C, Tohyama K, Yokota R, Nitatori T, Onodera S. Schwann cell basal lamina and nerve regeneration. Brain Res 1983;288(1-2):61-75.

187. y Cajal SR. Degeneration & regeneration of the nervous system. Oxford University Press, Humphrey Milford; 1928.

188. Bunge RP, Bunge MB. Interrelationship between schwann cell function and extracellular matrix production. Trends Neurosci 1983;6:499-505.

189. Martini R, Schachner M. Immunoelectron microscopic localization of neural cell adhesion molecules (L1, N-CAM, and myelin-associated glycoprotein) in regenerating adult mouse sciatic nerve. J Cell Biol 1988;106(5):1735-46.

190. Chen YG, Brushart TM. The effect of denervated muscle and schwann cells on axon collateral sprouting. J Hand Surg Am 1998, Nov;23(6):1025-33.

191. Fu SY, Gordon T. The cellular and molecular basis of peripheral nerve regeneration. Mol Neurobiol 1997;14(1-2):67.

192. Ide C, Osawa T, Tohyama K. Nerve regeneration through allogeneic nerve grafts, with special reference to the role of the schwann cell basal lamina. Prog Neurobiol 1990;34(1):1-38.

193. Sulaiman OAR, Boyd JG, Gordon T. 36. Axonal regeneration in the peripheral nervous system of mammals. Neuroglia 2004;1(9):454-67.

194. Redfern PA. Neuromuscular transmission in new-born rats. J Physiol 1970, Aug;209(3):701-9.

195. Brown MC, Booth CM. Postnatal development of the adult pattern of motor axon distribution in rat muscle. 1983.

196. Purves D, Hadley RD. Changes in the dendritic branching of adult mammalian neurones revealed by repeated imaging in situ. Nature 1985;315(6018):404-6.

197. Rich MM, Lichtman JW. In vivo visualization of pre- and postsynaptic changes during synapse elimination in reinnervated mouse muscle. J Neurosci 1989, May;9(5):1781-805.

198. Balice-Gordon RJ, Lichtman JW. In vivo observations of pre- and postsynaptic changes during the transition from multiple to single innervation at developing neuromuscular junctions . The Journal of Neuroscience 1993;73(2):834-55.

199. Colman H, Nabekura J, Lichtman JW. Alterations in synaptic strength preceding axon withdrawal. Science 1997;275(5298):356.

200. Laskowski MB, Colman H, Nelson C, Lichtman JW. Synaptic competition during the reformation of a neuromuscular map. J Neurosci 1998, Sep 15;18(18):7328-35.

201. Lichtman JW, Colman H. Synapse elimination and indelible memory. Neuron 2000, Feb;25(2):269-78.

202. Mackinnon SE, Dellon AL, O'Brien JP. Changes in nerve fiber numbers distal to a nerve repair in the rat sciatic nerve model. Muscle Nerve 1991, Nov;14(11):1116-22.

203. Gutmann E, Sanders FK. Recovery of fibre numbers and diameters in the regeneration of peripheral nerves. J Physiol 1943, Mar 25;101(4):489-518.

204. Sanders FK, Whitteridge D. Conduction velocity and myelin thickness in regenerating nerve fibres. J Physiol 1946, Sep 18;105(2):152-74.

205. Weiss P, Taylor AC. Further experimental evidence against neurotropism in nerve regeneration. Journal of Experimental Zoology 1944;95(2):233-57.

206. Sanders FK, Whitteridge D. Conduction velocity and myelin thickness in regenerating nerve fibres. J Physiol 1946, Sep 18;105(2):152-74.

207. Gordon T, Stein RB. Reorganization of motor-unit properties in reinnervated muscles of the cat. J Neurophysiol 1982, Nov;48(5):1175-90.

208. Voyvodic JT. Peripheral target regulation of dendritic geometry in the rat superior cervical ganglion. J Neurosci 1989, Jun;9(6):1997-2010.

209. Duncan D. A relation between axone diameter and myelination determined by measurement of myelinated spinal root fibers. J Comp Neurol 1934, Dec;60(3):437-71.

210. MacQuillan AH, Grobbelaar AO, Baiarda FU. A theory explaining the development of late-onset tightening or contracture in patients who have undergone facial reanimation surgery with free functional muscle transfers. Plast Reconstr Surg 2009;124(5):254e.

211. CRAGG BG, THOMAS PK. THE CONDUCTION VELOCITY OF REGENERATED PERIPHERAL NERVE FIBRES. J Physiol 1964, May;171:164-75.

212. Gutmann E, Sanders FK. Recovery of fibre numbers and diameters in the regeneration of peripheral nerves. J Physiol 1943, Mar 25;101(4):489-518.

213. Sunderland S. Degeneration of the axon and associated changes. Nerves and Nerve Injuries 1978:108-32.

214. Merle M, Amend P, Foucher G, Michon J. [Plea for the primary microsurgical repair of peripheral nerve lesions. A comparative study of 150 injuries of the median or the ulnar nerve with a follow-up of more than 2 years]. Chirurgie 1984;110(8-9):761-71.

215. Birch R, Raji AR. Repair of median and ulnar nerves. Primary suture is best. J Bone Joint Surg Br 1991, Jan;73(1):154-7.

216. Bowden REM. Muscle changes in denervation and re-innervation. Br Med J 1945;2(4423):487-8.

217. Mussini I, Favaro G, Carraro U. Maturation, dystrophic changes and the continuous production of fibers in skeletal muscle regenerating in the absence of nerve. J Neuropathol Exp Neurol 1987, May;46(3):315-31.

218. Schmalbruch H, al-Amood WS, Lewis DM. Morphology of long-term denervated rat soleus muscle and the effect of chronic electrical stimulation. J Physiol 1991, Sep;441:233-41.

219. Bagust J, Lewis DM, Westerman RA. Motor units in cross-reinnervated fast and slow twitch muscle of the cat. J Physiol 1981;313:223-35.

220. Fu SY, Gordon T. Contributing factors to poor functional recovery after delayed nerve repair: Prolonged denervation. J Neurosci 1995, May;15(5 Pt 2):3886-95.

221. Brown MC, Ironton R. Sprouting and regression of neuromuscular synapses in partially denervated mammalian muscles. J Physiol 1978, May;278:325-48.

222. Rafuse VF, Gordon T, Orozco R. Proportional enlargement of motor units after partial denervation of cat triceps surae muscles. J Neurophysiol 1992, Oct;68(4):1261-76.

223. Luff AR, Torkko K. Long-term persistence of enlarged motor units in partially denervated hindlimb muscles of cats. J Neurophysiol 1990, Oct;64(4):1261-9.

224. Rochel S, Robbins N. Effect of partial denervation and terminal field expansion on neuromuscular transmitter release and nerve terminal structure. J Neurosci 1988, Jan;8(1):332-8.

225. Slack JR, Hopkins WG. Neuromuscular transmission at terminals of sprouted mammalian motor neurones. Brain Res 1982, Apr 8;237(1):121-35.

226. Fu SY, Gordon T. Contributing factors to poor functional recovery after delayed nerve repair: Prolonged denervation. J Neurosci 1995, May;15(5 Pt 2):3886-95.

227. Rich MM, Lichtman JW. In vivo visualization of pre- and postsynaptic changes during synapse elimination in reinnervated mouse muscle. J Neurosci 1989, May;9(5):1781-805.

228. Kang H, Tian L, Thompson W. Terminal schwann cells guide the reinnervation of muscle after nerve injury. J Neurocytol 2003;32(5-8):975-85.

229. Brown AG, Fyffe RE. Direct observations on the contacts made between ia afferent fibres and alpha-motoneurones in the cat's lumbosacral spinal cord. J Physiol 1981;313:121-40.

230. Aldskogius H, Molander C, Persson J, Thomander L. Specific and nonspecific regeneration of motor axons after sciatic nerve injury and repair in the rat. J Neurol Sci 1987, Sep;80(2-3):249-57.

231. Bernstein JJ, Guth L. Nonselectivity in establishment of neuromuscular connections following nerve regeneration in the rat. Exp Neurol 1961, Sep;4:262-75.

232. Brushart TM, Mesulam M-. Alteration in connections between muscle and anterior horn motoneurons after peripheral nerve repair. Science 1980;208(4444):603-5.

233. Mizuno N, Uemura-Sumi M, Matsuda K, Takeuchi Y, Kume M, Matsushima R. Non-selective distribution of hypoglossal nerve fibers after section and resuture: A horseradish peroxidase study in the cat. Neurosci Lett 1980, Aug;19(1):33-7.

234. Brushart TM. Preferential reinnervation of motor nerves by regenerating motor axons. Journal of Neuroscience 1988;8(3):1026.

235. Aldskogius H, Molander C, Persson J, Thomander L. Specific and nonspecific regeneration of motor axons after sciatic nerve injury and repair in the rat. J Neurol Sci 1987, Sep;80(2-3):249-57.

236. Uschold T, Robinson GA, Madison RD. Motor neuron regeneration accuracy: Balancing trophic influences between pathways and end-organs. Exp Neurol 2007, May;205(1):250-6.

237. Madison RD, Robinson GA, Chadaram SR. The specificity of motor neurone regeneration (preferential reinnervation). Acta Physiologica 2007;189(2):201-6.

238. Robinson GA, Madison RD. Influence of terminal nerve branch size on motor neuron regeneration accuracy. Exp Neurol 2009, Feb;215(2):228-35.

239. Brown MC, Booth CM. Postnatal development of the adult pattern of motor axon distribution in rat muscle. 1983.

240. Balice-Gordon RJ, Lichtman JW. Long-term synapse loss induced by focal blockade of postsynaptic receptors. Nature 1994, Dec 8;372(6506):519-24.

241. Marques MJ, Conchello JA, Lichtman JW. From plaque to pretzel: Fold formation and acetylcholine receptor loss at the developing neuromuscular junction. J Neurosci 2000, May 15;20(10):3663-75.

242. Balice-Gordon RJ, Breedlove SM, Bernstein S, Lichtman JW. Neuromuscular junctions shrink and expand as muscle fiber size is manipulated: In vivo observations in the androgen-sensitive bulbocavernosus muscle of mice. J Neurosci 1990, Aug;10(8):2660-71.

243. Kang H, Tian L, Thompson W. Terminal schwann cells guide the reinnervation of muscle after nerve injury. J Neurocytol 2003;32(5-8):975-85.

244. Shimomura O, Johnson FH, Saiga Y. Extraction, purification and properties of aequorin, a bioluminescent protein from the luminous hydromedusan, aequorea. J Cell Comp Physiol 1962, Jun;59:223-39.

245. Prasher DC, Eckenrode VK, Ward WW, Prendergast FG, Cormier MJ. Primary structure of the aequorea victoria green-fluorescent protein. Gene 1992, Feb 15;111(2):229-33.

246. Chalfie M, Tu Y, Euskirchen G, Ward WW, Prasher DC. Green fluorescent protein as a marker for gene expression. Science (New York, NY) 1994;263(5148):802.

247. Wang S, Hazelrigg T. Implications for bcd mrna localization from spatial distribution of exu protein in drosophila oogenesis. Nature 1994, Jun 2;369(6479):400-3.

248. Heim R, Prasher DC, Tsien RY. Wavelength mutations and posttranslational autoxidation of green fluorescent protein. Proc Natl Acad Sci U S A 1994, Dec 20;91(26):12501-4.

249. Zimmer M. GFP: From jellyfish to the nobel prize and beyond. Chem Soc Rev 2009, Oct;38(10):2823-32.

250. Feng G, Mellor RH, Bernstein M, Keller-Peck C, Nguyen QT, Wallace M, et al. Imaging neuronal subsets in transgenic mice expressing multiple spectral variants of GFP. Neuron 2000;28(1):41-51.

251. Lichtman JW, Sanes JR. Watching the neuromuscular junction. J Neurocytol 2003;32(5-8):767-75.

252. Lu J, Fiala JC, Lichtman JW. Semi-automated reconstruction of neural processes from large numbers of fluorescence images. PLoS One 2009;4(5):e5655.

253. Nguyen QT, Son YJ, Sanes JR, Lichtman JW. Nerve terminals form but fail to mature when postsynaptic differentiation is blocked: In vivo analysis using mammalian nerve-muscle chimeras. J Neurosci 2000, Aug 15;20(16):6077-86.

254. Kasthuri N, Lichtman JW. The role of neuronal identity in synaptic competition. Nature 2003;424(6947):426-30.

255. Feng G, Mellor RH, Bernstein M, Keller-Peck C, Nguyen QT, Wallace M, et al. Imaging neuronal subsets in transgenic mice expressing multiple spectral variants of GFP. Neuron 2000;28(1):41-51.

256. Rasband WS. ImageJ. US national institutes of health, bethesda, MD, USA 1997:

257. Yushkevich PA, Piven J, Hazlett HC, Smith RG, Ho S, Gee JC, Gerig G. User-guided 3D active contour segmentation of anatomical structures: Significantly improved efficiency and reliability. Neuroimage 2006, Jul 1;31(3):1116-28.

258. Feir BJ, Toothaker LE. The ANOVA f-test versus the kruskal-wallis test: A robustness study. 1974.

259. Khan A, Rayner GD. Robustness to non-normality of common tests for the many-sample location problem. Journal of Applied Mathematics & Decision Sciences 2003;7(4):187-206.

260. Mendes M, Pala A. Evaluation of four tests when normality and homogeneity of variance assumptions are violated. Journal of Applied Sciences 2004;4(1):38-42.

261. MacQuillan AH, Grobbelaar AO, Baiarda FU. A theory explaining the development of late-onset tightening or contracture in patients who have undergone facial reanimation surgery with free functional muscle transfers. Plast Reconstr Surg 2009;124(5):254e.

262. MacQuillan AH, Grobbelaar AO, Baiarda FU. A theory explaining the development of late-onset tightening or contracture in patients who have undergone facial reanimation surgery with free functional muscle transfers. Plast Reconstr Surg 2009;124(5):254e.

263. Lu J, Fiala JC, Lichtman JW. Semi-automated reconstruction of neural processes from large numbers of fluorescence images. PLoS One 2009;4(5):e5655.

264. Nguyen QT, Sanes JR, Lichtman JW. Pre-existing pathways promote precise projection patterns. Nat Neurosci 2002, Sep;5(9):861-7.

265. Waller A. New method for the study of the nervous system. London Journal of Medicine 1852;2(43):609.

266. Levinthal R, Brown WJ, Rand RW. Comparison of fascicular, interfascicular and epineural suture techniques in the repair of simple nerve lacerations. J Neurosurg 1977, Nov;47(5):744-50.

267. Lundborg G, Rosén B, Dahlin L, Danielsen N, Holmberg J. Tubular versus conventional repair of median and ulnar nerves in the human forearm: Early results from a prospective, randomized, clinical study. J Hand Surg Am 1997, Jan;22(1):99-106.

268. Siemionow M, Brzezicki G. Chapter 8: Current techniques and concepts in peripheral nerve repair. Int Rev Neurobiol 2009;87:141-72.

269. Millesi H. Indications and techniques of nerve grafting. In: Gelberman R, editors. Operative Nerve Repair and Reconstruction. Philadelphia: JB Lippincott; 1991. p. 525-43.

270. Miyamoto Y. Experimental study of results of nerve suture under tension vs. Nerve grafting. Plast Reconstr Surg 1979, Oct;64(4):540-9.

271. Nunley J. Donor nerves for grafting. In: Gelberman R, editors. Operative Nerve Repair and Reconstruction. Philadelphia: JB Lippincott; 1991. p. 545-52.

272. Birch R, Raji AR. Repair of median and ulnar nerves. Primary suture is best. J Bone Joint Surg Br 1991, Jan;73(1):154-7.

273. Millesi H, Meissl G, Berger A. The interfascicular nerve-grafting of the median and ulnar nerves. J Bone Joint Surg Am 1972, Jun;54(4):727-50.

274. Millesi H. Bridging defects: Autologous nerve grafts. Acta Neurochir Suppl 2007;100:37-8.

275. Mackinnon SE, Doolabh VB, Novak CB, Trulock EP. Clinical outcome following nerve allograft transplantation. Plast Reconstr Surg 2001, May;107(6):1419-29.

276. Fox IK, Mackinnon SE. Experience with nerve allograft transplantation. Semin Plast Surg 2007, Nov;21(4):242-9.

277. Chu TH, Du Y, Wu W. Motor nerve graft is better than sensory nerve graft for survival and regeneration of motoneurons after spinal root avulsion in adult rats. Exp Neurol 2008, Aug;212(2):562-5.

278. Moradzadeh A, Borschel GH, Luciano JP, Whitlock EL, Hayashi A, Hunter DA, Mackinnon SE. The impact of motor and sensory nerve architecture on nerve regeneration. Exp Neurol 2008, Aug;212(2):370-6.

279. Nichols CM, Brenner MJ, Fox IK, Tung TH, Hunter DA, Rickman SR, Mackinnon SE. Effects of motor versus sensory nerve grafts on peripheral nerve regeneration. Exp Neurol 2004, Dec;190(2):347-55.

280. Strauch B. Use of nerve conduits in peripheral nerve repair. Hand Clin 2000, Feb;16(1):123-30.

281. Itoh S, Shinomiya K, Samejima H, Ohta T, Ishizuki M, Ichinose S. Experimental study on nerve regeneration through the basement membrane tubes of the nerve, muscle, and artery. Microsurgery 1996;17(10):525-34.

282. Chiu DT, Janecka I, Krizek TJ, Wolff M, Lovelace RE. Autogenous vein graft as a conduit for nerve regeneration. Surgery 1982, Feb;91(2):226-33.

283. Battiston B, Geuna S, Ferrero M, Tos P. Nerve repair by means of tubulization: Literature review and personal clinical experience comparing biological and synthetic conduits for sensory nerve repair. Microsurgery 2005;25(4):258-67.

284. Schlosshauer B, Dreesmann L, Schaller HE, Sinis N. Synthetic nerve guide implants in humans: A comprehensive survey. Neurosurgery 2006, Oct;59(4):740-7; discussion 747-8.

285. Pabari A, Yang SY, Seifalian AM, Mosahebi A. Modern surgical management of peripheral nerve gap. J Plast Reconstr Aesthet Surg 2010, Dec;63(12):1941-8.

286. Lichtman JW, Magrassi L, Purves D. Visualization of neuromuscular junctions over periods of several months in living mice. J Neurosci 1987, Apr;7(4):1215-22.

287. Wernig A, Herrera AA. Sprouting and remodelling at the nerve-muscle junction. Prog Neurobiol 1986;27(3):251-91.

288. MacQuillan AH, Grobbelaar AO, Baiarda FU. A theory explaining the development of late-onset tightening or contracture in patients who have undergone facial reanimation surgery with free functional muscle transfers. Plast Reconstr Surg 2009;124(5):254e.

289. Lu J, Tapia JC, White OL, Lichtman JW. The interscutularis muscle connectome. PLoS Biol 2009, Feb 10;7(2):e32.

290. Nguyen QT, Sanes JR, Lichtman JW. Pre-existing pathways promote precise projection patterns. Nat Neurosci 2002, Sep;5(9):861-7.

291. Purves D, Sakmann B. The effect of contractile activity on fibrillation and extrajunctional acetylcholine-sensitivity in rat muscle maintained in organ culture. J Physiol 1974, Feb;237(1):157-82.

292. Campanelli JT, Roberds SL, Campbell KP, Scheller RH. A role for dystrophin-associated glycoproteins and utrophin in agrin-induced achr clustering. Cell 1994, Jun 3;77(5):663-74.

293. Nastuk MA, Lieth E, Ma JY, Cardasis CA, Moynihan EB, McKechnie BA, Fallon JR. The putative agrin receptor binds ligand in a calcium-dependent manner and aggregates during agrin-induced acetylcholine receptor clustering. Neuron 1991, Nov;7(5):807-18.

294. Sanes JR, Lichtman JW. Induction, assembly, maturation and maintenance of a postsynaptic apparatus. Nat Rev Neurosci 2001, Nov;2(11):791-805.

295. Misgeld T, Kummer TT, Lichtman JW, Sanes JR. Agrin promotes synaptic differentiation by counteracting an inhibitory effect of neurotransmitter. Proc Natl Acad Sci U S A 2005, Aug 2;102(31):11088-93.

296. Rich MM, Lichtman JW. In vivo visualization of pre- and postsynaptic changes during synapse elimination in reinnervated mouse muscle. J Neurosci 1989, May;9(5):1781-805.

297. Son YJ, Trachtenberg JT, Thompson WJ. Schwann cells induce and guide sprouting and reinnervation of neuromuscular junctions. Trends Neurosci 1996, Jul;19(7):280-5.

298. Sanes JR, Lichtman JW. Can molecules explain long-term potentiation? Nat Neurosci 1999, Jul;2(7):597-604.

299. Wood MD, Kemp SW, Weber C, Borschel GH, Gordon T. Outcome measures of peripheral nerve regeneration. Ann Anat 2011, Jul;193(4):321-33.

300. Wood MD, Kemp SW, Weber C, Borschel GH, Gordon T. Outcome measures of peripheral nerve regeneration. Ann Anat 2011, Jul;193(4):321-33.

301. Bray GM, Aguayo AJ. Regeneration of peripheral unmyelinated nerves. Fate of the axonal sprouts which develop after injury. J Anat 1974, Jul;117(Pt 3):517-29.

302. Duel AB. The operative treatment of facial palsy. Br Med J 1934;2(3857):1027.

303. Vizoso AD, Young JZ. Internode length and fibre diameter in developing and regenerating nerves. J Anat 1948, Apr;82(Pt 1-2):110-134.1.

304. SHAWE GD. On the number of branches formed by regenerating nerve-fibres. Br J Surg 1955, Mar;42(175):474-88.

305. Ide C. Peripheral nerve regeneration. Neurosci Res 1996;25(2):101-21.

306. Ide C, Osawa T, Tohyama K. Nerve regeneration through allogeneic nerve grafts, with special reference to the role of the schwann cell basal lamina. Prog Neurobiol 1990;34(1):1-38.

307. Aitken JT, Sharman M, Young JZ. Maturation of regenerating nerve fibres with various peripheral connexions. J Anat 1947, Jan;81(1):1-22.

308. SHAWE GD. On the number of branches formed by regenerating nerve-fibres. Br J Surg 1955, Mar;42(175):474-88.

309. Urso-Baiarda F, Grobbelaar AO. Practical nerve morphometry. J Neurosci Methods 2006;156(1-2):333-41.

310. Ashur H, Vilner Y, Finsterbush A, Rousso M, Weinberg H, Devor M. Extent of fiber regeneration after peripheral nerve repair: Silicone splint vs. Suture, gap repair vs. Graft. Exp Neurol 1987, Aug;97(2):365-74.

311. Colman H, Lichtman JW. Cartellian competition at the neuromuscular junction. Trends Neurosci 1992;15(6):197-9.

312. Colman H, Nabekura J, Lichtman JW. Alterations in synaptic strength preceding axon withdrawal. Science 1997;275(5298):356.

313. Laskowski MB, Colman H, Nelson C, Lichtman JW. Synaptic competition during the reformation of a neuromuscular map. J Neurosci 1998, Sep 15;18(18):7328-35.

314. Lichtman JW, Colman H. Synapse elimination and indelible memory. Neuron 2000, Feb;25(2):269-78.

315. Walsh MK, Lichtman JW. In vivo time-lapse imaging of synaptic takeover associated with naturally occurring synapse elimination. Neuron 2003, Jan 9;37(1):67-73.

316. Valdez G, Tapia JC, Kang H, Clemenson GD, Gage FH, Lichtman JW, Sanes JR. Attenuation of age-related changes in mouse neuromuscular synapses by caloric restriction and exercise. Proc Natl Acad Sci U S A 2010;107(33):14863.

317. Mackinnon SE, Dellon AL, O'Brien JP. Changes in nerve fiber numbers distal to a nerve repair in the rat sciatic nerve model. Muscle Nerve 1991, Nov;14(11):1116-22.

318. Balice-Gordon RJ, Lichtman JW. Long-term synapse loss induced by focal blockade of postsynaptic receptors. Nature 1994, Dec 8;372(6506):519-24.

319. Keller-Peck CR, Walsh MK, Gan WB, Feng G, Sanes JR, Lichtman JW. Asynchronous synapse elimination in neonatal motor units: Studies using GFP transgenic mice. Neuron 2001, Aug 16;31(3):381-94.

320. Buffelli M. Activity-Dependent synaptic competition at mammalian neuromuscular junctions. News in Physiological Sciences 2004, Jun 1;19(3):85-91.

321. Balice-Gordon RJ, Breedlove SM, Bernstein S, Lichtman JW. Neuromuscular junctions shrink and expand as muscle fiber size is manipulated: In vivo observations in the androgen-sensitive bulbocavernosus muscle of mice. J Neurosci 1990, Aug;10(8):2660-71.

322. Balice-Gordon RJ, Breedlove SM, Bernstein S, Lichtman JW. Neuromuscular junctions shrink and expand as muscle fiber size is manipulated: In vivo observations in the androgen-sensitive bulbocavernosus muscle of mice. J Neurosci 1990, Aug;10(8):2660-71.

323. Wood MD, Kemp SW, Weber C, Borschel GH, Gordon T. Outcome measures of peripheral nerve regeneration. Ann Anat 2011, Jul;193(4):321-33.

324. Kawabuchi M, Zhou CJ, Wang S, Nakamura K, Liu WT, Hirata K. The spatiotemporal relationship among schwann cells, axons and postsynaptic acetylcholine receptor regions during muscle reinnervation in aged rats. Anat Rec 2001, Oct 1;264(2):183-202.

325. Harii K, Ohmori K, Torii S. Free gracilis muscle transplantation, with microneurovascular anastomoses for the treatment of facial paralysis. A preliminary report. Plast Reconstr Surg 1976, Feb;57(2):133-43.

326. Terzis JK, Sweet RC, Dykes RW, Williams HB. Recovery of function in free muscle transplants using microneurovascular anastomoses. J Hand Surg Am 1978, Jan;3(1):37-59.

327. Frey M, Gruber H, Freilinger G. Is a crossover to the contralateral side by nerve transplants a satisfactory source for reinnervation of a muscle transplant? An experimental study in the rectus femoris muscle of the rabbit. Microsurgery 1983;4(1):41-50.

328. Urso-Baiarda F, Grobbelaar AO. A comparison of one-versus two-stage surgery in an experimental model of functional muscle transfer with interposed nerve grafting. Journal of Plastic, Reconstructive & Aesthetic Surgery 2009;62(8):1042-7.

329. Fu SY, Gordon T. Contributing factors to poor functional recovery after delayed nerve repair: Prolonged axotomy. J Neurosci 1995, May;15(5 Pt 2):3876-85.

330. Johnson EO, Zoubos AB, Soucacos PN. Regeneration and repair of peripheral nerves. Injury 2005, Nov;36 Suppl 4:S24-9.

331. Pestronk A, Drachman DB, Griffin JW. Effects of aging on nerve sprouting and regeneration. Exp Neurol 1980, Oct;70(1):65-82.

332. Jacob JM, Robbins N. Age differences in morphology of reinnervation of partially denervated mouse muscle. J Neurosci 1990, May;10(5):1530-40.

333. Jacob JM, Robbins N. Differential effects of age on neuromuscular transmission in partially denervated mouse muscle. J Neurosci 1990, May;10(5):1522-9.

334. Vaughan DW. Effects of advancing age on peripheral nerve regeneration. J Comp Neurol 1992, Sep 8;323(2):219-37.

335. Ferreira MC, Besteiro JM, Tuma Júnior P. Results of reconstruction of the facial nerve. Microsurgery 1994;15(1):5-8.

336. Kimura J, Rodnitzky RL, Okawara SH. Electrophysiologic analysis of aberrant regeneration after facial nerve paralysis. Neurology 1975, Oct;25(10):989-93.

337. Bento RF, Miniti A. Anastomosis of the intratemporal facial nerve using fibrin tissue adhesive. Ear Nose Throat J 1993, Oct;72(10):663.

338. Kerrebijn JD, Freeman JL. Facial nerve reconstruction: Outcome and failures. Journal of Otolaryngology-Head & Neck Surgery 1998;27(4):183.

339. Anonsen CK, Trachy RE, Hibbert J, Cummings CW. Assessment of facial reinnervation by use of chronic electromyographic monitoring. Otolaryngol Head Neck Surg 1986, Jan;94(1):32-6.

340. Baker RS, Stava MW, Nelson KR, May PJ, Huffman MD, Porter JD. Aberrant reinnervation of facial musculature in a subhuman primate: A correlative analysis of eyelid kinematics, muscle synkinesis, and motoneuron localization. Neurology 1994, Nov;44(11):2165-73.

341. Morris JH, Hudson AR, Weddell G. A study of degeneration and regeneration in the divided rat sciatic nerve based on electron microscopy. I. The traumatic degeneration of myelin in the proximal stump of the divided nerve. Z Zellforsch Mikrosk Anat 1972;124(1):76-102.

342. Ito M, Kudo M. Reinnervation by axon collaterals from single facial motoneurons to multiple muscle targets following axotomy in the adult guinea pig. Acta Anat (Basel) 1994;151(2):124-30.

343. Brown AG, Fyffe RE. Direct observations on the contacts made between ia afferent fibres and alpha-motoneurones in the cat's lumbosacral spinal cord. J Physiol 1981;313:121-40.

344. Guntinas-Lichius O, Irintchev A, Streppel M, Lenzen M, Grosheva M, Wewetzer K, et al. Factors limiting motor recovery after facial nerve transection in the rat: Combined structural and functional analyses. Eur J Neurosci 2005, Jan;21(2):391-402.

345. Carmignoto G, Finesso M, Siliprandi R, Gorio A. Muscle reinnervation--i. Restoration of transmitter release mechanisms. Neuroscience 1983;8(3):393-401.

346. Madison RD, Robinson GA, Chadaram SR. The specificity of motor neurone regeneration (preferential reinnervation). Acta Physiol (Oxf) 2007, Feb;189(2):201-6.

347. Lefebvre JL, Kostadinov D, Chen WV, Maniatis T, Sanes JR. Protocadherins mediate dendritic self-avoidance in the mammalian nervous system. Nature 2012, Aug 23;488(7412):517-21.

348. Ranson SW. Degeneration and regeneration of nerve fibers. ; 1912.

349. Jenq CB, Coggeshall RE. Long-term patterns of axon regeneration in the sciatic nerve and its tributaries. Brain Res 1985, Oct 14;345(1):34-44.

350. Chor H, Cleveland D, Davenport H, Dolkart R, Beard G. Atrophy and regeneration of the gastrocnemius-soleus muscles. J Am Med Assoc-1939-CHOR-1029-33.pdf .

351. Mackinnon SE, Dellon AL, O'Brien JP. Changes in nerve fiber numbers distal to a nerve repair in the rat sciatic nerve model. Muscle Nerve 1991, Nov;14(11):1116-22.

352. Wehrmacher WH, Thomson JD, Hines HM. Effects of electrical stimulation on denervated skeletal muscle. Arch. Phys. Med 1945;26(261):1045.

353. Hines HM, Wehrmacher WH, Thomson JD. Functional changes in nerve and muscle after partial denervation. Am J Physiol 1945, Nov;145:48-53.

354. Weiss P, Edds MV. Sensory-motor nerve crosses in the rat. J Neurophysiol 1945;8(3):173-93.

355. Exner S. Die innervation des kehlkopfes. ; 1884.

356. Van Harreveld A. Re-innervation of denervated muscle fibers by adjacent functioning motor units. American Journal of Physiology--Legacy Content 1945;144(4):477-93.

357. Edds MV, Small WT. The behavior of residual axons in partially denervated muscles of the monkey. J Exp Med 1951, Mar;93(3):207-16.

358. Edds MV. Collateral nerve regeneration. Q Rev Biol 1953, Sep;28(3):260-76.

359. Hoffman H. Local re-innervation in partially denervated muscle; a histophysiological study. Aust J Exp Biol Med Sci 1950, Jul;28(4):383-97.

360. Ironton R, Brown MC, Holland RL. Stimuli to intramuscular nerve growth. Brain Res 1978, Nov 10;156(2):351-4.

361. Slack JR, Hopkins WG, Williams MN. Nerve sheaths and motoneurone collateral sprouting. Nature 1979, Nov 29;282(5738):506-7.

362. Burkel WE. The histological fine structure of perineurium. Anat Rec 1967, Jun;158(2):177-89.

363. Causey G, Hoffman H. Axon sprouting partially deneurotized nerves. Brain 1955;78(4):661-8.

364. Duchen LW. An electron microscopic study of the changes induced by botulinum toxin in the motor end-plates of slow and fast skeletal muscle fibres of the mouse. J Neurol Sci 1971, Sep;14(1):47-60.

365. Thompson W, Jansen JK. The extent of sprouting of remaining motor units in partly denervated immature and adult rat soleus muscle. Neuroscience 1977;2(4):523-35.

366. Brown MC, Holland RL, Ironton R. Variations in the amount and type of alpha-motoneurone sprouting following partial denervation of different mouse muscles [proceedings]. J Physiol 1978, Nov;284:177P-8P.

367. Luff AR, Hatcher DD, Torkko K. Enlarged motor units resulting from partial denervation of cat hindlimb muscles. J Neurophysiol 1988, May;59(5):1377-94.

368. Madison RD, Sofroniew MV, Robinson GA. Schwann cell influence on motor neuron regeneration accuracy. Neuroscience 2009;163(1):213-21.

369. Happak W, Liu J, Burggasser G, Flowers A, Gruber H, Freilinger G. Human facial muscles: Dimensions, motor endplate distribution, and presence of muscle fibers with multiple motor endplates. Anat Rec 1997, Oct;249(2):276-84.